uOttawa

L'Université canadienne
Canada's university

FACULTÉ DES ÉTUDES SUPÉRIEURES ET POSTOCTORALES

uOttawa

L'Université canadienne
Canada's university

FACULTY OF GRADUATE AND POSDOCTORAL STUDIES

Mona Hosseini-Abardeh

AUTEUR DE LA THÈSE / AUTHOR OF THESIS

M.Sc. (Cellular and Molecular Medicine)

GRADE / DEGREE

Department of Cellular and Molecular Medicine

FACULTÉ, ÉCOLE, DÉPARTEMENT / FACULTY, SCHOOL, DEPARTMENT

The Regulation of α-Actinin-4 in Podocytes and its Role in Focal Segmental Glomerulosclerosis

TITRE DE LA THÈSE / TITLE OF THESIS

Dr. C. Kennedy

DIRECTEUR (DIRECTRICE) DE LA THÈSE / THESIS SUPERVISOR

CO-DIRECTEUR (CO-DIRECTRICE) DE LA THÈSE / THESIS CO-SUPERVISOR

EXAMINATEURS (EXAMINATRICES) DE LA THÈSE / THESIS EXAMINERS

Dr. J. Copeland

Dr. R. Hebert

Gary W. Slater

Le Doyen de la Faculté des études supérieures et postdoctorales / Dean of the Faculty of Graduate and Postdoctoral Studies

THE REGULATION OF α-ACTININ-4 IN PODOCYTES AND ITS ROLE IN FOCAL SEGMENTAL GLOMERULOSCLEROSIS

Mona Hosseini-Abardeh

Thesis submitted to the Department of Cellular and Molecular Medicine in partial fulfillment of the requirements for the degree of Master of Science

©Mona Hosseini-Abardeh
Faculty of Medicine
University of Ottawa
Ottawa, Ontario, Canada
April 2007

Library and Archives Canada

Published Heritage Branch

395 Wellington Street
Ottawa ON K1A 0N4
Canada

Bibliothèque et Archives Canada

Direction du Patrimoine de l'édition

395, rue Wellington
Ottawa ON K1A 0N4
Canada

Your file Votre référence
ISBN: 978-0-494-49211-6
Our file Notre référence
ISBN: 978-0-494-49211-6

NOTICE:
The author has granted a non-exclusive license allowing Library and Archives Canada to reproduce, publish, archive, preserve, conserve, communicate to the public by telecommunication or on the Internet, loan, distribute and sell theses worldwide, for commercial or non-commercial purposes, in microform, paper, electronic and/or any other formats.

The author retains copyright ownership and moral rights in this thesis. Neither the thesis nor substantial extracts from it may be printed or otherwise reproduced without the author's permission.

AVIS:
L'auteur a accordé une licence non exclusive permettant à la Bibliothèque et Archives Canada de reproduire, publier, archiver, sauvegarder, conserver, transmettre au public par télécommunication ou par l'Internet, prêter, distribuer et vendre des thèses partout dans le monde, à des fins commerciales ou autres, sur support microforme, papier, électronique et/ou autres formats.

L'auteur conserve la propriété du droit d'auteur et des droits moraux qui protège cette thèse. Ni la thèse ni des extraits substantiels de celle-ci ne doivent être imprimés ou autrement reproduits sans son autorisation.

In compliance with the Canadian Privacy Act some supporting forms may have been removed from this thesis.

While these forms may be included in the document page count, their removal does not represent any loss of content from the thesis.

Conformément à la loi canadienne sur la protection de la vie privée, quelques formulaires secondaires ont été enlevés de cette thèse.

Bien que ces formulaires aient inclus dans la pagination, il n'y aura aucun contenu manquant.

Canada

ABSTRACT

α-Actinin-4 is an actin crosslinking protein that supports the foot process architecture of the podocytes. Mutations in the *ACTN4* gene underlie an autosomal dominant form of the glomerular lesion - Focal Segmental Glomerulosclerosis (FSGS). Affected individuals have a defective filtration barrier causing protein to leak into the urine. The K256E mutation dramatically increases α-actinin-4/actin affinity, alters α-actinin-4's intracellular localization in podocytes, and impairs cytoskeletal-dependent cell spreading and migration. Due to its mislocalization and enhanced affinity for F-actin, we hypothesized that the phosphorylation and interaction of K256E α-actinin-4 with its known binding partners would be disrupted. Furthermore, K256E α-actinin-4 would diminish the dynamic nature of the podocyte actin cytoskeleton upon exposure to mechanical stretch – a mimic of the in vivo intraglomerular capillary pressure. Tyrosine phosphorylation of α-actinin-4 could not be detected in cells overexpressing focal adhesion kinase (FAK) or in response to sodium orthovanadate – a tyrosine phosphatase inhibitor. Immunofluorescence, immunoprecipitation, and immunoblot approaches revealed that K256E α-actinin-4 exhibits reduced interaction with the adherens junction protein, β-catenin, and affects distribution of the actin binding protein, synaptopodin, along stress fibers. Finally expression of K256E α-actinin-4 dramatically alters the morphology of podocytes, reducing the cytoplasmic surface area, in response to mechanical stretch. These findings demonstrate that the K256E α-actinin-4 is sequestered away from specific subcellular domains such that it cannot interact with some of its endogenous binding partners, while severely impacting the dynamic nature of the actin cytoskeleton. These perturbations may therefore underlie podocyte dysfunction in actinin-associated FSGS.

The most exciting phrase to hear in science, the one that heralds the most discoveries, is not "I found it!" but "That's funny..."

~Isaac Asimov

ACKNOWLEDGMENTS

I would like to express my immense gratitude to Dr. Chris Kennedy for his guidance, inspiration and understanding throughout my studies. His teaching methods and patience were paramount to my success. I am extremely grateful for the opportunity of being his student.

In addition, I would like to thank the members of my advisory committee, Dr. John Copeland and Dr. Dennis Bulman for their great insights and suggestions.

A special thanks to Jean-Louis Michaud for all his help and advice. I really appreciate all the time he took to simplify and explain things to me; he is truly a great teacher.

I would also like to thank the lab members Erin Stitt, Anthony Carter, Kaeda Gomi, Wissam Faour, and Hiba Yusuf for making the lab environment an exciting one to work in.

I would like to thank Pauline Messier, Donna Hooper, and the entire Kidney Research Centre for all their help in the past few years.

Finally I am deeply indebted to my husband, my parents and my brothers for their support and encouragement through my studies.

DECLARATION

I certify that this thesis does not incorporate without acknowledgement any material previously submitted for a degree in any university. To the best of my knowledge this thesis does not contain material previously written by another except where due reference is made in the text.

I authorize the University of Ottawa to reproduce this thesis in whole or in part at the request of another institution for the purpose of academic research.

Mona Hosseini-Abardeh

TABLE OF CONTENTS

LIST OF FIGURES

LIST OF ABBREVIATIONS

ABD	actin-binding domain
ANOVA	Analysis of VAriance
BSA	bovine serum albumin
BCA	bicinchoninic Acid
°C	degree celsius
CaM	C-terminal calmodulin-like
CD2AP	CD2-associated protein
CH	calponin-homology
DAPI	4',6-diamidino-2-phenylindole
DMEM	Dulbecco's modified eagle's basal medium
E-cadherin	epithelial-cadherin
EGTA	ethylene glycol tetraacetic acid
EDTA	ethylenediamine tetraacetic acid
EM	electron microscopy
FBS	fetal bovine serum
FAK	focal adhesion kinase
FSGS	focal segmental glomerulosclerosis
g	gram
g	gravity
hOSE	human ovarian surface epithelial
GBM	glomerular basement membrane
GFP	green fluorescence protein

GFR	glomerular filtration rate
HA	hemagglutinin
HEK	human embryonic kidney
hrs	hours
IFN	interferon
mg	milligram
ml	milliliter
MAGUK	Membrane-Associated GUanylate Kinase
MAGI-1	MAGUK-with inverted orientation
MOI	multiplicity of infection
NFP	net filtration pressure
NP-40	ninodet-40
P-cadherin	placental-cadherin
PBS	phosphate buffered saline
PCR	polymerase chain reaction
Pfu	plaque forming units
PI	phosphoinositide
PI3-kinase	phosphoinositide 3 kinase
PMSF	phenylmethylsulphonyl fluoride
RT	room temperature
RPMI-1640	Roswell Park Memorial Institute
SDS	sodium dodecyl sulphate
SDS-PAGE	SDS-polyacrylamide gel electrophoresis
Smurf-1	SMAD-specific ubiquitin regulatory factor 1

SV40	Simian Vacuolating virus 40
TBS-T	tris-buffered saline tween-20
TRPC6	transient receptor potential cation channel 6
µg	microgram
µl	microliter
ZO-1	zonula occludens-1

1 INTRODUCTION

1.1 THE KIDNEY

The kidney is an indispensable organ that removes toxic waste products, and excess water and salts from the blood. It also plays a part in controlling blood pressure, produces erythropoietin which stimulates red blood cell production and prevents anaemia, helps to keep calcium and phosphate in balance for healthy bones, and maintains the blood in a neutral (i.e. non acidic) state [4, 5]. The kidneys receive 20-25% of the resting cardiac output and filter/retain key plasma components (i.e. albumin) which helps keep a proper oncotic balance throughout the body, thereby preventing edema. Homeostasis is maintained through 1-1.5 million nephrons – the basic structural and functional units of the kidney.

1.2 THE NEPHRON

The chief function of the nephron is to reabsorb solute components of blood and secrete waste products. Each nephron (Figure 1.1) consists of a glomerulus, where blood plasma is filtered, and renal tubules, where the filtered fluid passes through and secretion and reabsorption of plasma components is carried out [4, 5]. The beginning of the nephron – the glomerulus - is composed of the glomerular capillaries and Bowman's capsule, the epithelial sac-like structure that surrounds the glomerular capillaries (Figure 1.2) [5].

Blood enters the glomerulus via the afferent arteriole of the renal circulation. The glomerulus filters the blood and the fluid that enters the Bowman's capsule is called the glomerular filtrate. The glomerulus filters approximately 150 and 180 liters of blood in females and males, respectively.

The glomerular filtrate then passes into the renal tubules as it exits from Bowman's capsule. The filtered fluid from the proximal convoluted tubule then passes through the loop of Henle (descending limb and ascending limp) and the distal convoluted tubule where it finally empties into a single collecting duct (Figure 1.1) [5]. Urine from all the collecting ducts flows into renal pelvis, and eventually empties into the bladder by way of the ureter.

The remainder of the blood, not filtered into the glomerulus, passes into the efferent arteriole and then moves into the vasa recta, the long loop-shaped capillaries that intertwine the renal tubules through the interstitial space (Figure 1.1). The reabsorbed water and solutes (Na^+, K^+, Cl^-, H^+, etc.) enter into the vasa recta from the renal tubules via interstitial space. The efferent venules then combine with those surrounding other nephrons to merge into the renal vein, and exit the kidney to join the main bloodstream. At this point, 99% of the filtrate returns to the bloodstream via renal tubule reabsorption, and only 1-2 liters are excreted as urine.

1.3 THE GLOMERULUS

The glomerulus (Figure 1.2) is the basic filtration unit of the nephron. It consists of a collection of elaborate capillary loops receiving blood supply from the afferent

arteriole of the renal circulation. The rate at which blood is filtered is called the glomerular filtration rate (GFR) [4]. The GFR of a given nephron is established by a pressure gradient set up by a number of forces (Figure 1.3). The glomerular capillary pressure consists of two main forces: First, the hydrostatic pressure, which is the blood pressure in glomerular capillaries and capsular space. Second, the colloid oncotic pressure, which is the pressure in the capillaries (caused by the presence of proteins such as albumin) and capsular space. The net filtration pressure (NFP), that takes into account all the pressures, is the driving force that causes the blood to be filtered into the Bowman's capsule from the glomerulus. GFR is then calculated to be the surface area available for filtration (the ultrafiltration coefficient - K_f) multiplied by NFP, [GFR = K_f x NFP].

The cellular components in the glomerulus that form the basic filtration unit and contribute to the architecture/function of glomerulus are mesangial cells and cells in the glomerular filtration barrier.

Mesangial cells are smooth muscle-like pericytes that are found in the interstitium between the capillaries of the glomerulus [6]. The role of the contractile smooth muscle-like pericytes is to regulate the intraglomerular blood flow [7], thus, the presumptive role of mesangial cells is to regulate glomerular filtration by modulating the surface area of each capillary loop to control the blood flow [6]. Therefore mesangial cells are not part of the filtration barrier per se, but instead participate indirectly in filtration.

The glomerular filtration barrier consists of the glomerular basement membrane (GBM) which is covered by fenestrated endothelial cells on the inner blood-facing surface and visceral epithelial cells called podocytes that cover the outer surface of each

capillary [5]. The endothelial cells of the glomerulus contain numerous pores (fenestrae) large enough to allow anything smaller than a red blood cell to pass through. The GBM is very thick (100-200 nm) compared to most basement membranes (40-50 nm), and it consists of collagen IV, laminin, and glycosaminoglycans such as heparan sulfate that are negatively charged molecules. This helps prevent passage of negatively charged proteins (e.g. albumin) into the Bowman's capsule as the negatively charged basement membrane repels them. Inasmuch as the endothelial cells and GBM help establish the initial obstacle for plasma albumin, the final barrier for filtration is established and maintained by the podocytes.

Figure 1.1 The Nephron

Each nephron consists of a glomerulus and renal tubules. Blood enters the nephron via the afferent arteriole from renal system. The beginning of the nephron – The Glomerulus - filters the blood and the filtrate fluid enters the Bowman's capsule. The glomerular filtrate then passes into the renal tubules, the proximal convoluted tubule, the loop of Henle (descending limb and ascending limp), the distal convoluted tubule, and finally the collecting duct. The blood, not filtered into the Bowman's capsule, passes into the efferent arteriole and then moves into the vasa recta, surrounding the renal tubules. The reabsorbed water and solutes enter into the vasa recta from the renal tubules to return to the main bloodstream. Image from (Ross M.H. et al., 2003)

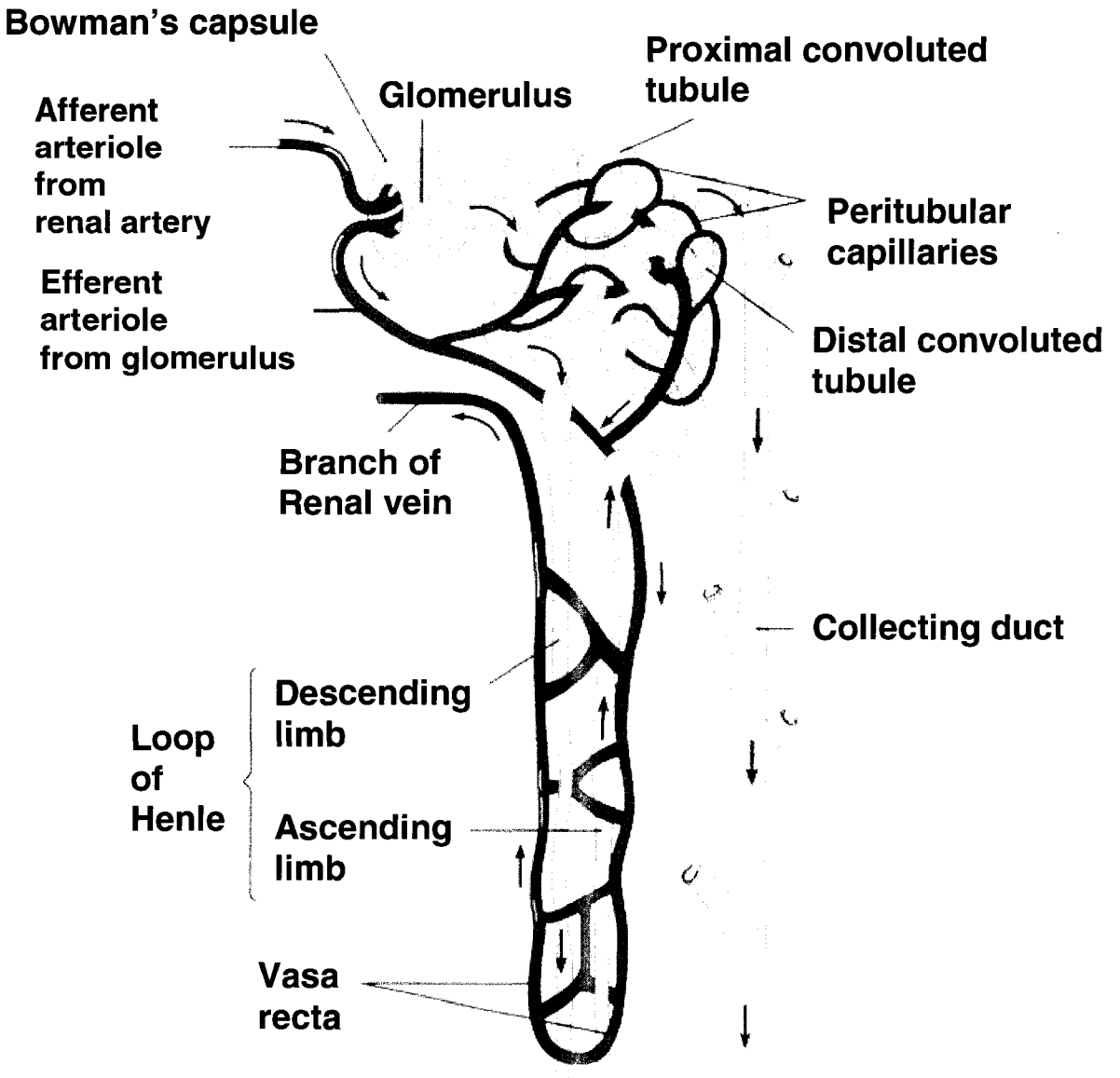
Bowman's capsule
Glomerulus
Proximal convoluted tubule
Afferent arteriole from renal artery
Peritubular capillaries
Efferent arteriole from glomerulus
Distal convoluted tubule
Branch of Renal vein
Collecting duct
Loop of Henle
Descending limb
Ascending limb
Vasa recta

Figure 1.2 The Glomerulus

The glomerulus is the basic filtration unit of the nephron that consists of capillary loops covered by podocytes and Bowman's capsule. **A** - Scanning electron microscopy (EM) of the glomerular capillaries covered by podocytes. **B** - Glomerulus (Bowman's capsule, podocytes) and the mesangial cells. Image (A) from Renal Pathology Scanning Microscopy site (http://www.med.niigata-u.ac.jp/npa/rpa/rpa.html).

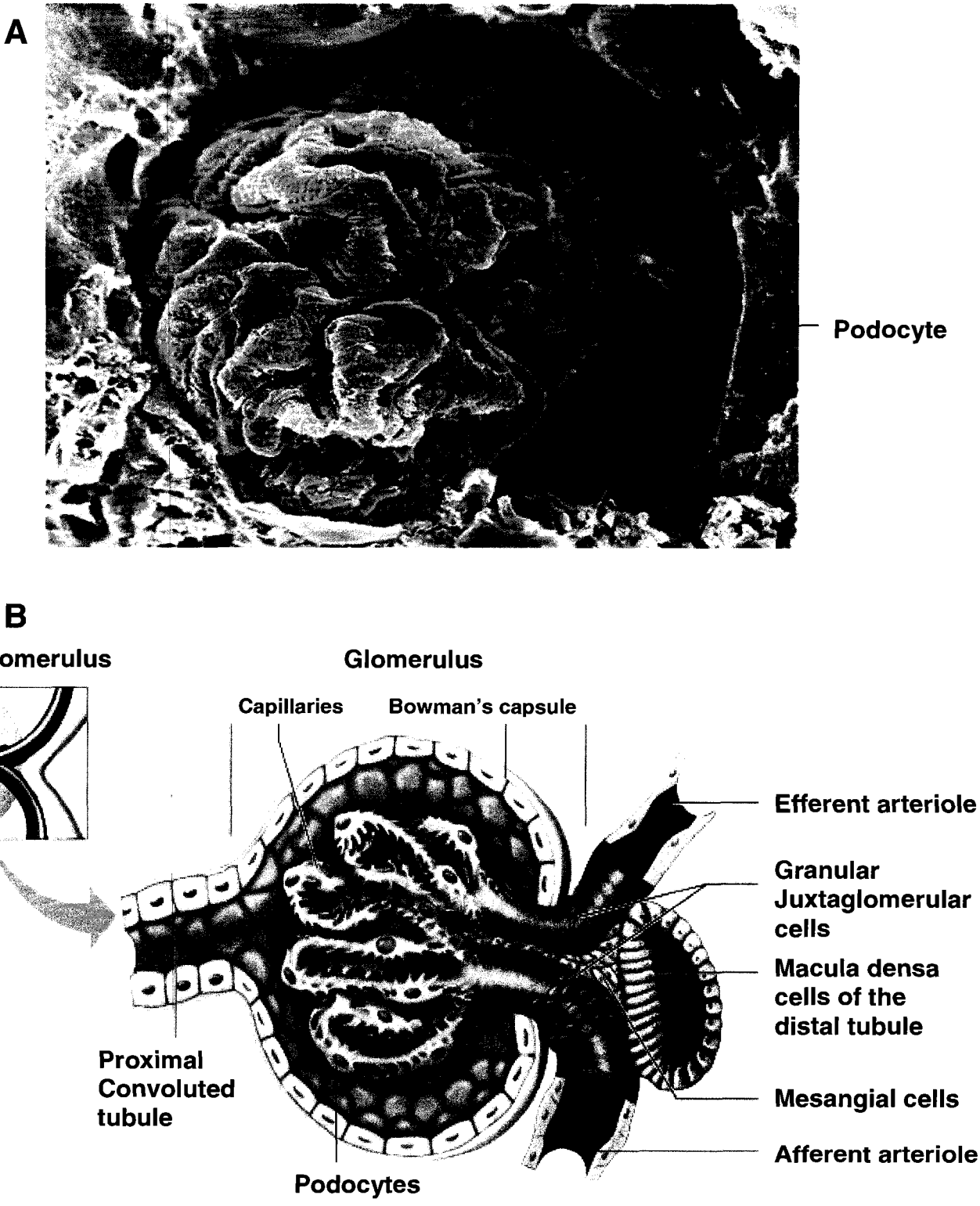

copyright © 2001, Benjamen cummings,
an imprint of Addison Wesley Longman, Inc.

Figure 1.3 Blood Flow and Pressure in Glomerulus

Blood enters the glomerulus via the afferent arteriole of the renal circulation. The glomerulus filters the blood and the filtrate enters Bowman's capsule.
The rate at which blood is filtered is called the glomerular filtration rate (GFR). The net filtration pressure (NFP), which is the net pressure of the glomerular capillary pressure (hydrostatic and colloid oncotic pressure), is the driving force that causes the blood to be filtered into the Bowman's capsule from the glomerulus. GFR is then calculated to be: [GFR = K_f x NFP]. Where K_f is the ultrafiltration coefficient. Image modified from the following URL: (http://www.mscd.edu/~biology/2320course/2320info.htm

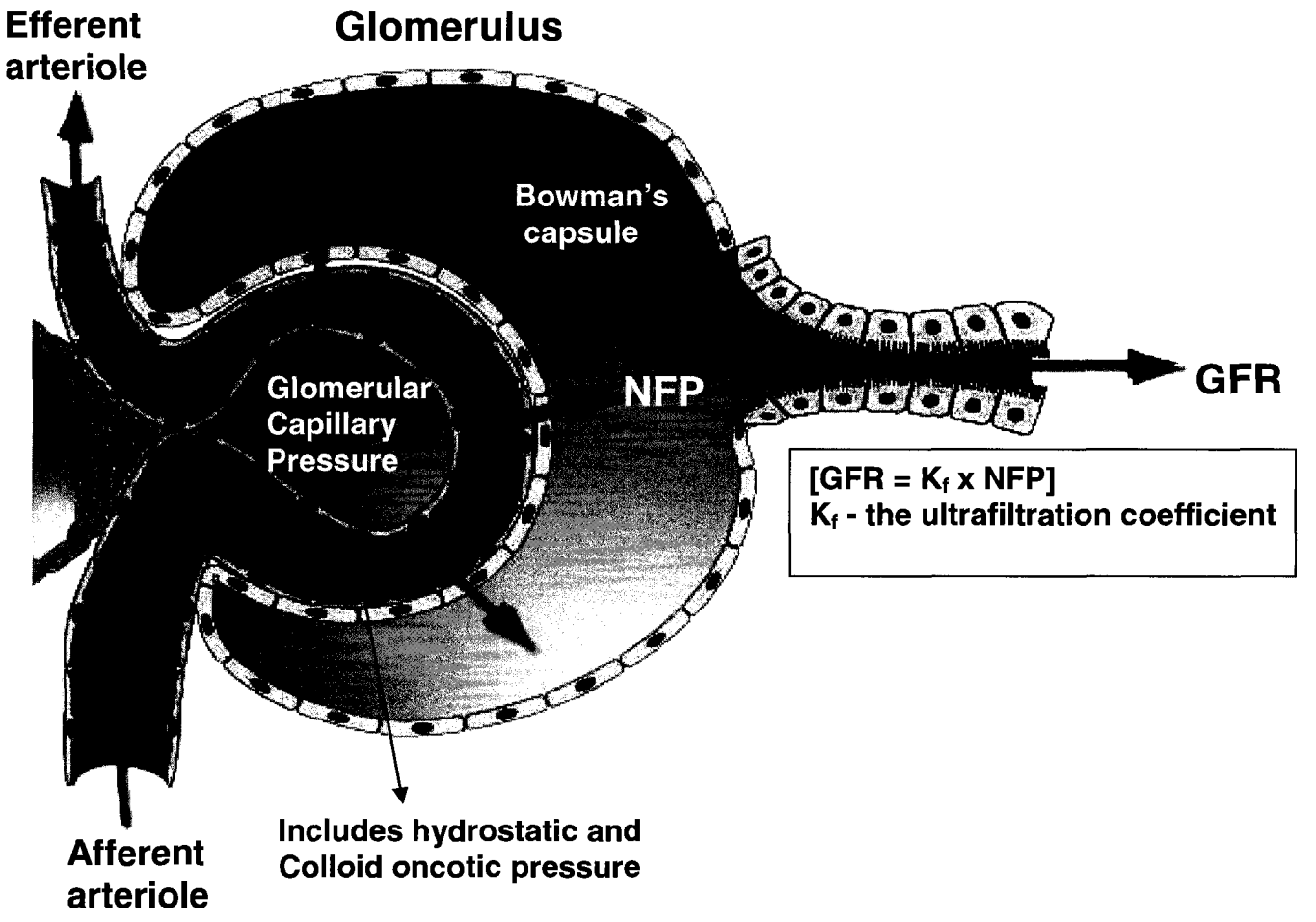
Efferent arteriole
Glomerulus
Bowman's capsule
Glomerular Capillary Pressure
NFP
GFR
[GFR = K_f x NFP]
K_f - the ultrafiltration coefficient
Afferent arteriole
Includes hydrostatic and Colloid oncotic pressure

1.4 THE PODOCYTES

The ability of the glomerulus to produce a filtrate free of protein is mainly achieved by podocytes. The function of podocytes depends on an elaborate and complex structure and cellular morphology. The structure of podocytes (Figure 1.4) consists of the cell body, the primary and secondary processes, also known as foot processes, and the slit diaphragm.

The cell body of the podocytes bulges into the urinary space and gives rise to primary processes that extend toward the glomerular capillaries by use of their longitudinally arranged bundles of microtubules (Figure 1.5B shown in green) [8]. Primary processes then branch out as numerous foot processes and completely enwrap the glomerular capillaries by use of their actin-base contractile apparatus (Figure 1.5B shown in red). By interdigitating with the foot processes of adjacent podocytes, foot processes form a sieve bridged by an extracellular structure, known as the slit diaphragm (Figure 1.6) [8].

The slit diaphragm establishes a barrier to molecules based on their size, charge and shape. Furthermore, the role of the slit diaphragm tends to be more complex than simply a physical sieve, as it participates in intracellular signaling mechanisms necessary to maintain the functional integrity and survival of podocytes [9].

1.5 THE SLIT DIAPHRAGM

The structure of the slit diaphragm is essentially a modified adherens junction [8, 10]. During the early stage of glomerular development, podocytes are connected by

structures resembling tight junctions as they express zonula occludens-1 (ZO-1) [11] and desmosomal proteins [12], the common tight junction proteins. Normally, cell to cell contacts are maintained through such highly organized junctional structures. Two major types of junctions are adherens junctions and tight junctions [13] by transmembrane adhesive proteins that are linked to intracellular binding partners, which anchor to the actin cytoskeleton and stabilize the junctions [13]. As podocytes begin to form their foot processes and slit membrane, the desmosomal proteins disappear [12] and the ZO-1 protein migrates to where the albumin-restrictive slit membrane develops and the slit diaphragm associated proteins, nephrin, podocin, and CD2-associated protein (CD2AP) are expressed (Figure 1.6B) [8].

Nephrin (180kDa) is an adhesion protein and member of the Ig superfamily and an essential structural component of the slit diaphragm [14]. It's extracellular domain is part of the slit diaphragm that forms a zipper-like structure, which bridges the distance between interdigitating podocyte foot processes to interact with the extracellular domain of another nephrin molecule expressed on an adjacent foot process (Figure 1.7) [14].

Mutations in the gene encoding nephrin (NPHS1) have been linked to a familial form of nephrotic syndrome [15], a condition characterized by massive leakage of protein into the urine. In addition, NPHS1 inactivation in mice leads to effacement of podocyte foot processes, and neonatal death [16]. These phenotypes indicate that nephrin is a key component of the slit diaphragm and the glomerular filtration barrier.

Nephrin also contains a short cytoplasmic tail with a number of tyrosine residues that are phosphorylated and tightly regulated by the src kinase family member Fyn [17]. When activated by phosphorylation, nephrin is believed to trigger anti-apoptotic

signaling; this is achieved by interacting with phosphoinositide 3 kinase (PI3-kinase), which activates the serine-threonine kinase, Akt [9]. Akt then mediates phosphorylation of several target proteins such as Bad, a proapoptotic protein of the Bcl-2 family. Upon inactivation of Bad by phosphorylation, apoptosis is avoided [9], suggesting that the nephrin-PI3-kinase-mediated Akt activity can regulate cellular survival pathways in podocytes.

An expanding list of other slit diaphragm associated proteins include P (placental) - cadherin, the MAGUK with inverted orientation-1 (MAGI-1), α-catenin, and β-catenin (Figure 1.6B). Such molecular components are believed to be important in maintaining the structure and function of slit diaphragm; either by associating with the slit diaphragm directly/indirectly to link it to the cytoskeleton or by participating in signaling pathways that considered to be important in podocytes survival. Importantly, the integrity of the slit diaphragm complex is dependent upon its being tethered to a structurally secure cytoskeletal network. It is becoming clear that factors which disrupt the podocyte cytoskeleton in a disease state have an immediate impact upon the viability of the slit diaphragm and its ability to restrict the passage of albumin into the urine.

Figure 1.4 The Podocyte

Scanning EM of podocytes enwrapping the outer aspect of the glomerular capillaries. Podocyte structure consists of the cell body, primary processes, and the secondary processes also known as foot processes. Scanning EM image from (Smoyer, W.E. and Mundel P., 1998).

Glomerulus

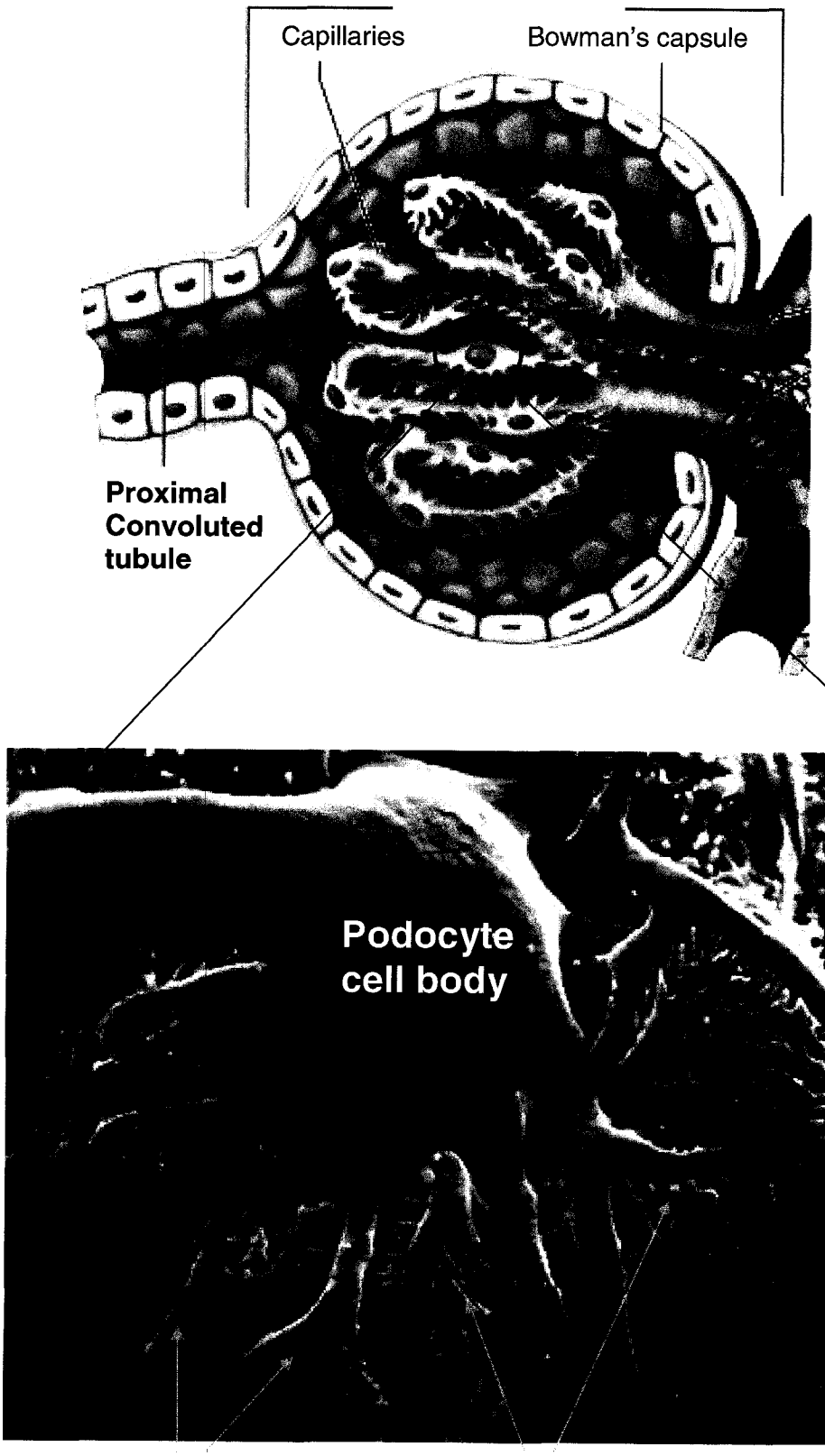

copyright © 2001, Benjamen cummings, an imprint of Addison Wesley Longman, Ir

Figure 1.5 Cytoskeleton of Podocyte Foot Processes

A - Cross section of a glomerular capillary loop covered by foot processes of the podocytes. **B –** View from the top - Arranged bundles of microtubules in primary processes (green) and actin-bundles of contractile apparatus in foot processes (red). Image from (Pavenstadt H., et al., 2003).

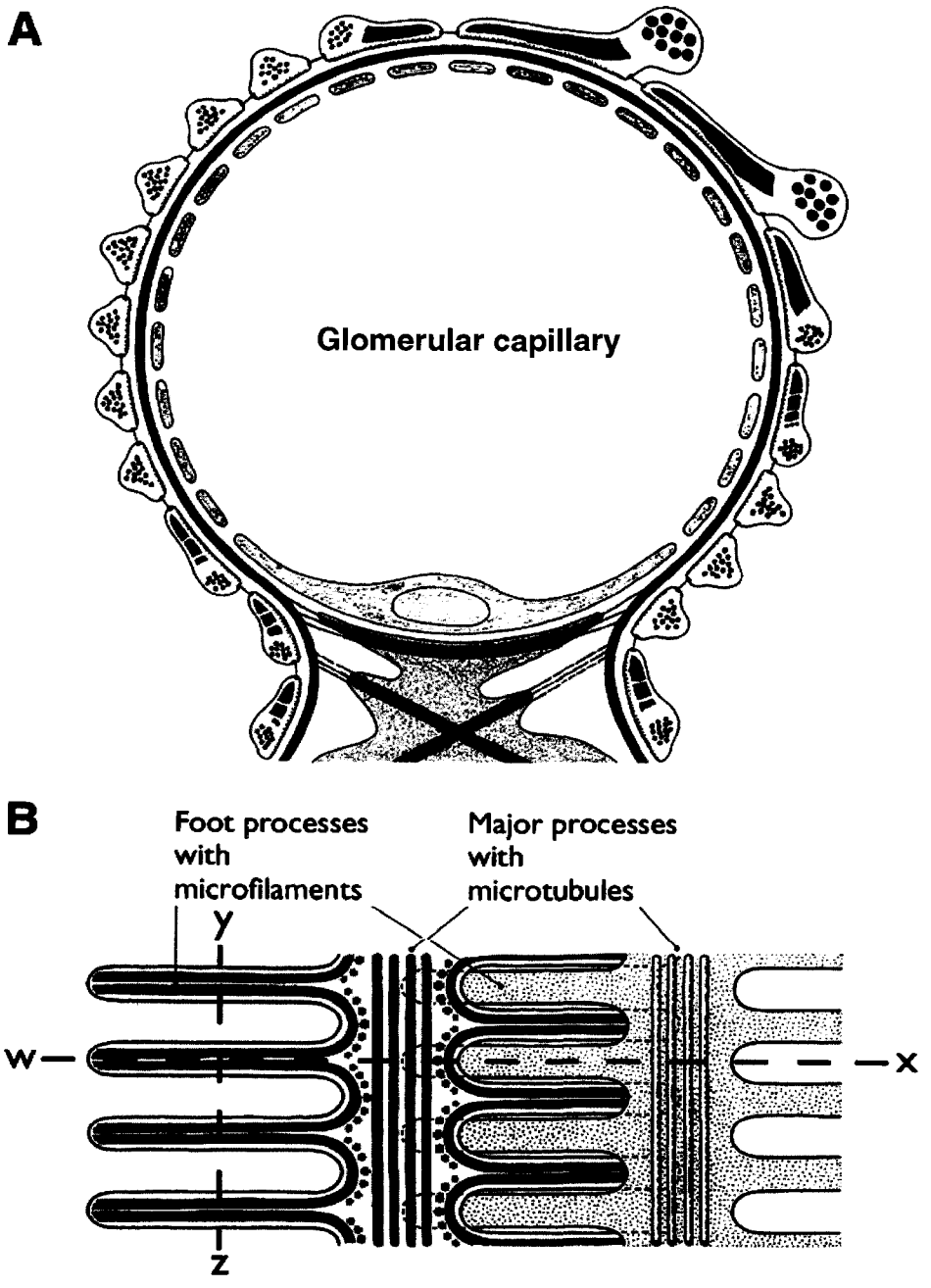
A
Glomerular capillary
B
Foot processes with microfilaments
Major processes with microtubules
y
w
x
z

Figure 1.6 Foot Processes and Slit Diaphragm of Podocytes

The foot processes are extensions of the podocyte that contact the GBM and interdigitate with the foot processes of the neighboring podocytes. The slit diaphragm bridges the space between two foot processes and forms the sieve that substances cross to reach the urinary space. **A** – Illustrates a transmission EM of podocyte foot processes. Image from (Lahdenkari A.T. et al., 2004). **B** – Illustrates a drawing of two foot processes and most of the molecular components required in podocytes to develop and maintain their structure and function as the main filtration barrier. Nephrin, P-cadherin, β-catenin, synaptopodin, vinculin, and MAGI-1 discussed in introduction are all included in this figure. Image from (Michaud J.L., and Kennedy C.R., 2007).

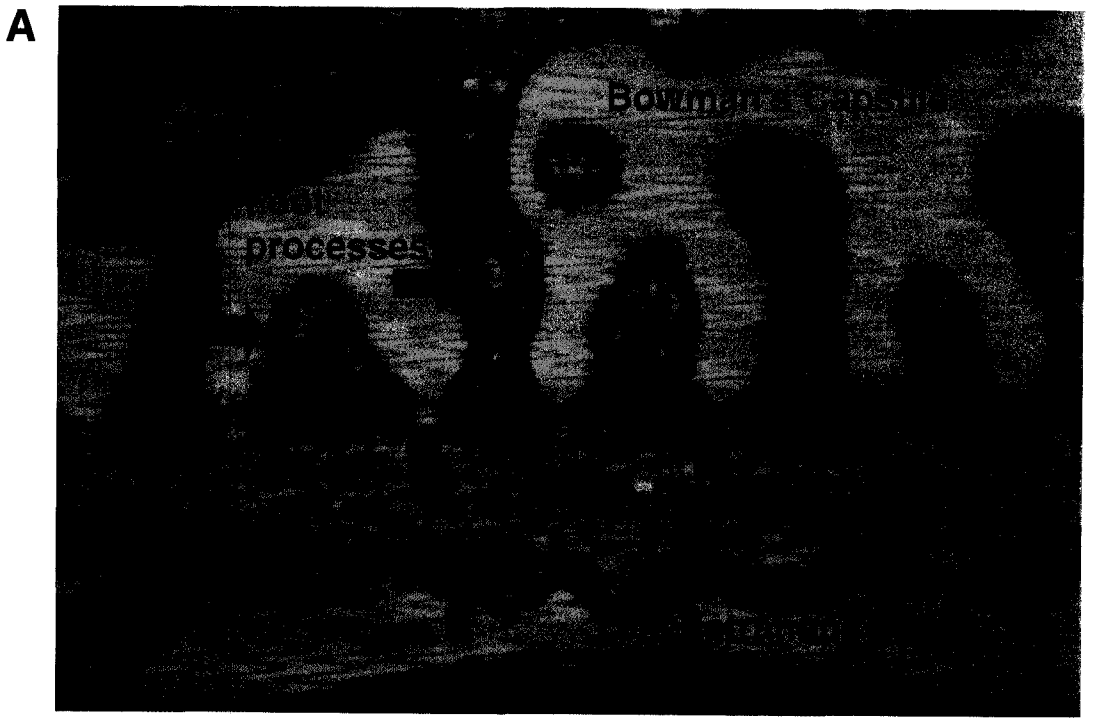
A
Bowman's Capsule
processes

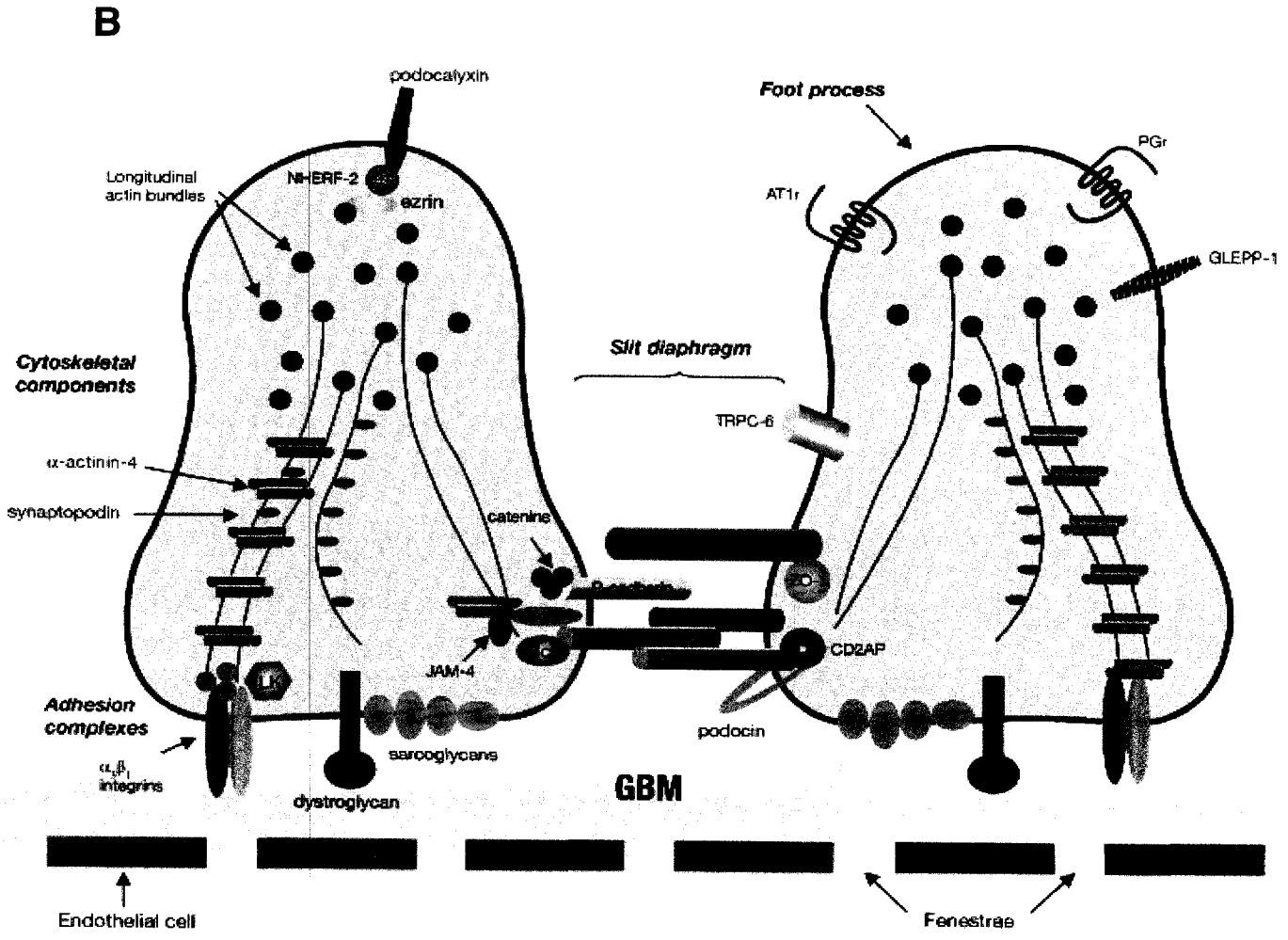
B
podocalyxin
Foot process
PGr
Longitudinal actin bundles
NHERF-2
ezrin
AT1r
GLEPP-1
Cytoskeletal components
Slit diaphragm
TRPC-6
α-actinin-4
synaptopodin
catenins
JAM-4
CD2AP
Adhesion complexes
podocin
sarcoglycans
GBM
dystroglycan
Endothelial cell
Fenestrae

Figure 1.7 Nephrin

Nephrin is an essential structural component of the slit diaphragm. Its extracellular domain forms a zipper-like structure, which bridges the distance between interdigitating podocyte foot processes. This structure forms pores that establish a barrier to molecules based on their size, charge and shape.

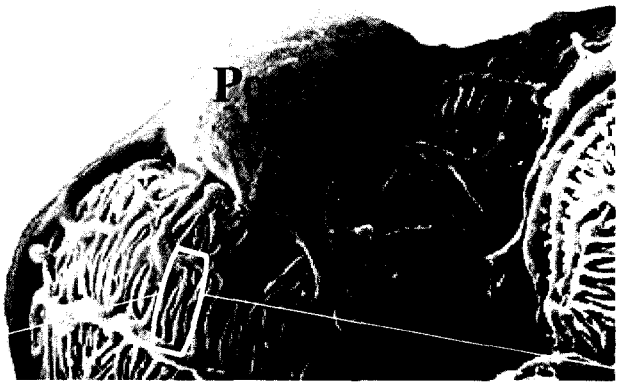

Nephrin

View from the top

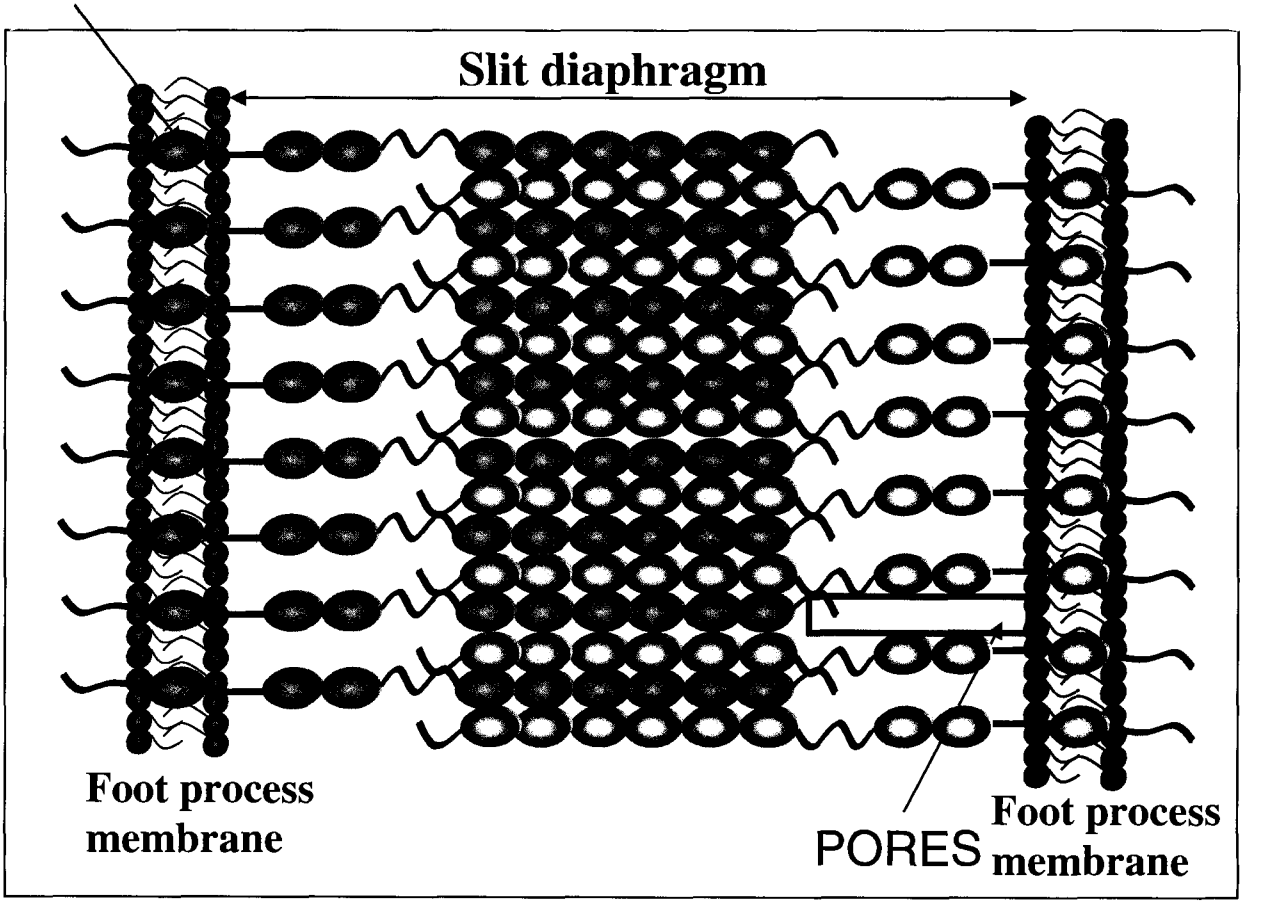

1.6 FOCAL SEGMENTAL GLOMERULOSCLEROSIS

A number of diseases target the roughly one million glomeruli in each kidney. When the glomerulus is damaged, it allows protein (albumin) to leak into the urine, commonly called proteinuria. Over time, the excess protein within the tubular lumen becomes toxic to the kidney. The ensuing damage will eventually lead to kidney failure, which requires life-sustaining dialysis or kidney transplant.

One class of glomerular diseases is called focal segmental glomerulosclerosis (FSGS), which is one of the leading causes of end-stage renal disease. FSGS is actually a type of lesion that occurs when scar tissue forms in some of the glomeruli of the kidney. The term "focal" means that some of the glomeruli are scarred, while others remain unaffected. The term "segmental" means that only part of an individual glomerulus is damaged.

The scarring process is initiated from podocyte damage. When podocytes are injured, the cell-cell contacts at the slit diaphragm, cell-matrix contacts and the cytoskeletal structure of the foot processes are altered and eventually the cell takes on an "effaced" phenotype (Figure 1.8). Foot process effacement is also referred to as process simplification, retraction, or fusion [8]. The mechanism by which cells develop an effaced phenotype, is not fully understood, however, it is commonly accepted that disappearance of the structure of the slit diaphragm and development of proteinuria are accompanied by increased deposition of actin filaments along the base of foot processes – an event that likely contributes to effacement and the loss of the slit diaphragm.

Most people affected by FSGS do not have a family history of kidney disease. However, familial FSGS is considered in families with two or more family members with FSGS and, most have mutation in genes encoding nephrin [15, 16], podocin [18], CD2AP [19], TRPC6 (transient receptor potential cation channel, subfamily C, member 6) [20] and α-actinin-4 [21].

Figure 1.8 Podocyte Foot Process Effacement

When podocytes are damaged, the cells exhibit an effaced phenotype. The cell-cell contacts at the slit diaphragm of the foot processes show an abnormal phenotype and eventually lead to the disappearance of the slit diaphragm. **A** – Illustrates a scanning EM of normal foot processes of podocytes. **B** – Illustrates a scanning EM of effaced foot processes. **C** – Illustrates a scanning EM of the normal podocytes **D** – Illustrates a scanning EM of the diseased podocytes, possibly detaching from the GBM. Image A and B from (Lahdenkari A.T. et al., 2004) and Image B and C from (http://biology.ucf.edu/~logiudice/zoo3713/ZOO%203713 and http://www.nephrohus.org/uz/article.php3?id_article=137)

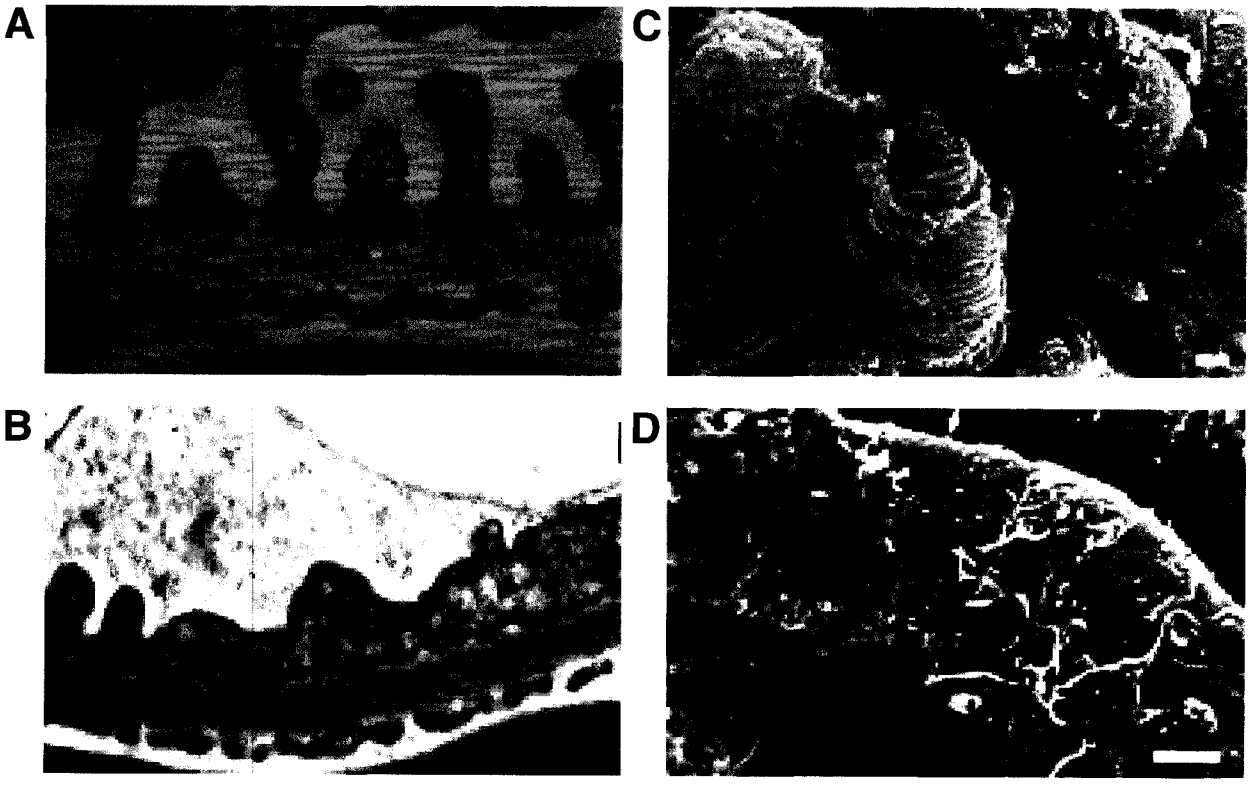
A
C
B
D

1.7 α-ACTININ-4

α-Actinin is a ubiquitous actin-bundling/crosslinking protein belonging to the spectrin superfamily [22, 23]. The α-actinin family consists of two non-muscle isoforms (α-actinins 1 and 4) and two skeletal muscle isoforms (α-actinin-2 and 3) [24, 25]. The muscle-specific isoforms, α-actinin-2 and α-actinin-3 cross-link F-actin together in the region of the Z-disc of the sarcomeres in striated muscle cells [22, 26, 27]. The bundling/crosslinking abilities of α-actinin-2 and α-actinin-3 are insensitive to calcium [26] while those of α-actinin-1 and α-actinin-4 are responsive to calcium [28]. Thus, the binding affinity of the α-actinins (1,4) can be regulated by calcium.

α-Actinin-1 and α-actinin-4 are widely expressed, though only α-actinin 4 (~100kDa) is highly expressed in the glomerular podocytes [1]. α-Actinin-4 was first discovered by S. Hirohashi's group in 1998 as a new molecular marker that is associated with cell motility and cancer invasion [29]. In podocytes, α-actinin-4 co-localizes with focal adhesions, stress fibres and adherens junctions while being excluded from the nucleus. On the other hand, in some cancer cell lines, α-actinin-1 localizes to focal adhesions and adherens junctions, while, α-actinin-4 does not localize to these sites and is mostly found in the cytoplasm and in the nucleus upon inhibition of PI3-kinase [29]. These findings suggest that α-actinin-1 and α-actinin-4 might have some redundant and some distinct roles depending on the cell line and they might compensate for one another in case the expression of the other isoform is not significant.

Interestingly, mutations in the gene encoding α-actinin-4 (*ACTN4*) account for approximately 4% of familial FSGS in families with an autosomal dominant pattern of inheritance [1, 30]. Thus, α-actinin 4 is thought to be important for maintaining the structure and function of podocytes.

1.7.1 Structure of α-Actinin-4

The putative structure of the α-actinin-4 protein is shown in Figure 1.9. α-actinin-4 exists as an antiparallel homo-dimer equipped with several regulatory domains: an N-terminal actin-binding domain (ABD) composed of two calponin-homology (CH) domains, where the second calponin-domain contains a phosphoinositide binding site (PI), a central region with four α–helical spectrin-like repeats (R1-R4) which allows α-actinin-4 to dimerize and gives it a significant elasticity [25], and a C-terminal calmodulin-like (CaM) domain with two EF-hand motifs [25]. Interestingly, the FSGS causing mutations are found in a highly-conserved region located in the linker sequence between the ABD and first spectrin-like repeat (Figure 1.9). These regulatory domains may function to relay a number of specific intracellular signals in order to modulate the binding of α-actinin-4 to actin filaments or other associating proteins and thereby alter its intracellular location and function.

Figure 1.9 Structure of α-Actinin-4

α-actinin-4 forms an anti-parallel dimmer. It consists of an actin-binding domain (ABD) (composed of two calponin-homology domains) at the N-terminus of each monomer with a phosphoinositide binding site (PI). α-actinin-4 also contains four spectrin-like repeats (R1-R4) and two EF-hand calcium regulation domains (EF). FSGS-associated mutations are found in the linker region between the actin binding domain and the 1st spectrin like repeat.

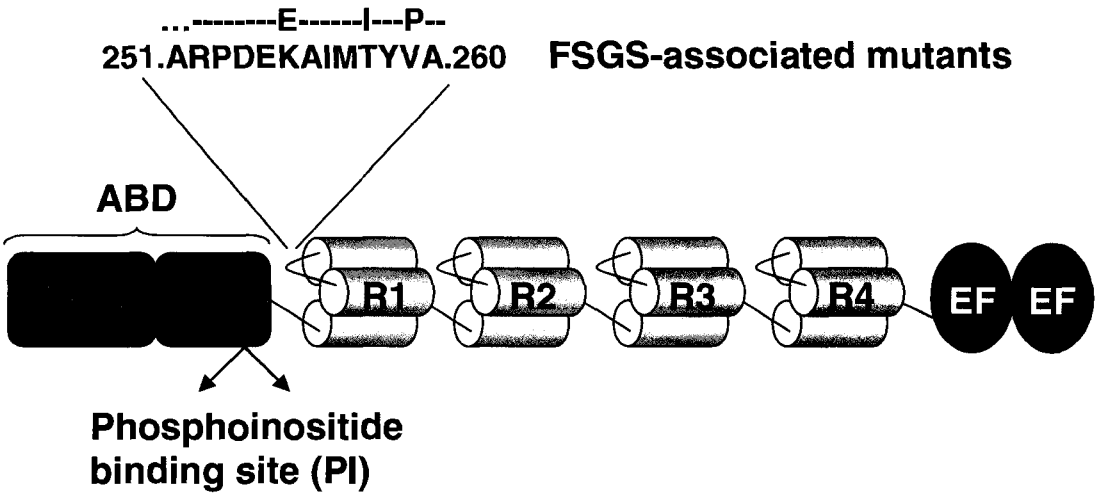
...--------E------I---P--
251.ARPDEKAIMTYVA.260
FSGS-associated mutants
ABD
R1
R2
R3
R4
EF
EF
Phosphoinositide
binding site (PI)

1.8 REGULATION AND FUNCTION OF α-ACTININ-4

1.8.1 Function of α-Actinin-4

Further studies from our lab demonstrated that α-actinin-4 localizes to distinct subcellular domains of podocytes, including the cortical actin network, focal adhesions, and actin stress fibers. In contrast, the disease-causing K256E α-actinin-4 dramatically increases the affinity of α-actinin-4 for F-actin thereby excluding α-actinin-4 from the cell periphery while impairing cell migration, spreading and formation of foot process-like projections in cultured podocytes [3] suggesting that the podocyte cytoskeleton is dysregulated.

To better understand the progression of α-actinin-4 associated-FSGS a transgenic mouse model was developed in our lab [2]. Mice expressing the α-actinin-4 transgene, with a K256E mutation, in a podocyte-specific manner using the nephrin promoter developed proteinuria, foot process effacement and glomerular sclerosis [2]. These findings strongly supported a role for podocyte α-actinin-4 in the maintenance of the glomerular filtration barrier.

At the same time, Pollak's group developed a mouse model lacking the *ACTN4* gene [31]. Mice homozygous for the *ACTN4* null alleles developed damaged podocytes leading to proteinuria and progressive glomerular disease while heterozygous ACTN4 null mice showed no apparent phenotype [31]. Furthermore, they developed knock-in mice expressing the FSGS-associated mutant and showed an increased degradation of mutated α-actinin-4 in fibroblasts taken from these mice [32]. These mice also developed

foot process effacement in podocytes leading to progressive proteinuria and glomerular disease.

1.8.2 Flexibility of α-Actinin-4

A recent study has shown that α-actinin is a flexible cross-linker of actin filaments by studying 2D electron micrographs of F-actin cross-linked with α-actinin [33]. They showed 8000 actin crossover repeats, each with one to five α-actinin molecules bound that can turn 60°, 120° and 180° about its ABD. These properties of α-actinin may explain the non-flexibility of actin filaments observed when FSGS-associated K256E α-actinin-4 is associated with them, possibly resulting in inhibition of their structural flexibility.

1.8.3 Regulation of α-Actinin-4 Function

The putative regulatory domains housed within the α-actinin-4 protein sequence suggest that the binding affinity of this molecule may be modulated by intracellular signal transduction. In fact, a group showed that PI3-kinase derived phosphoinositides that bind to the PI binding site of α-actinin may regulate actin stress fiber formation in cells by controlling the extent to which microfilaments are bundled [34, 35]. Furthermore the EF hands of α-actinin-4 appear to be responsive to calcium since our lab demonstrated that wildtype α-actinin-4 is displaced from F-actin with increasing levels of

Ca^{2+} whereas the K256E α-actinin-4 remains tightly associated with actin (unpublished data).

1.8.4 Regulation of α-Actinin-1 by Focal Adhesion Kinase

Focal adhesion kinase (FAK) is a key component of the signal transduction pathways triggered by integrins [36], which is important in regulation of cell spreading, migration, survival, and proliferation [37]. Activation and autophosphorylation of FAK is achieved by association of FAK with integrins via cytoskeletal proteins at focal adhesions. Upon autophosphorylation, FAK associates with a number of signaling molecules containing the Src homology 2 domain [38], including Src family members, resulting in activation of these kinases. The activation of the FAK/Src complex leads to tyrosine phosphorylation of a number of other substrates, which are involved in cell adhesion, cell proliferation, and survival. The signaling function of FAK is dependent upon its localization to focal adhesions since a FAK mutant that fails to localize to focal adhesions exhibits impaired autophosphorylation in response to cell adhesion and fails to phosphorylate downstream substrates [39].

One group showed that α-actinin-1, an isoform of α-actinin-4, can act as a substrate for FAK and can be phosphorylated on tyrosine 12 (corresponding to Y32 of murine α-actinin-4) in activated human platelets [40]. α-Actinin-1 was not phosphorylated in cells lacking FAK, while re-expression of FAK in these cells restored α-actinin phosphorylation [41]. They also showed that phosphorylation of α-actinin-1 negatively regulates the binding of α-actinin-1 to actin [41]. These findings suggest that

α-actinin-4 could be another substrate of FAK that leads to regulation of cell adhesion, cell proliferation and survival when tyrosine phosphorylated.

1.8.5 Interaction of α-Actinin-4 with β-Catenin

In addition to its interaction with actin filaments, α-actinin-4 may serve as a docking protein that binds a number of other intracellular proteins to form complex multimeric structures within the podocyte. An important interaction was association of α-actinin-4 with β-catenin at adherens junctions in colorectal cancer cells [42]. This interaction is extremely interesting because it is involved in the structure of adherens junctions (slit diaphragm in the case of podocytes). The importance of the adherens junction is that it determines cellular morphogenesis, maintains cellular architecture and regulates major cellular processes including motility, polarity, growth, differentiation, and survival [43].

In cancer cells, when α-actinin-4 interacts with β-catenin, β-catenin's binding to E (epithelial)-cadherin is reduced [42]. However, podocytes do not express E-cadherin but instead express P (placental)-cadherin. P-cadherin (120kDa) is another adhesion-transmembrane protein of podocytes with an extracellular domain that also contributes to the zipper-like structure between the interdigitating foot processes. It consists of a cytoplasmic domain that links to β-catenin and/or gamma-catenin. P-cadherin and nephrin link to the actin cytoskeleton in podocytes, via the adaptors, ZO-1, CD2AP, α/β-catenin, and α-actinin [8]. However, β-catenin does not bind to actin filaments directly

but mediates the linkage via α-actinin. This suggests that interaction of α-actinin-4 with β-catenin might play a role in establishing the structure of slit diaphragms in podocytes.

1.8.6 Interaction of α-Actinin-4 with Synaptopodin

Synaptopodin is a 110 kDa proline-rich protein associated with actin filaments and it is expressed in the foot processes of podocytes and in the dendritic spines of the telencephalic synapses [44]. Synaptopodin appears almost as a linear protein without any globular domain structure and this may result in a side to side arrangement along the actin microfilaments (Figure 1.6B) [44].

Synaptopodin is believed to modulate the actin-based architecture and motility of the podocyte foot processes as its expression begins in the capillary loop stage, at which podocytes begin to form their foot processes and slit diaphragm [45].

Synaptopodin-deficient mice are viable and fertile and the structure of their podocytes appears to be normal [46]. Furthermore, the number and length of their dendritic spines are normal, however, the spine apparatuses are completely absent from their hippocampal neurons [46]. Subsequently, Mundel's group showed that synaptopodin-deficient podocytes exhibit difficulty in re-forming their actin filaments in vivo and in vitro [47]. These phenotypes were explained by their discovery that synaptopodin has three isoforms, neuronal Synpo-short, renal Synpo-long, and Synpo-T (which consists of only the C terminus of Synpo-long). They showed that Synpo-T acts in a redundant manner for Synpo-long only in podocytes since in mice deficient synaptopodin, Synpo-T is not upregulated in the brain.

Synaptopodin is also involved in stress fibre assembly and regulation of cytoskeletal dynamics through RhoA (small GTPase) [48]. RhoA is involved in regulating many signal transduction pathways including cytoskeletal dynamics by promoting the formation of actin-myosin-stress fibres and cell migration [49, 50]. Thus, by blocking the activity of SMAD-specific ubiquitin regulatory factor 1 (Smurf-1), which is responsible for degradation of RhoA, synaptopodin is able to regulate RhoA signaling such as cytoskeletal dynamics and cell migration [48]

Importantly, synaptopodin interacts with α-actinin-4 in podocytes to facilitate actin filament elongation and to prevent the formation of short branched filaments [47]. This indicates that the interaction of the two actin bundling proteins found in podocytes is important in the regulation of the actin cytoskeleton.

1.8.7 Interaction of α-Actinin-4 with MAGI-1

The MAGUK with inverted orientation (MAGI) proteins consist of three members that make up a subfamily of a larger group of proteins known as the MAGUKs (Membrane-Associated GUanylate Kinase) [51]. MAGUK proteins are proposed to function as molecular scaffolds within cells. They are found at several types of cell junctions, postsynaptic densities within neurons as well as the tight and adherens junctions of epithelial cells [51].

MAGI-1 (137 kDa) is expressed in podocytes and localizes to the slit diaphragm (Figure 1.6B). As a scaffold protein, MAGI-1 might be involved in the molecular

architecture of the slit diaphragm since it interacts with nephrin [52], and links to the actin cytoskeleton by interacting with synaptopodin and α-actinin-4 [51].

1.8.8 Interaction of α-Actinin-4 with Vinculin

The delicate foot process architecture of glomerular podocytes depends on maintaining the slit diaphragm (cell-cell adhesion) and integrin mediated cell-GBM interaction. Foot processes of podocytes are attached to their underlying GBM through complex transmembrane structures known as focal adhesions. These are complexes that provide a molecular bridge between the extracellular matrix, the plasma membrane, and the actin cytoskeleton. In podocytes, focal adhesions are composed of integrins ($\alpha_3\beta_1$), major cell surface receptors for extracellular matrix molecules (Collagen IV and laminin), and membrane-cytoplasmic linker proteins, such as vinculin, and other proteins such as talin and paxillin, that are involved in linkage of integrin to the actin cytoskeleton [53].

Vinculin is a 117 kDa membrane-cytoskeletal protein and consists of a globular head domain that contains binding sites for talin and α-actinin as well as a tyrosine phosphorylation site, while the tail region contains binding sites for paxillin and lipids [54, 55]. Cells that lack vinculin exhibit impairment in cell adhesion, spreading and stress fiber formation. They also form fewer focal adhesions and lamellipodia [55-57]. These phenotypes indicate that vinculin's ability to interact with the cytoskeleton via other focal adhesion proteins appears to be critical for control of cell migration and motility.

In an early study, α-actinin-1, an isoform of α-actinin-4, was shown to bind to vinculin [58]. The downstream of this interaction was not investigated, however, we believe that this interaction may be related to the phenotypes our laboratory recently observed in podocytes expressing the FSGS-associated α-actinin-4 (i.e. impairment in cell migration, spreading and fewer cytoplasmic extensions).

1.8.9 Interaction of α-Actinin-4 with Akt

Akt (also known as protein kinase B) is a member of the serine/threonine-specific protein kinase family [59]. Akt is a downstream effector of PI3-kinase and it was shown to be involved in cellular survival pathways [60]. Akt needs to be translocated to the plasma membrane via its pleckstrin homology domain in order to be activated [61, 62] and is dependent upon the product of PI3-kinase, (3,4,5) phosphoinositide [63].

The three isoforms of Akt are named Akt-1, Akt-2 and Akt-3. All Akt isoforms are assumed to have identical or similar substrate specificity [64, 65]. In most tissues, expression of Akt1 is the predominant isoform [59]. Akt1-null mice exhibit growth deficiency [66], and Akt2-null mice exhibit mild growth deficiency, loss of adipose tissue, and insulin resistance with elevated plasma triglycerides [67]. These phenotypes indicate that both Akt1 and Akt2 participate in the regulation of growth.

Akt activation is involved with inhibition of the apoptosis pathway, induction of the protein synthesis pathways leading to tissue growth, and metabolic functions of insulin and growth factors such as protein and lipid synthesis, carbohydrate metabolism,

and transcription [60]. Another important pathway that Akt is involved in is actin filament remodeling through PI3-kinase [68].

Recent work revealed that α-actinin-4 associates with Akt1 [69]. When α-actinin-4 interacts with Akt1 in human ovarian surface epithelial (hOSE) cells it regulates Akt phosphorylation by mediating its translocation to the cell membrane [69]. This suggests that α-actinin-4 might also regulate phosphorylation of Akt in podocytes and the K256E α-actinin-4 mutant might fail to translocate Akt to the cell membrane due to its inability to dissociate from actin filaments.

In summary, FSGS-associated mutations in α-actinin-4 may compromise cytoskeletal dynamics and thereby result in defective podocyte function leading to FSGS. To date, the interaction of β-catenin, synaptopodin, MAGI-1, vinculin FAK and Akt with the FSGS-associated mutant α-actinin-4 has not been studied; however uncovering whether such interactions are impaired by the disease-associated K256E mutant could give us insights into the development of podocyte damage during the early stages of FSGS.

2 RATIONALE

Due to its altered affinity for F-actin and aberrant subcellular localization, the question arises as to whether signaling through the various regulatory domains, or interactions with other proteins no longer exerts influence over actin/α-actinin-4 association, its intracellular location, and its effects on cellular dynamics. Therefore we sought to investigate the interaction of FSGS-associated mutant α-actinin-4 with a number of putative binding partners to understand the mechanism by which K256E α-actinin-4 leads to defective podocyte function.

3 HYPOTHESIS

The FSGS-associated mutant K256E α-actinin-4 exhibits altered association and regulation by its intracellular binding partners.

4 OBJECTIVES

1) To determine if α-actinin-4 is tyrosine phosphorylated.

To determine the influence of phosphorylation on the actin affinity of wildtype and K256E α-actinin-4 for F-actin.

2) To identify differences between wildtype and K256E α-actinin-4 with various interacting partners expressed in podocytes.

3) To examine morphological changes of podocytes expressing wildtype and K256E α-actinin-4 by mimicking glomerular pressure in vitro.

5 MATERIALS AND METHODS

5.1 CONSTRUCTS

5.1.1 Vectors

pcDNA3 HA-FAK – Cloning site is between Xbal and EcoRV of pcDNA3. Hemagglutinin (HA) epitope tag was introduced at the N-terminus of FAK. This construct was provided by Dr. Luc Sabourin (Ottawa Health Research Institute, Ottawa, ON)

pEGFP-N1- α-actinin-1 – Human α-actinin-1 was cloned into the Hind III site of pEGFP-N1. The green fluorescence protein (GFP) epitope tag was introduced at the C-terminus of α-actinin-1. This construct was provided by Dr. Carol A. Otey (University of North Carolina).

pcDNA3 HA-α-actinin-4 – Wildtype and K256E constructs were generated by cloning the murine HA-ACTN4 cDNA into pcDNA3 as described previously by our laboratory [2]. The double-HA epitope tag was introduced at the N-terminus of α-actinin-4.

pEGFP- α-actinin-4 –pCDNA3 HA-α-actinin-4 constructs (wildtype or K256E) were sub-cloned into pEGFP-N2. The stop codon was changed to an XmaI site by polymerase chain reaction (PCR) and the GFP epitope tag was introduced at the C-terminus of α-actinin-4.

5.1.2 Adenoviral Constructs

pcDNA3 HA-α-actinin-4 – The HA-tagged wildtype and K256E adenoviral constructs were developed in collaboration with Dr. R. Parks (Ottawa Health Research Institute, Ottawa, ON). As previously described by our lab [3], the HA-ACTN4 expression cassette replaced the E1-region and transcription is directed rightward, relative to the conventional human adenovirus serotype 5 map. The E1-deleted, first-generation adenovirus vectors used in these studies were constructed using a combination of conventional cloning techniques and RecA-mediated recombination [70, 71], and were grown and titred on Human Embryonic Kidney-293 (HEK) cells, as described previously [72].

pEGFP- α-actinin-4 – Two constructs of pEGFP-α-actinin-4 (wildtype, K256E) were sub-cloned into pShuttle-CMV to be used in the AdEasy Adenoviral Vector System (Stratagene, La Jalla, CA). The adenoviral constructs were then given to University of Ottawa Adenoviral Core Facility to sub-clone the pShuttle vector into pAdEasy-1 Vector and to thereby derive the adenoviruses.

5.2 TRANSIENT TRANSFECTION OF COS-7 AND NIH 3T3 CELLS

Transformed African Green Monkey Kidney Fibroblast (Cos-7) and Mouse embryonic fibroblast (NIH 3T3) cells were grown on collagen I coated plastic culture plates in Dulbecco's Modified Eagle's basal Medium (DMEM) supplemented with 10% Fetal Bovine Serum (FBS) (Invitrogen Corp., Carlsbad, CA), and penicillin-streptomycin solution (100 units/ml penicillin and 0.1 mg/ml streptomycin; Invitrogen Corp., Carlsbad, CA). Cells were passaged every 3-5 days and maintained at 37 ^{o}C and 5% CO_2.

Prior to any experiment, media was aspirated and the cells were rinsed twice with phosphate buffered saline (PBS). Transient transfection of Cos-7 and NIH 3T3 cells was carried out using the PolyFect Reagent (Qiagen Inc., Valencia, CA). Where indicated, the HA-tagged FAK construct (2μg) was co-transfected along with constructs for either α-actinin-4 (2μg) or α-actinin-1 (2μg). After 48 hours of transfection, cells were treated with 200μM of sodium orthovanadate (Sigma-Aldrich Co., St. Louis, MI) for 2 hours prior to cell lysis.

5.3 CELL CULTURE OF PODOCYTES

Conditionally immortalized mouse podocytes were provided by Dr. K. Endlich (University of Heidelberg, Germany). These cells were grown from isolated glomeruli of mice, carrying the temperature-sensitive mutant of the immortalizing Simian Vacuolating Virus-40 (SV40) large T antigen [73]. The inactivation of the temperature-sensitive mutant of the SV40 large T antigen is enhanced at 38°C- matching the body temperature of the mouse. These cell lines exhibit stable expression of nephrin and essential podocyte proteins such as P-cadherin, podocin, CD2AP, ZO-1, synaptopodin, cortactin, etc. Formation of cell-cell contacts is also visible in these cell lines [73].

Podocytes were grown on Collagen I coated plastic culture plates in normal podocyte growth medium (Roswell Park Memorial Institute (RPMI-1640)) supplemented with 10% FBS, 100ug/ml normocin (Cedarlane Labortories Limited, Hornby, ON) and penicillin-streptomycin solution (100 units/ml penicillin and 0.1 mg/mL streptomycin)). Cells were passaged (between 18 to 35) every 3-5 days and propagated at 33 ^{o}C with the addition of 10unit/ml γ-interferon (IFN) (Invitrogen Corp., Carlsbad, CA). To induce podocyte differentiation, the cells were then cultured in podocyte differentiation media (without γ-IFN) at 38 ^{o}C for ten to fourteen days.

Prior to any experiment media was aspirated and the cells were rinsed twice with PBS. Podocytes were infected with adenoviral constructs encoding either wildtype or K256E α-actinin-4 tagged with GFP (multiplicity of infection (MOI) of 200 plaque forming unit (pfu)/ml), or adenoviral constructs encoding wildtype or K256E tagged with HA (MOI of 25 pfu/ml). Adenoviral constructs were added to podocytes in Opti-mem I

Reduced Serum Medium (Invitrogen Corp., Carlsbad, CA). After one hour of incubation, normal podocyte growth media was added to the cells. The cells were then incubated at 38 ^{o}C for three days without media change and experiments performed on the fourth day.

5.4 PULLDOWN ASSAY

Following transient transfection of Cos-7 cells with either wildtype or K256E α-actinin-4 constructs, cells were washed twice with PBS and were scraped in 1 ml of PBS and collected in 1.5 ml microcentrifuge tubes. The cells were centrifuged at 16 000 *x g* for 10 minutes and were lysed in 500µl of sedimentation buffer (10mM Tris, pH 7.4, 150mM NaCl, 1mM ethylene glycol tetraacetic acid (EGTA), 1mM ethylenediamine tetraacetic acid (EDTA), 1% Triton X-100, and 0.5% ninodet-40 (NP-40)) containing protease inhibitor cocktail (5ul; Sigma-Aldrich Co., St. Louis, MI) and 1mM of phenylmethylsulphonyl fluoride (PMSF). Samples were incubated at room temperature (RT) for 10 minutes. 400µl of the sample was collected and put in a new 1.5 ml microcentrifuge tube and the rest was used for whole lysate analysis. Samples were centrifuged for 15 minutes at speed of 16 000 *x g* at RT. Supernatant was collected and put in a small microcentrifuge glass tubes and centrifuged at 100 000 *x g* for 30 minutes. Supernatant (Triton X-100 soluble) was collected for further analysis. Pellets (Triton X-100 insoluble) from low speed and high speed fractions were resuspended and sonicated in 400µl of ddH_2O. Protein concentration of each sample was determined using a bicinchoninic Acid (BCA) Protein Assay Kit (Pierce Biotechnology Inc., Rockford, IL). Equal amounts of protein were loaded for each sample onto 10% sodium dodecyl

sulphate- polyacrylamide gel electrophoresis (SDS-PAGE) resolving gel and processed for immunoblot analysis.

5.5 PROTEIN EXTRACTION AND QUANTITATION

Cells were washed twice with PBS and were scraped with 1 ml of PBS and collected in 1.5 ml microcentrifuge tubes. The cells were centrifuged at 16,000 *x g* for 10 minutes and lysed using M-PER Mammalian Protein Extraction Reagent (Pierce Biotechnology Inc., Rockford, IL) containing protease inhibitor cocktail (5ul; Sigma-Aldrich Co., St. Louis, MI). For phosphorylation analyses, phosphatase inhibitors, sodium orthovanadate (Sigma-Aldrich Co., St. Louis, MI), sodium fluoride (Sigma-Aldrich Co., St. Louis, MI) and di-sodium dihydrogen pyrophosphate (VWR International, Mississauga, ON) were included in the buffer. Elimination of cell debris was obtained by centrifuging the cell lysate at 16,000 *x g* for 5 minutes. Supernatants were collected and protein concentration was determined using BCA Protein Assay Kit (Pierce Biotechnology Inc., Rockford, IL).

5.6 IMMUNOPRECIPITATION ANALYSIS

Equal volumes of protein lysate (~300µg/µl) were transferred to 1.5 ml microcentrifuge tubes. 20µl of Immunopure-Immobilized protein A/G (Pierce Biotechnology Inc., Rockford, IL) was added and incubated for 1 hour at 4°C on a rotating apparatus to remove non-specifically bound proteins. The beads were then

centrifuged and supernatant was transferred to a new 1.5 ml microcentrifuge tube. 2-5μg of antibody (GFP or β-catenin) was added to supernatant. 25μl of protein A/G were then added and the sample was incubated overnight at 4°C on a rotating apparatus. The beads were then centrifuged and supernatant was removed. The beads were washed five times with 1ml of cold PBS for 2 minutes each wash. Supernatant was discarded from final wash and the pellets were re-suspended in 35μl of 2 X sodium dodecyl sulphate (SDS) sample buffer. The samples were boiled for 5 minutes and centrifuged for 1 minute. 25μl of supernatant was loaded on one 7.5% SDS-PAGE resolving gel and the remaining sample (10μl) was loaded on another 7.5% SDS-PAGE resolving gel to determine efficiency of immunoprecipitation.

5.7 IMMUNOBLOT ANALYSIS

Equal amounts of protein were loaded for each fraction onto 7.5-10% SDS-PAGE resolving gel. Gels were run at 130 V using the Bio-Rad Power Pac 300 and then electro-transferred to Hybond-ECL nitrocellulose membrane (Amersham Pharmacia Biotech, Piscataway, NJ). After performing the electrotransfer, membranes were incubated in blocking buffer (5% milk in tris-buffered saline tween-20 (TBS-T)) overnight at 4°C. Following the blocking step appropriate primary antibodies were diluted in 2% skim milk in TBS-T and the membrane probed for 1 hour at RT. Membranes were then washed in TBS-T three times for 10 minutes each and subsequently incubated in 2% skim milk in TBS-T containing anti-rabbit IgG, horseradish peroxidase-linked whole antibody from

donkey or anti-mouse IgG, horseradish peroxidase-linked whole antibody from sheep (Amersham Pharmacia Biotech, Piscataway, NJ) for 1 hour at RT.

The membranes were washed again in TBS-T three times for 10 minutes. Proteins were detected using Super Signal West Pico Chemiluminescent detection kit and in case of lower expression the Super Signal West Femto Maximum Sensitivity Substrate (Pierce Biotechnology Inc., Rockford, IL) and exposed to Kodak X-Omat Blue film for an appropriate exposure time.

5.8 ANTIBODIES

β-catenin Rabbit Polyclonal IgG: Upstate Cell Signaling Solutions (Lake Placid, NY). 1:1000 and 1:100 dilutions used for immunoblot and immunofluorescence respectively. 2μg/500μg of protein concentration used for immunoprecipitation.

BD Living Colors Full Length A.v. Rabbit Polycolonal IgG: BD biosciences-Clontech Laboratories, Inc. (Mountain View, CA). 1:1000 dilutions used for immunoblot and 1μg/500μg for immunoprecipitation.

HA-7 Mouse Monoclonal IgG: Monoclonal Anti-HA H 9685. Sigma-Aldrich Co. (St. Louis, MI). 1:1000 and 1:100 dilutions used for immunoblot and immunofluorescence respectively.

HA Rabbit Polycolonal IgG: BD Biosciences-Clontech Laboratories, Inc. (Mountain View, CA). 1:1000 and 1:100 dilutions used for immunoblot and immunofluorescence respectively.

MAGI-1 (H-70) Rabbit Polyclonal IgG: Santa Cruz Biotechnology, Inc. (Santa Cruz, CA). 1:100 and 1:50 dilutions used for Immunoblot and immunofluorescence respectively.

Phospho AKT (Ser473) Rabbit Polyclonal IgG: Cell Signaling Technology, Inc. (Danvers, MA). 1:1000 dilutions used for immunoblot.

Phosphotyrosine Mouse Monoclonal IgG: Upstate Cell Signaling Solutions (Lake Placid, NY). 1:500 dilutions used for immunoblot.

Synaptopodin Monoclonal IgG: Fitzgerald Industries International, Inc. (Concord, MA). 1:50 and 1:10 used for immunoblot and immunofluorescence respectively.

Total AKT Rabbit Polyclonal IgG: Cell Signaling Technology, Inc. (Danvers, MA). 1:1000 dilutions used for immunoblot.

Vinculin Mouse Monoclonal IgG: Sigma-Aldrich Co. (St. Louis, MI). 1:200 and 1:50 dilutions used for immunoblot and immunofluorescence respectively.

5.9 IMMUNOFLUORESCENCE

Differentiated podocytes were plated (~ 10 000 cells) onto collagen I coated glass coverslips in 12-well culture dishes and infected with the various adenoviral constructs. 72 hours after infection, the coverslips were washed twice with PBS and were fixed by incubating in cold 4% paraformaldehyde in PBS for 30 minutes at RT. Fixed cells were then washed with PBS containing 1mM Mg^{++} and 0.5 mM Ca^{++} and permeablized with 0.2% Triton X-100 in PBS for 15 minutes at RT. After cells were washed with PBS/Mg^{++}/Ca^{++}, permeabilized cells were incubated in blocking solution (2% BSA, 0.1% Triton X-100, PBS/ Mg^{++} /Ca^{++}) for 15 minutes at RT. The specific primary antibody for each experiment was left to incubate for 1 hour at RT. After cells were washed with PBS/0.1% Triton/Mg^{++} /Ca^{++} the secondary antibodies (Alexa Fluor 488 anti-rabbit, anti-mouse, Alexa Fluor 555 anti-rabbit, Alexa Fluor 594 anti-mouse, or Alexa Fluor 488-Phalloidin) (Molecular Probes, Eugene, Oregon) depending on the primary antibody were added for 1 hour at RT. To visualize nuclei, cells were also incubated with 4',6-diamidino-2-phenylindole (DAPI) (dilution 1:5000; Roche, Indianapolis, IN). Cells were once again washed with PBS/0.1% Triton/Mg^{++} /Ca^{++} and then coverslips were mounted using Vestashield fluorescent mounting media (Fluoromount G; Electron Microscopy

Sciences, Hatfield, PA). Podocytes were then visualized under a fluorescence microscope (Zeiss Axioskop 2 MOT, Zeiss Germany) and images were taken using a Zeiss AxioCam.

5.10 EQUIBIAXIAL CYCLIC STRETCH

Differentiated podocytes were plated onto six-well collagen I coated stretch plates (Flexcell International, Hillsborough, NC) (~ 2 x 10^5 cells) (Figure 5.1A). After allowing for attachment and spreading for 48-72 hours, the cells were infected with adenovirus for either wildtype or K256E α-actinin-4 tagged with GFP. Following three days of infection, the media of the podocytes was replaced with fresh podocyte growth media, and the silicone plates were mounted onto vaccum based 25mm loading stations of the Flexercell FX-4000 apparatus (Flexcell International, Hillsborough, NC) (Figure 5.1B). Podocytes were then subjected to 10% elongation at a frequency of 0.5 Hz for various times (1 hour to 24 hours) using the FX-4000T computer-regulated bioreactor (Figure 5.1C). The control (non-stretched) cells were not subjected to mechanical stress, but were nevertheless cultured on the collagen I coated silicone membrane six-well plates.

5.11 STATISTICAL ANALYSIS

Statistical analysis was performed using Graph Pad Prism software. Unpaired Student t-test was used to compare 2 groups. One way Analysis of Variance (ANOVA) was used to determine the significant differences among groups of more than 2 conditions. Statistically significant results were denoted at a P-value of < 0.05.

5.12 DENSITOMETRIC QUANTIFICATION

Densitometric quantification was performed for immunoblot analysis and surface area measurement of cells using ID Kodak Project Manager software. The cell perimeters were traced and the enclosed cytoplasmic area was measured in pixels. The pixels obtained from ID Kodak Project Manager software was multiplied by the square of micron (μm) per pixel determined by the fluorescence microscope objectives (Zeiss AxioCam).

5.13 QUANTIFICATION ANALYSIS

Cells were manually counted in a blinded manner using DAPI stained cells to obtain number of cells in stretch experiments.

Figure 5.1 Mechanical Stretch Device

A - The six-well collagen I coated stretch plates. These culture plates have flexible, matrix-bonded growth surfaces of silicone. **B** - Vacuum based 25mm loading stations. **C** - The FX-4000T computer-regulated bioreactor that can deliver equibiaxial cyclic stress (0.5 Hz and 10% linear strain) over the time course of 1 to 24 hours. Stretch is regulated by vacuum pressure. Image from Flexcell International official website (http://www.flexcellint.com/)

A

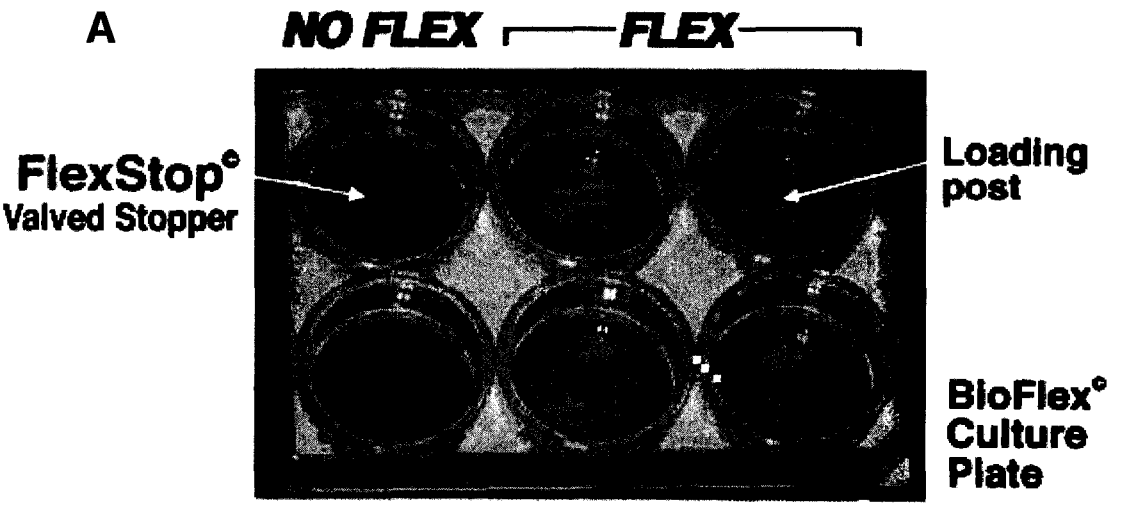
NO FLEX
FLEX
FlexStop©
Valved Stopper
Loading post
BioFlex©
Culture
Plate

B

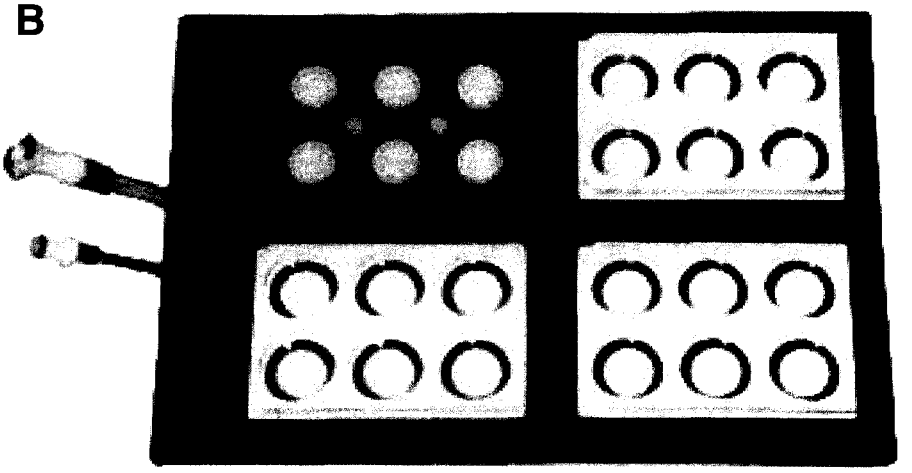

C

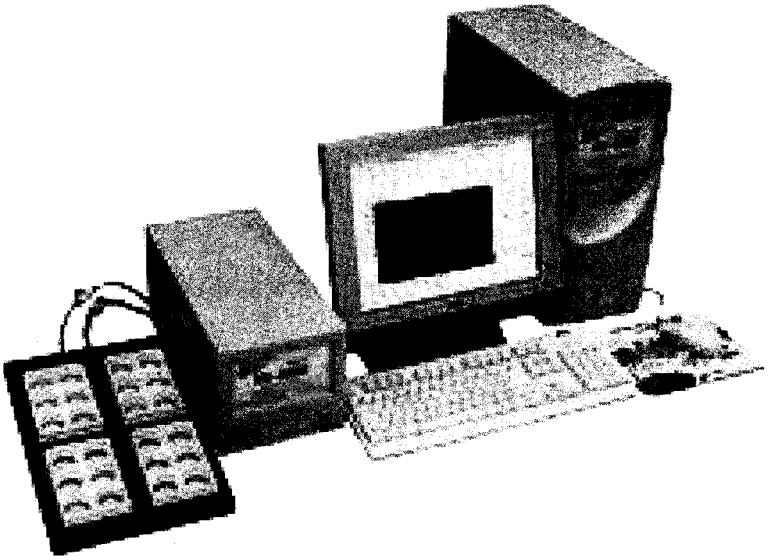

6 RESULTS

6.1 PHOSPHORYLATION OF α-ACTININ-4

6.1.1 Tyrosine Phosphorylation of α-Actinin-4 in NIH 3T3 and Cos-7 Cells

Cell survival requires the coordination of many processes including cytoplasmic spreading, cell migration and proliferation. These functions involve the assembly/disassembly of many structures such as focal adhesion complexes. Several protein-protein interactions have been identified at focal adhesions and most of these proteins have multiple binding partners [53]. These interactions are involved in a variety of signaling pathways, allowing cells to adapt to matrices of diverse properties. Tyrosine phosphorylation is one of the key signaling events occurring at focal adhesions. FAK is a tyrosine kinase localized to focal adhesions which participates in cell proliferation and survival by phosphorylating and activating a variety of proteins as cells adhere to extracellular matrix [74-76].

Previous studies have shown that α-actinin-1, an isoform of α-actinin-4, is tyrosine phosphorylated by FAK in Cos-7 cells [40]. Phosphorylation of α-actinin-1 negatively regulates its binding to actin, suggesting a role in the turnover of focal adhesions that occurs during migration and motility [41].

This was of great interest since our laboratory has shown that the K256E mutation in α-actinin-4 impairs migration and spreading of podocytes. We therefore investigated whether α-actinin-4 is likewise regulated by FAK-induced phosphorylation.

To determine tyrosine phosphorylation of α-actinin-4, NIH 3T3 cells were transfected with either α-actinin-4 or α-actinin-1 constructs (both GFP-tagged) (Figure 6.1, lanes 2-3) and co-transfected with a FAK construct (HA tagged) (Figure 6.1, lanes 5-6). Cells were then treated with sodium orthovanadate for 2 hours to block endogenous tyrosine phosphatase activity. Immunoblotting of cell lysates with an anti-GFP antibody was carried out to verify transfection efficiency (Figure 6.1A). Anti-GFP antibody was used to immunoprecipitate either wildtype α-actinin-4 or α-actinin-1 and the samples were then subjected to immunoblotting using an anti-GFP antibody (Figure 6.1B) or an anti-phosphotyrosine antibody (Figure 6.1C). Our data showed that neither α-actinin-4 nor α-actinin-1 were phosphorylated in NIH 3T3 cells in conjunction with FAK overexpression or in the presence of sodium orthovanadate.

To determine tyrosine phosphorylation of α-actinin-4, Cos-7 cells were transfected with either wildtype α-actinin-4 or α-actinin-1 (GFP-tagged) (lanes 2 and 3) and co-transfected with a FAK construct (HA tagged) (Figure 6.2, lanes 7-8). Cells were then treated with sodium orthovanadate (Figure 6.2, lanes 4-8). An anti-GFP antibody was used to immunoprecipitate α-actinin-4 or α-actinin-1 and the immunoblots were probed with an anti-GFP antibody (Figure 6.2A) or an anti-phosphotyrosine antibody (Figure 6.2B). Our data showed that neither α-actinin-4 nor α-actinin-1 were phosphorylated in Cos-7 cells, regardless of the overexpression of FAK, or the presence of sodium orthovanadate.

To illustrate the efficiency of the immunoprecipitation method to study phosphorylation of actinin-4, we transfected Cos-7 cells with HA tagged FAK (Figure 6.3). We then used an anti-HA antibody to immunoprecipitate FAK (Figure 6.3A) and

probed the immunoblots with an anti-phosphotyrosine antibody. We were able to detect autophosphorylation of FAK following immunoprecipitation (Figure 6.3B). Furthermore, cell lysates expressing wildtype or K256E α-actinin-4 were either left untreated, or treated with sodium orthovanadate to block tyrosine phosphatases (Figure 6.4). The blots were then probed with an anti-phosphotyrosine antibody. Our results indicate that treating the samples with sodium orthovanadate indeed inhibits the tyrosine phosphatases, as seen by the increased tyrosine phosphorylation of FAK, and that of the cell lysates. Thus, our conditions were suitable to determine phosphorylation of α-actinin-4.

These results clearly show that our experimental conditions, while able to promote total cellular tyrosine phosphorylation, including FAK autophosphorylation, were unable to achieve tyrosine phosphorylation of α-actinin-4 or α-actinin-1 in either NIH 3T3 or Cos-7 cells.

Figure 6.1 Tyrosine Phosphorylation of α-Actinin-4 in NIH-3T3 Cells

A – Cells were un-transfected (lane 1) and transfected with either α-actinin-1 or α-actinin-4 (lanes 2 and 3) and co-transfected with FAK (lanes 5 and 6). Cells were then treated with sodium orthovanadate (200μM) for 2 hrs and cell lysates were processed for immunoblotting using an anti-GFP antibody to verify transfection. **B** - Samples were subjected to immunoprecipitation and immunoblotting using an anti-GFP antibody. **C** - Samples were subjected to immunoprecipitation using the anti-GFP antibody and an anti phosphotyrosine antibody for immunoblotting. Blots are representative of three repeated experiments.

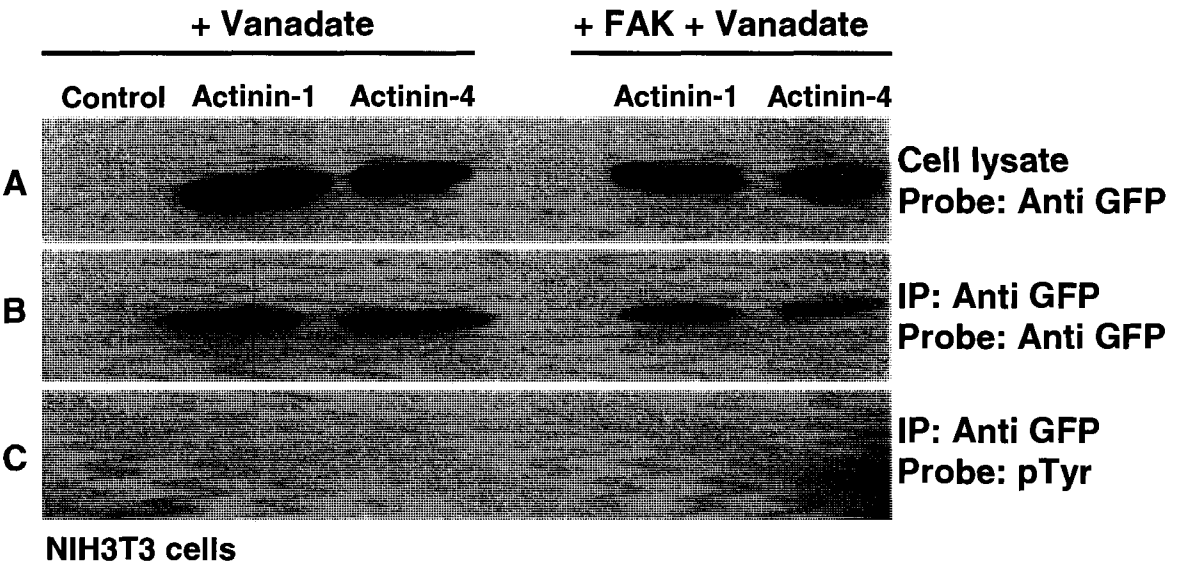
+ Vanadate
+ FAK + Vanadate
Control
Actinin-1
Actinin-4
Actinin-1
Actinin-4
A
Cell lysate
Probe: Anti GFP
B
IP: Anti GFP
Probe: Anti GFP
C
IP: Anti GFP
Probe: pTyr
NIH3T3 cells

Figure 6.2 Tyrosine Phosphorylation of α-Actinin-4 in Cos-7 Cells

Lanes 1-3 - Cells were either un-transfected or transfected with constructs overexpressing either α-actinin-1 or α-actinin-4. **Lanes 4-6 -** Cells were treated with sodium orthovanadate (200 μM) for 2 hrs. **Lanes 7-8 -** Cells were co-transfected with FAK and treated with sodium orthovanadate (200μM) for 2hrs. **A -** Samples were subjected to immunoprecipitation and immunoblotting using an anti-GFP antibody to verify immunoprecipitation. **B -** Samples were subjected to immunoprecipitation using an anti-GFP antibody and an anti-phosphotyrosine antibody for immunoblotting. Blots are representative of three repeated experiments.

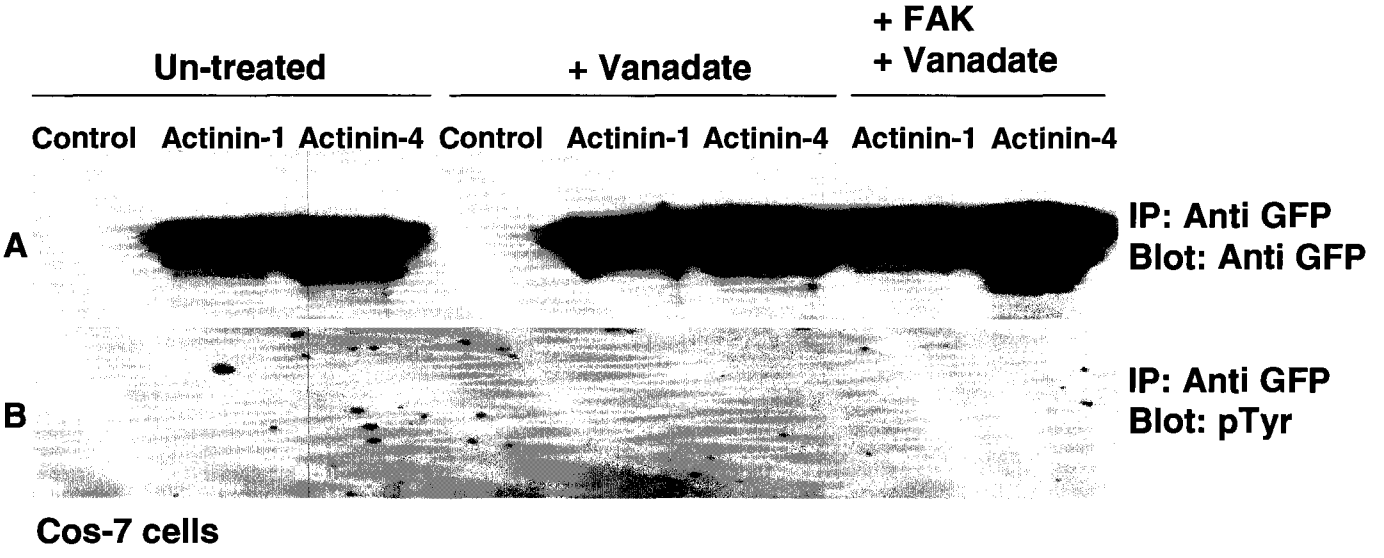
Un-treated
+ Vanadate
+ FAK
+ Vanadate
Control
Actinin-1
Actinin-4
Control
Actinin-1
Actinin-4
Actinin-1
Actinin-4
A
B
IP: Anti GFP
Blot: Anti GFP
IP: Anti GFP
Blot: pTyr
Cos-7 cells

Figure 6.3 Tyrosine Phosphorylation of FAK in Cos-7 Following Immunoprecipitation

Cells were either un-transfected (control) or transfected with FAK tagged with HA. **A –** Samples were subjected to immunoprecipitation and immunoblotting using an anti-HA antibody to verify immunoprecipitation. **B –** Samples were subjected to immunoprecipitation using an anti-HA antibody and an anti-phosphotyrosine antibody for immunoblotting. Blots are representative of two repeated experiments.

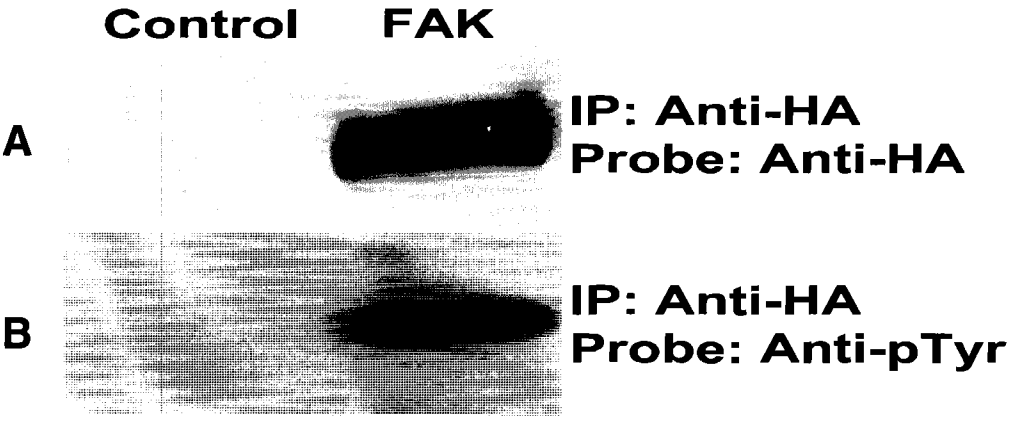
Control
FAK
A
IP: Anti-HA
Probe: Anti-HA
B
IP: Anti-HA
Probe: Anti-pTyr

Figure 6.4 Tyrosine Phosphorylation of Cos-7 Cell Lysates Promoted by Sodium Orthovanadate

Lanes 1-3 – Cos-7 cells were either un-transfected (control) or transfected with either wildtype or K256E α-actinin-4 without being treated with sodium orthovanadate. **Lanes4-6 –** Cells with no expression of α-actinin-4 (control) and cells overexpressing wildtype or K256E α-actinin-4 were treated with sodium orthovanadate (200 μM) for 2 hrs to verify the induction of tyrosine phosphorylation in Cos-7 cells due to inhibition of endogenous phosphatases. Blots are representative of two repeated experiments.

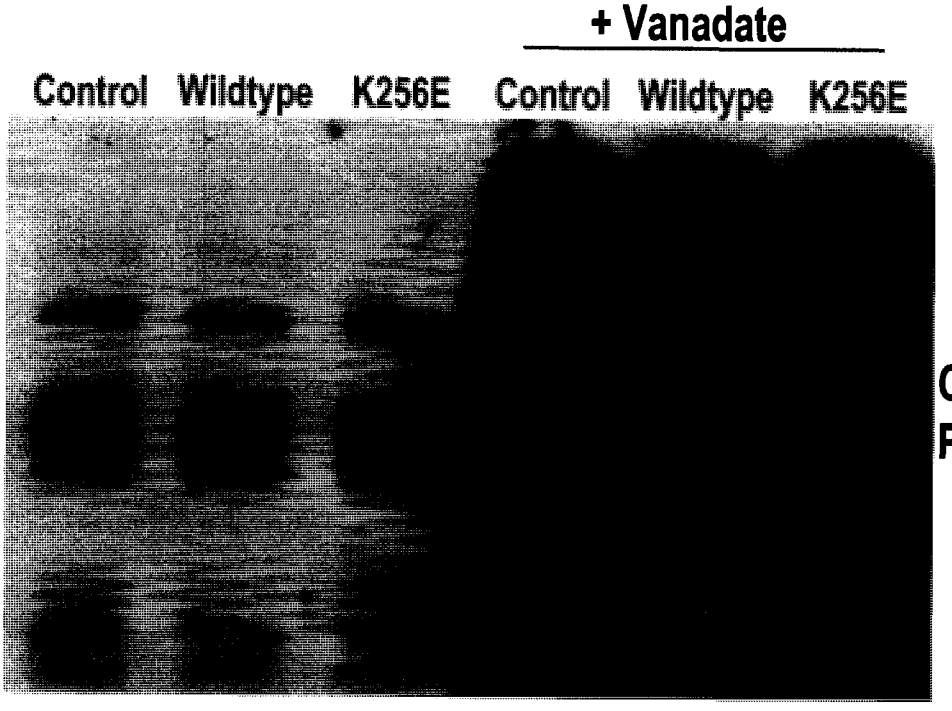
+ Vanadate
Control
Wildtype
K256E
Control
Wildtype
K256E
Cell lysate
Probe: Anti-pTyr

6.1.2 Influence of phosphorylation on Actin Affinity of Wildtype and K256E α-Actinin-4

Since we were unable to show direct tyrosine phosphorylation of α-actinin-4 we investigated whether other kinases within the cell may have an effect on the ability of α-actinin-4 to bind to F-actin indirectly.

To test whether the cellular tyrosine phosphorylation level regulates the affinity of α-actinin-4 for actin we performed an actin sedimentation assay using cell lysates from sodium orthovanadate-treated cells, in order to block tyrosine phosphatase activity within the cell.

Cos-7 cells were transfected with either HA-tagged wildtype or K256E α-actinin-4 and treated with sodium orthovanadate (200μM) for 2hrs. Lysates were processed to obtain Triton-X-100 soluble (containing unbound α-actinin-4, and non-crosslinked actin filaments) and Triton-X-100 insoluble fractions (containing α-actinin-4 crosslinked actin filaments/bundles). Immunoblots were probed with an HA-antibody to determine the proportion of α-actinin-4 in each pool after treatment with sodium orthovanadate (Figure 6.5). The data indicate that the distribution of wildtype and K256E α-actinin-4 in Triton X-100 fractions was not affected by elevating total cellular tyrosine phosphorylation levels, suggesting that the affinity of α-actinin-4 for F-actin may not be regulated by signaling pathways involving tyrosine kinases.

Figure 6.5 The Interaction of Wildtype and K256E α-Actinin-4 with The Actin Cytoskeleton Following Induction of Cellular Tyrosine Phosphorylation

A - Cos-7 cells were transfected with either wildtype or K256E α-actinin-4 without being treated with sodium orthovanadate. **B -** Cells were treated with sodium orthovanadate (200μM) for 2 hrs prior to obtaining triton X-100 soluble and insoluble fractions by centrifugation at 16,000 x *g*.
Lys: Cell lysate. **TI:** Triton insoluble fraction. **TS:P:** Triton soluble pellet. **TS:S:** Triton soluble supernatant. Blots are representative of one experiment.

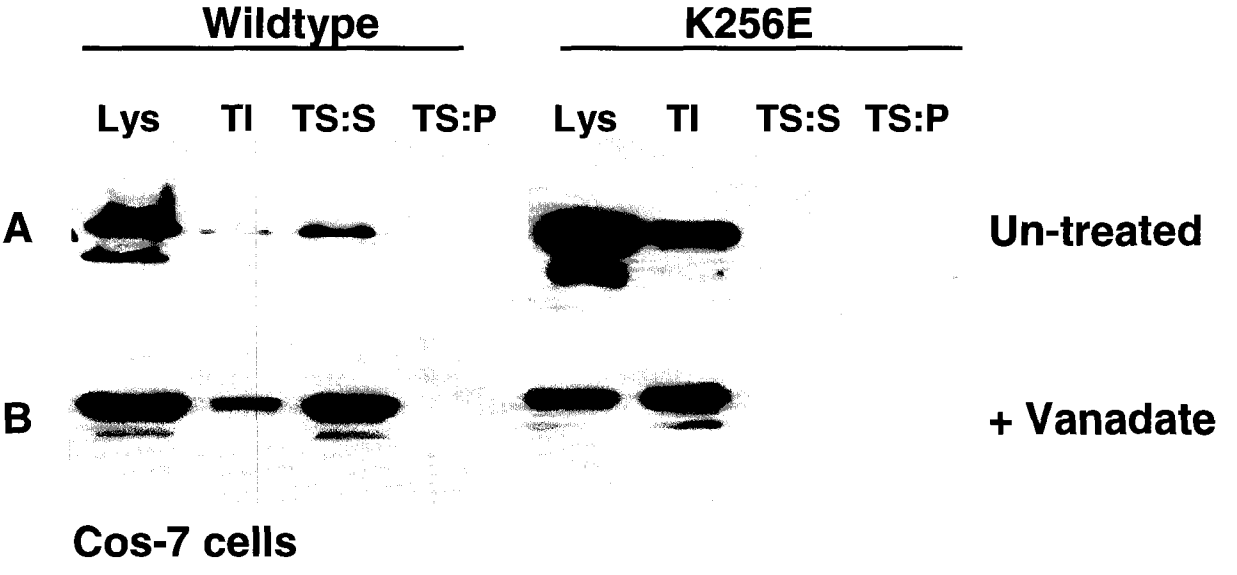
Wildtype
K256E
Lys
TI
TS:S
TS:P
Lys
TI
TS:S
TS:P
A
Un-treated
B
+ Vanadate
Cos-7 cells

6.2 INTERACTION AND CO-LOCALIZATION OF α-ACTININ-4 WITH BINDING PARTNERS

6.2.1 Interaction and Co-localization of α-Actinin-4 with β-Catenin in Podocytes

β-Catenin is an adherens junction protein with multifunctional properties and its interaction with different binding partners determines its role and subcellular localization [42, 77]. Although β-catenin is expressed in podocytes, its role in podocyte biology and injury is unclear. However, it likely acts as an adaptor between P-cadherin and actin filaments at the slit diaphragm in vivo.

Recent studies showed that α-actinin-4 is able to associate with β-catenin in cancer cells [52]. In that study, the authors showed that this interaction regulates binding of β-catenin with E-cadherin. We investigated the interaction of α-actinin-4 with β-catenin in podocytes and since K256E exhibits increased affinity for actin and an altered subcellular distribution. We therefore postulated that such mutations may challenge its ability to associate with β-catenin at the cell periphery.

To investigate the interaction of wildtype and K256E α-actinin-4 with β-catenin, podocytes were infected with adenovirus to overexpress either wildtype or K256E α-actinin-4 tagged with HA and cell lysates were immunoprecipitated using an anti-β-catenin antibody (Figure 6.6). The immunoblots were then probed with either an anti-HA antibody (Figure 6.6A) or an anti-β-catenin antibody (Figure 6.6B). Similar amounts of β-catenin were immunoprecipitated from each sample (Figure 6.6B) and an equal amount of α-actinin-4 was expressed within each cell lysate (Figure 6.6C). In contrast to wildtype, K256E α-actinin-4 exhibited minimal interaction with β-catenin (Figure 6.6A)

as confirmed by densitometric quantification (by 2.5 fold; Figure 6.6D). Results were normalized to total protein content of cell lysates ($n=3$, $p<0.01$).

For co-localization of wildtype and K256E α-actinin-4 with β-catenin, podocytes were infected with adenoviral constructs encoding HA-tagged wildtype or K256E α-actinin-4. Localization was determined by immunofluorescence using an anti-β-catenin and an anti-HA antibody (Figure 6.7). Wildtype α-actinin-4 co-localized with β-catenin at the cell periphery. Conversely, K256E α-actinin-4 associated predominantly along stress fibers and failed to associate with β-catenin at the cell periphery. However, our results also showed that intracellular localization of β-catenin was not altered in cells expressing either wildtype or K256E α-actinin-4.

These phenotypes indicate that the K256E mutation in α-actinin-4 diminishes the interaction of α-actinin-4 with β-catenin while not affecting the intracellular localization of β-catenin. Thus the subcellular localization of β-catenin is independent of its interaction with α-actinin-4. However, we cannot preclude whether the loss of a link to the actin cytoskeleton affects the function of β-catenin in K256E α-actinin-4 expressing podocytes.

Figure 6.6 Interaction of β-Catenin and α-Actinin-4 in Podocytes

β-catenin was immunoprecipitated from the podocyte lysates using an anti-β-catenin antibody and blots probed with either anti-HA or anti-β-catenin antibody (blots are representative of three repeated experiments). **A** - In contrast to wildtype, K256E α-actinin-4 exhibits minimal interaction with β-catenin. **B** - Similar amounts of β-catenin were immunoprecipitated from each sample. **C** - Equal expression of α-actinin-4 was detected within each cell lysate. **D** - Densitometric quantification representing the three repeated experiments shows that there was significantly less K256E α-actinin-4 immunoprecipitated with β-catenin. Results were adjusted for total HA-tagged protein content of the cell lysate and normalized to mutant
(n=3, **P<0.01).

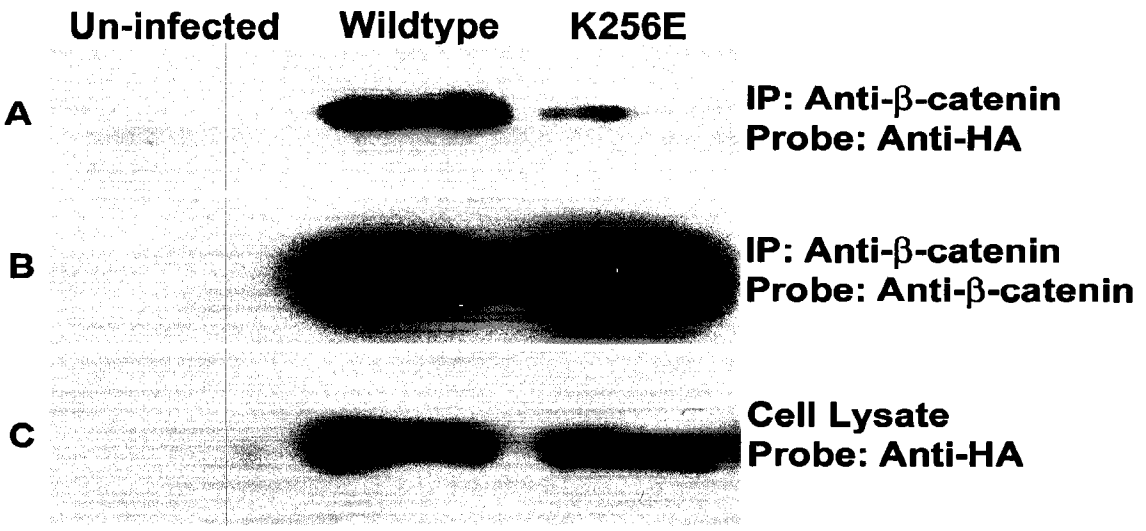
Un-infected
Wildtype
K256E
A
IP: Anti-β-catenin
Probe: Anti-HA
B
IP: Anti-β-catenin
Probe: Anti-β-catenin
C
Cell Lysate
Probe: Anti-HA

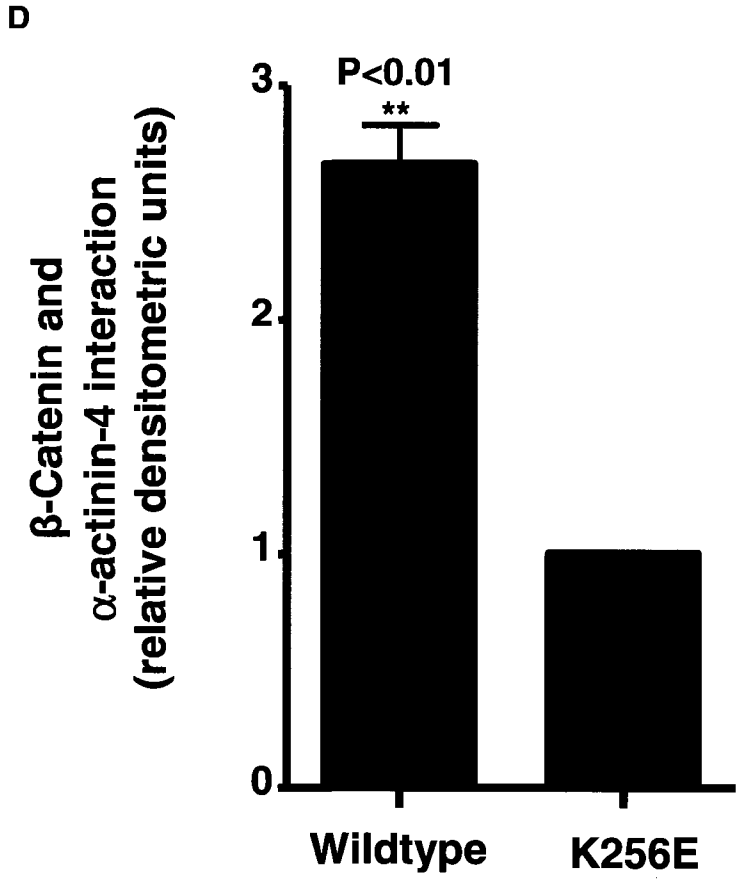
D
β-Catenin and
α-actinin-4 interaction
(relative densitometric units)
P<0.01
**
3
2
1
0
Wildtype
K256E

Figure 6.7 Co-localization of α-Actinin-4 with β-Catenin in Podocytes

Podocytes were infected with adenoviral constructs encoding either wildtype or K256E α-actinin-4 tagged with HA. Localization was determined by immunofluorescence using an anti-β-catenin (2° antibody conjugated to Alexa Fluor 555) and an anti-HA (2° antibody conjugated to Alexa Fluor 488) antibody (Images are representative of three repeated experiments). Wildtype α-actinin-4 co-localizes with β-catenin at the cell periphery (arrowheads). Conversely, K256E α-actinin-4 associates predominantly with stress fibers and not with β-catenin at the cell periphery (arrowheads).

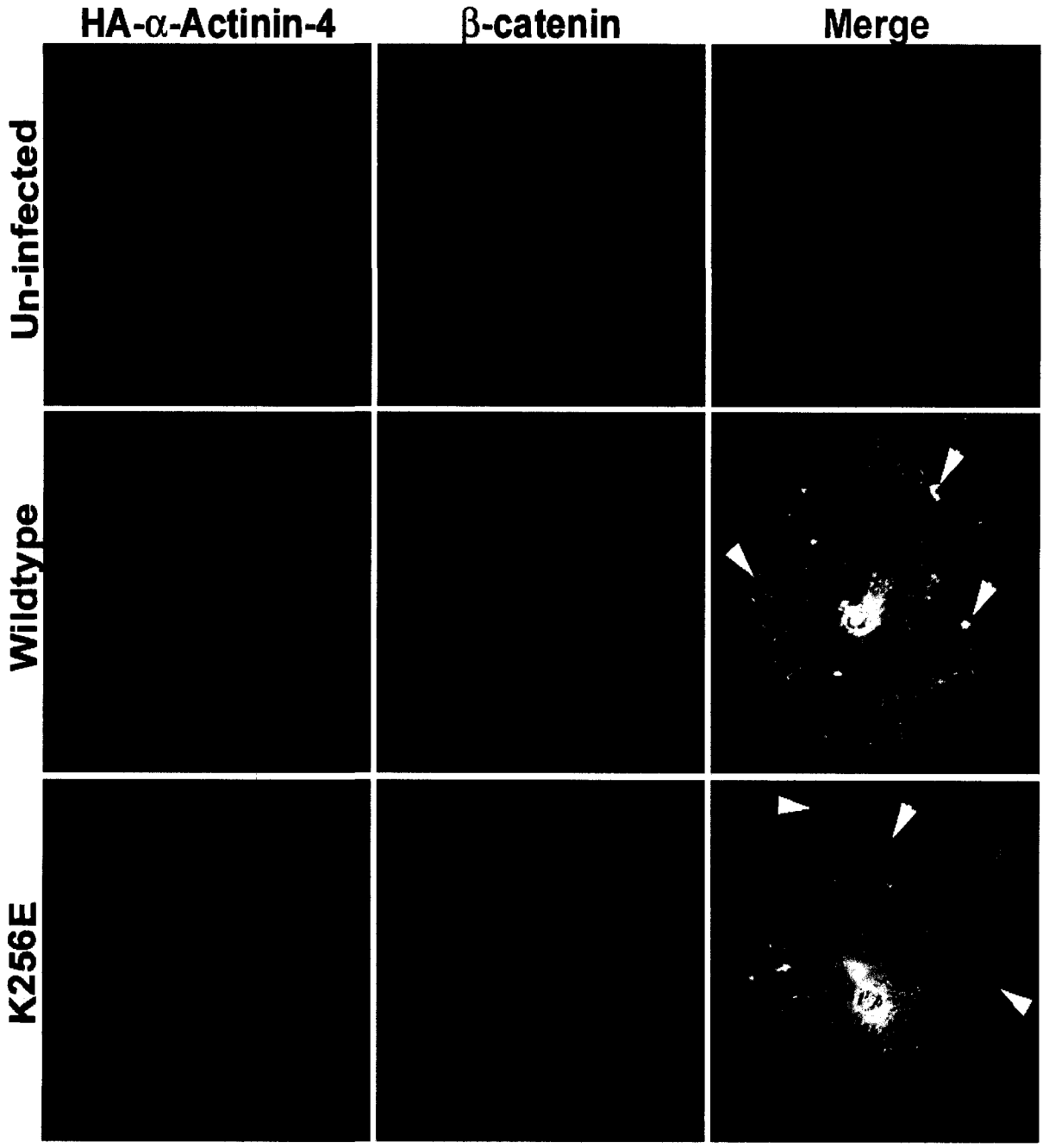
HA-α-Actinin-4
β-catenin
Merge
Un-infected
Wildtype
K256E

6.2.2 Interaction and Co-localization of α-Actinin-4 with Synaptopodin in Podocytes

Synaptopodin plays a role in actin-based cell shape and motility since it is an actin-associated protein in postsynaptic densities and podocytes [44], hence the name synapto-pod-in. Asanuma and colleagues demonstrated that the interaction of synaptopodin with α-actinin-4 promotes actin filament elongation [47]. However, the interaction of K256E α-actinin-4 with synaptopodin has not been investigated. Since K256E α-actinin-4 is strongly associated with actin filaments, we hypothesized that K256E α-actinin-4 would exhibit greater interaction with synaptopodin than wildtype α-actinin-4.

To investigate the interaction of wildtype and K256E α-actinin-4 with synaptopodin, an anti-GFP antibody was used to immunoprecipitate either wildtype or K256E α-actinin-4 tagged with GFP in podocytes. The immunoblots were probed with an anti-synaptopodin antibody (Figure 6.8A). Similar amounts of α-actinin-4 were immunoprecipitated from each sample (Figure 6.8B). Both wildtype and K256E α-actinin-4 interacted similarly with synaptopodin (Figure 6.8A). Densitometric quantification confirmed that there were no significant differences between the association of synaptopodin with either wildtype or K256E α-actinin-4 (Figure 6.8C).

For co-localization of wildtype and K256E α-actinin-4 with synaptopodin, podocytes were infected using adenoviral constructs encoding either wildtype or K256E α-actinin-4 tagged with GFP. Localization was determined by direct visualization of GFP fluorescence and by immunofluorescence using an anti-synaptopodin antibody (Figure 6.9). Wildtype α-actinin-4 co-localized with synaptopodin along stress fibers and

additionally, synaptopodin displayed a diffuse distribution within the cytoplasm. In contrast, synaptopodin expression along stress fibers is reduced in podocytes expressing K256E α-actinin-4.

Figure 6.8 Interaction of Synaptopodin and α-Actinin-4 in Podocytes

α-Actinin-4 was immunoprecipitated using an anti-GFP antibody and blots probed with either anti-synaptopodin or anti-GFP antibodies (blots are representative of three repeated experiments). **A** - Wildtype and K256E α-actinin-4 interact similarly with synaptopodin. **B** - Similar amounts of α-actinin-4 were immunoprecipitated from each cell lysate sample. **C** - Densitometric quantification representing the three repeated experiments shows no significant difference between association of synaptopodin with wildtype and K256E α-actinin-4. Results were adjusted for total protein content of cell lysate and normalized to mutant (n=3).

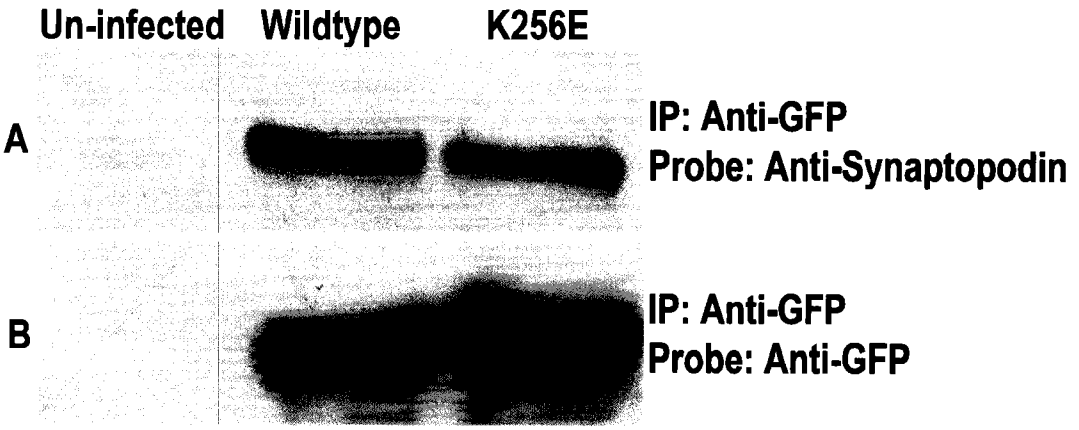
Un-infected
Wildtype
K256E
A
IP: Anti-GFP
Probe: Anti-Synaptopodin
B
IP: Anti-GFP
Probe: Anti-GFP

C

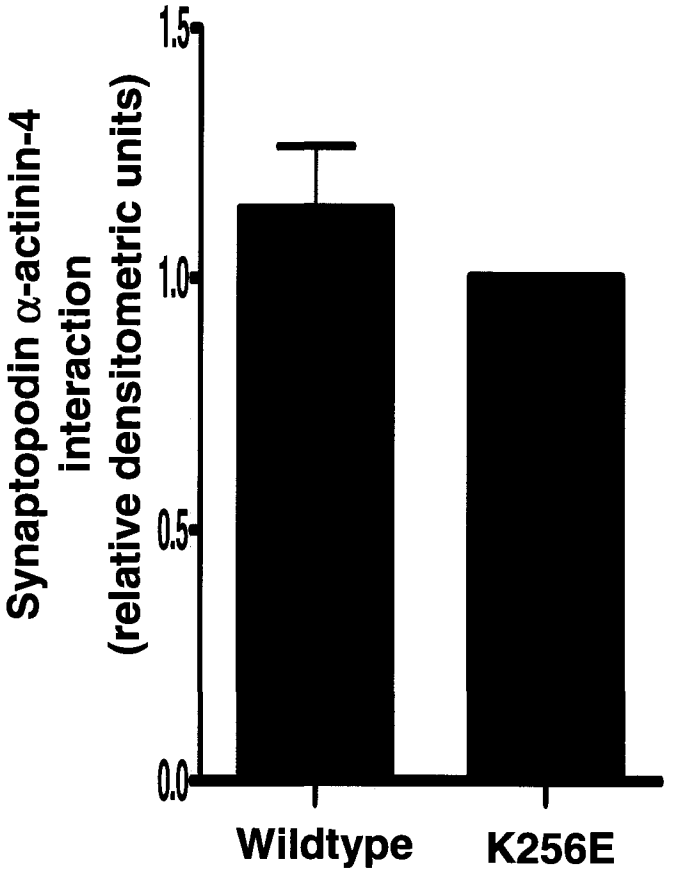
Synaptopodin α-actinin-4 interaction (relative densitometric units)
1.5
1.0
0.5
0.0
Wildtype
K256E

Figure 6.9 Co-localization of α-Actinin-4 with Synaptopodin in Podocytes

Podocytes were infected with adenoviral constructs encoding either wildtype or K256E α-actinin-4 tagged with GFP. Localization was determined by direct visualization of GFP fluorescence and by immunofluorescence using an anti-synaptopodin antibody (2° antibody conjugated to Alexa Fluor 594) (Images are representative of three repeated experiments). Wildtype α-actinin-4 co-localizes with synaptopodin along stress fibers. In these cells synaptopodin exhibits a diffuse distribution. In contrast, podocytes over-expressing K256E α-actinin-4 appear to express lower level of synaptopodin along stress fibers.

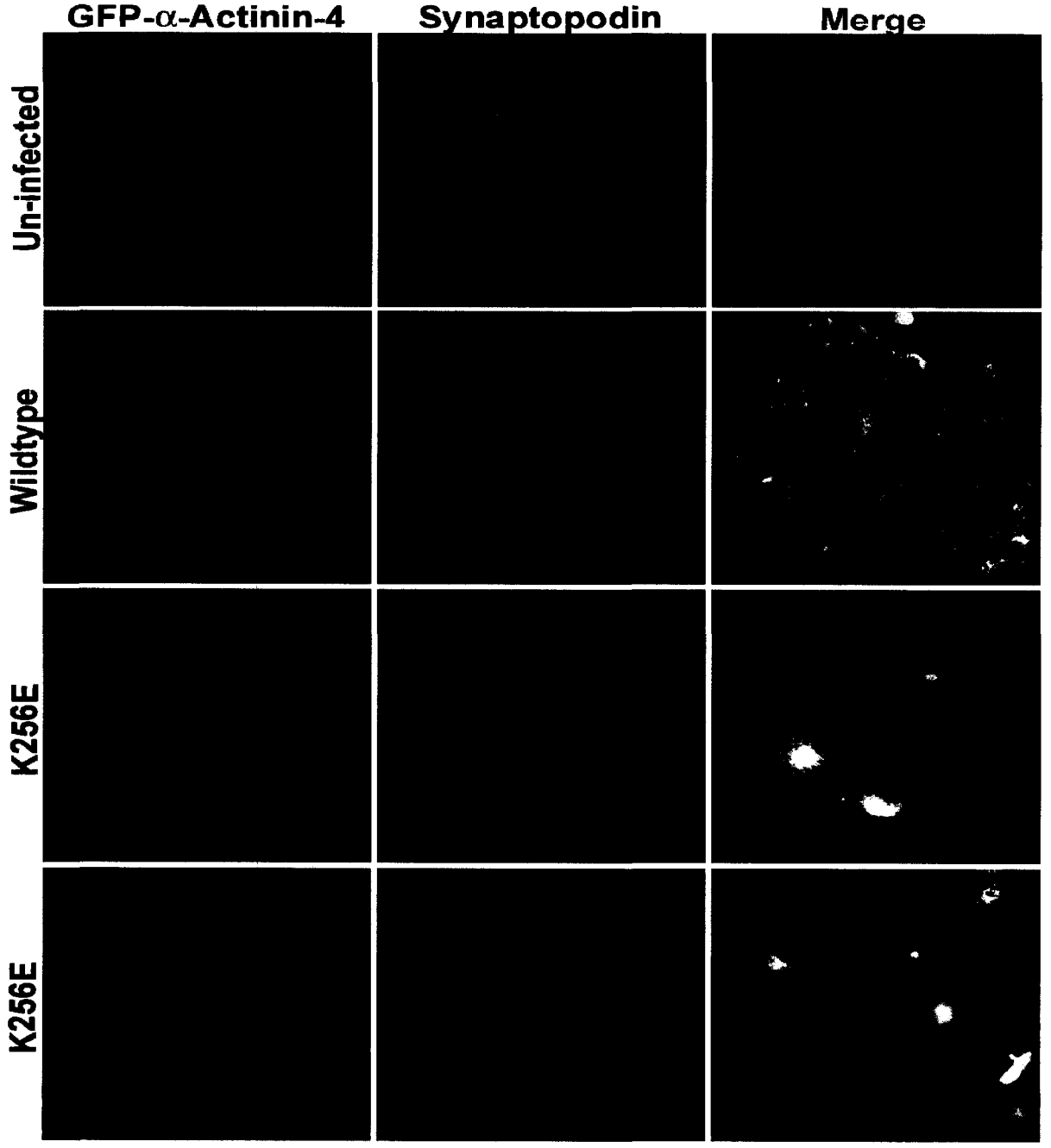
GFP-α-Actinin-4
Synaptopodin
Merge
Un-infected
Wildtype
K256E
K256E

6.2.3 Interaction and Co-localization of α-Actinin-4 with MAGI-1 in Podocytes

MAGI-1, a tight junction protein, plays a role as a non-F-actin binding molecular scaffold, facilitating the assembly of multiprotein complexes on the inner surface of the plasma membrane [78, 79]. In podocytes, MAGI-1 interacts with various proteins including nephrin [52, 80], suggesting that it may participate in the ordering of the slit diaphragm. Other studies showed that MAGI-1 links to the actin cytoskeleton via the two actin bundling proteins, synaptopodin and α-actinin-4 [51]. Since K256E α-actinin-4 exhibits abnormal intracellular localization due to its high affinity for actin we investigated the interaction of this mutant form of α-actinin-4 with MAGI-1 as compared to wildtype α-actinin-4.

To investigate the interaction of α-actinin-4 with MAGI-1, an anti-GFP antibody was used to immunoprecipitate wildtype and K256E α-actinin-4 tagged with GFP in podocytes and the immunoblots were probed with an anti-MAGI-1 antibody (Figure 6.10A). Similar amounts of α-actinin-4 were immunoprecipitated from each sample (Figure 6.10B). Our results show that both wildtype and K256E α-actinin-4 interact similarly with MAGI-1.

To study co-localization of wildtype and K256E α-actinin-4 with MAGI-1, podocytes were infected with adenoviral constructs encoding either wildtype or K256E α-actinin-4 tagged with GFP. Samples were then subjected to immunofluorescence and localization was determined by direct visualization of GFP fluorescence and by using indirect immunofluorescence with an anti-MAGI-1 antibody (Figure 6.11). Our findings indicate that MAGI-1 localizes at the cell periphery, along stress fibers, and in the

nucleus. Wildtype α-actinin-4 co-localizes with MAGI-1 at the cell periphery and along stress fibers while K256E α-actinin-4 co-localizes with MAGI-1 predominantly along stress fibers. Furthermore, our results show that intracellular localization of MAGI-1 is not altered in podocytes expressing either wildtype or K256E α-actinin-4. Thus, interaction of α-actinin-4 with MAGI-1 has no influence over intracellular localization of MAGI-1.

Figure 6.10 Interaction of MAGI-1 and α-Actinin-4 in Podocytes

α-Actinin-4 was immunoprecipitated using an anti-GFP antibody and blots probed with either an anti-MAGI-1 or an anti-GFP antibody (blots are representative of two repeated experiments). **A -** Wildtype and K256E α-actinin-4 interact similarly with MAGI-1. **B -** Similar amounts of α-actinin-4 were immunoprecipitated from each cell lysate sample.

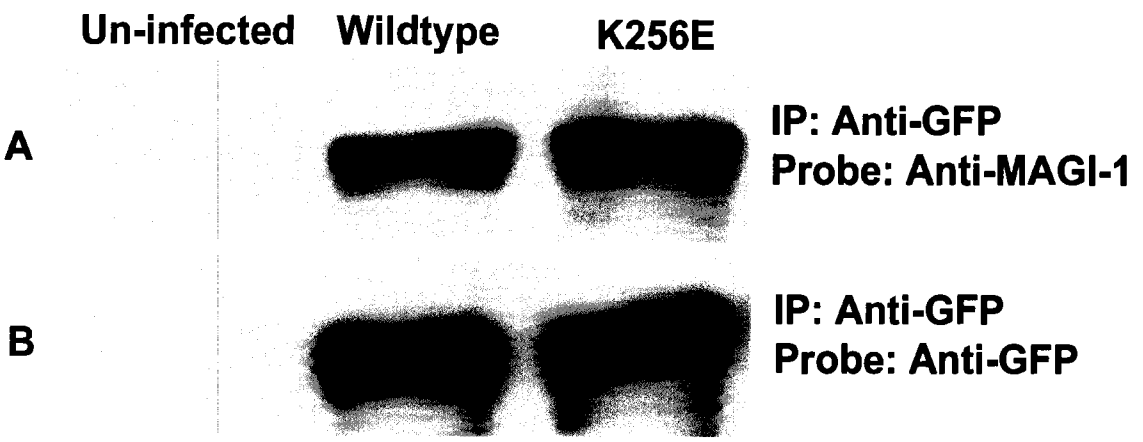
Un-infected
Wildtype
K256E
A
IP: Anti-GFP
Probe: Anti-MAGI-1
B
IP: Anti-GFP
Probe: Anti-GFP

Figure 6.11 Co-localization of α-Actinin-4 with MAGI-1 in Podocytes

Podocytes were infected with adenoviral constructs encoding either wildtype or K256E α-actinin-4 tagged with GFP. Localization was determined by direct visualization of GFP fluorescence and by immunofluorescence using an anti-MAGI-1 antibody (2° antibody conjugated to Alexa Fluor 555) (Images are representative of three repeated experiments.). MAGI-1 tends to localize around cell periphery, stress fibers and in the nucleus (arrowheads). Wildtype α-actinin-4 co-localizes with MAGI-1 along stress fibers and cell periphery (arrowheads). In contrast, K256E α-actinin-4 co-localizes with MAGI-1 along stress fibers (arrowhead).

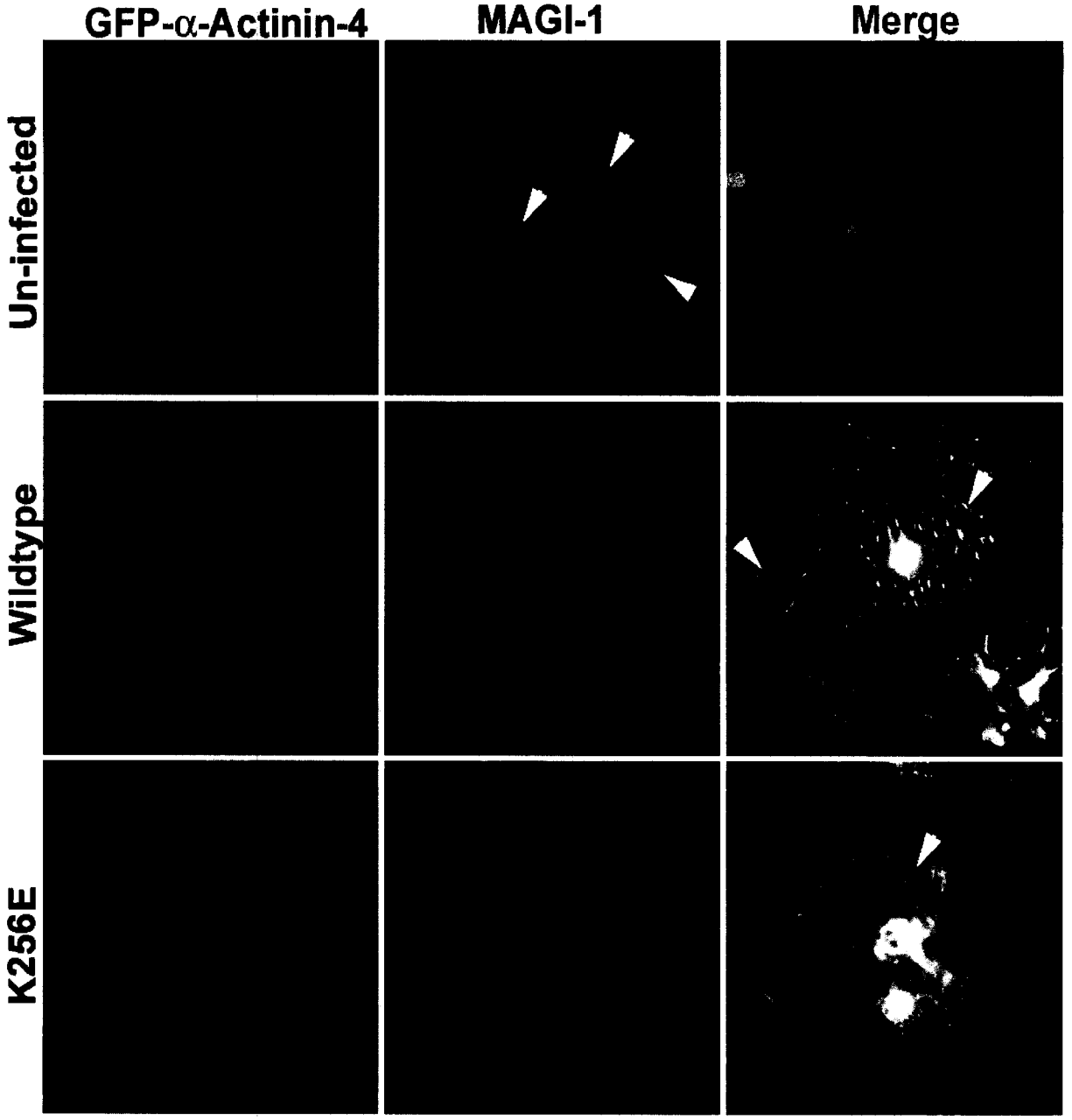
GFP-α-Actinin-4
MAGI-1
Merge
Un-infected
Wildtype
K256E

6.2.4 Interaction and Co-localization of α-Actinin-4 with Vinculin in Cos-7 and Podocyte Cells

Vinculin is a cytoskeletal focal adhesion protein that plays a role in cell adhesion, spreading and lamellipodia extension by interacting with other focal adhesion proteins [55-57]. Early studies by Belkin and Koteliansky showed that vinculin interacts with α-actinin-1 at focal adhesions [58]; however, the role of this interaction was not investigated. Cells deficient in vinculin exhibit impairment in cell adhesion, spreading, and display formation of fewer focal adhesions, and impairment of lamellipodia formation [55-57]. Since our lab has shown that podocytes expressing K256E α-actinin-4 also exhibit impairment in cell spreading, and formation of peripheral projections (similar to foot processes in vivo) [3], we investigated the interaction between vinculin and α-actinin-4, and whether such an association is disrupted by the K256E mutation.

To investigate the interaction of wildtype and K256E α-actinin-4 with vinculin, an anti-GFP antibody was used to immunoprecipitate wildtype and K256E α-actinin-4 tagged with GFP in either Cos-7 (Figure 6.12) or podocytes (Figure 6.13). The immunoblots were probed with an anti-vinculin antibody (Figure 6.12A and Figure 6.13A). Similar amounts of α-actinin-4 were immunoprecipitated from each sample (Figure 6.12B and Figure 6.13B) and similar amounts of endogenous vinculin could be detected within Cos-7 cell lysates irrespective of the expression of wildtype or K256E α-actinin-4 (Figure 6.12C). However, under the experimental conditions employed, we were unable to demonstrate association of either wildtype or K256E α-actinin-4 with vinculin by immunoprecipitation in Cos-7 cells or in podocytes (Figure 6.12A and Figure 6.13A respectively).

To study co-localization of wildtype and K256E α-actinin-4 with vinculin, podocytes were infected using adenoviral constructs encoding wildtype or K256E α-actinin-4 tagged with GFP. Localization was determined by direct visualization of GFP fluorescence and by indirect immunofluorescence using an anti-vinculin antibody (Figure 6.14). Our results show that wildtype α-actinin-4 co-localizes with vinculin at focal contacts. In contrast, while K256E α-actinin-4 associated strongly with stress fibers it mostly co-localizes with vinculin at mature focal adhesions while being absent from more newly formed focal contacts.

Figure 6.12 Interaction of Vinculin and α-Actinin-4 in Cos-7 Cells

A - α-actinin-4 was immunoprecipitated from un-transfected (control) and transfected cells using an anti-GFP antibody and blots were probed with an anti-vinculin antibody. These data show no association of wildtype and K256E α-actinin-4 with vinculin. **B -** Samples were subjected to immunoprecipitation and immunoblotting using the anti-GFP antibody to show similar amounts of α-actinin-4 were immunoprecipitated from each cell lysate. **C -** Similar amounts of endogenous vinculin are present within each cell lysate. Blots are representative of two repeated experiments.

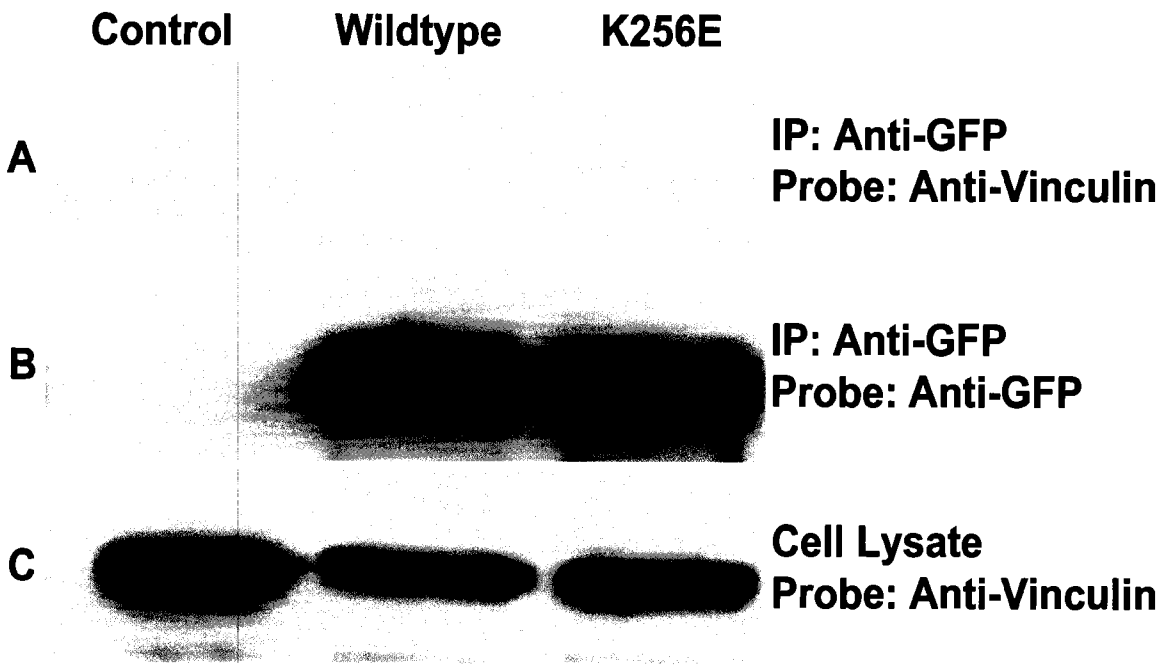
Control
Wildtype
K256E
A
IP: Anti-GFP
Probe: Anti-Vinculin
B
IP: Anti-GFP
Probe: Anti-GFP
C
Cell Lysate
Probe: Anti-Vinculin

Figure 6.13 Interaction of Vinculin and α-Actinin-4 in Podocytes

A - α-actinin-4 was immunoprecipitated using an anti-GFP antibody and blots were probed with an anti-vinculin antibody. These data show no association of wildtype and K256E α-actinin-4 with vinculin**. B -** Samples were subjected to immunoprecipitation and immunoblotting using an anti-GFP antibody to demonstrate similar amounts of α-actinin-4 immunoprecipitated from each cell lysate. Blots are representative of two repeated experiments.

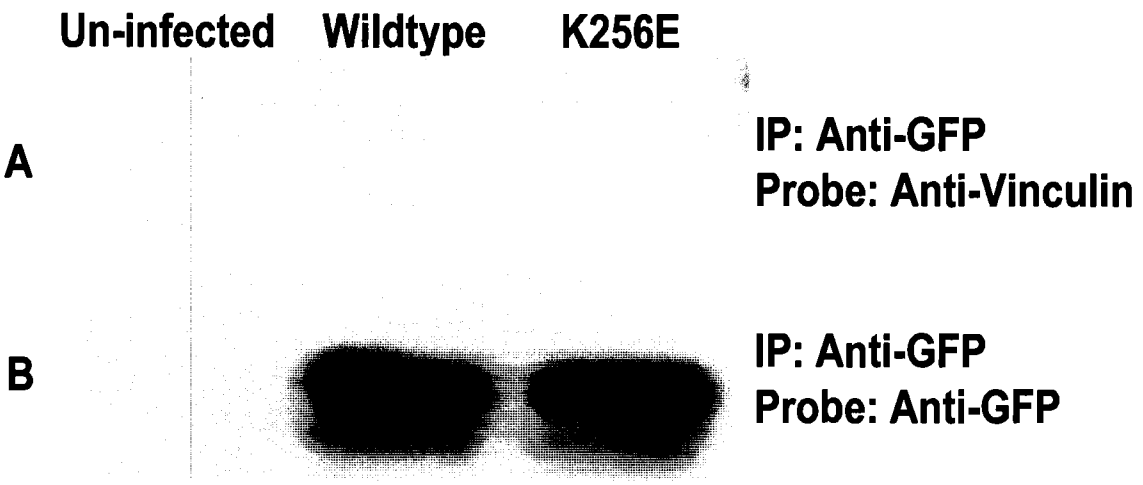
Un-infected
Wildtype
K256E
A
IP: Anti-GFP
Probe: Anti-Vinculin
B
IP: Anti-GFP
Probe: Anti-GFP

Figure 6.14 Co-localization of α-Actinin-4 with Vinculin in Podocytes

Podocytes were infected with adenoviral constructs encoding either wildtype or K256E α-actinin-4 tagged with GFP. Localization was determined by direct visualization of GFP fluorescence and by immunofluorescence using an anti-vinculin antibody (2° antibody conjugated to Alexa Fluor 594) (Images are representative of three repeated experiments). Wildtype α-actinin-4 co-localizes with vinculin at newly formed focal contacts (arrowheads). In contrast, K256E α-actinin-4 co-localizes with vinculin at mature focal adhesions (arrowheads).

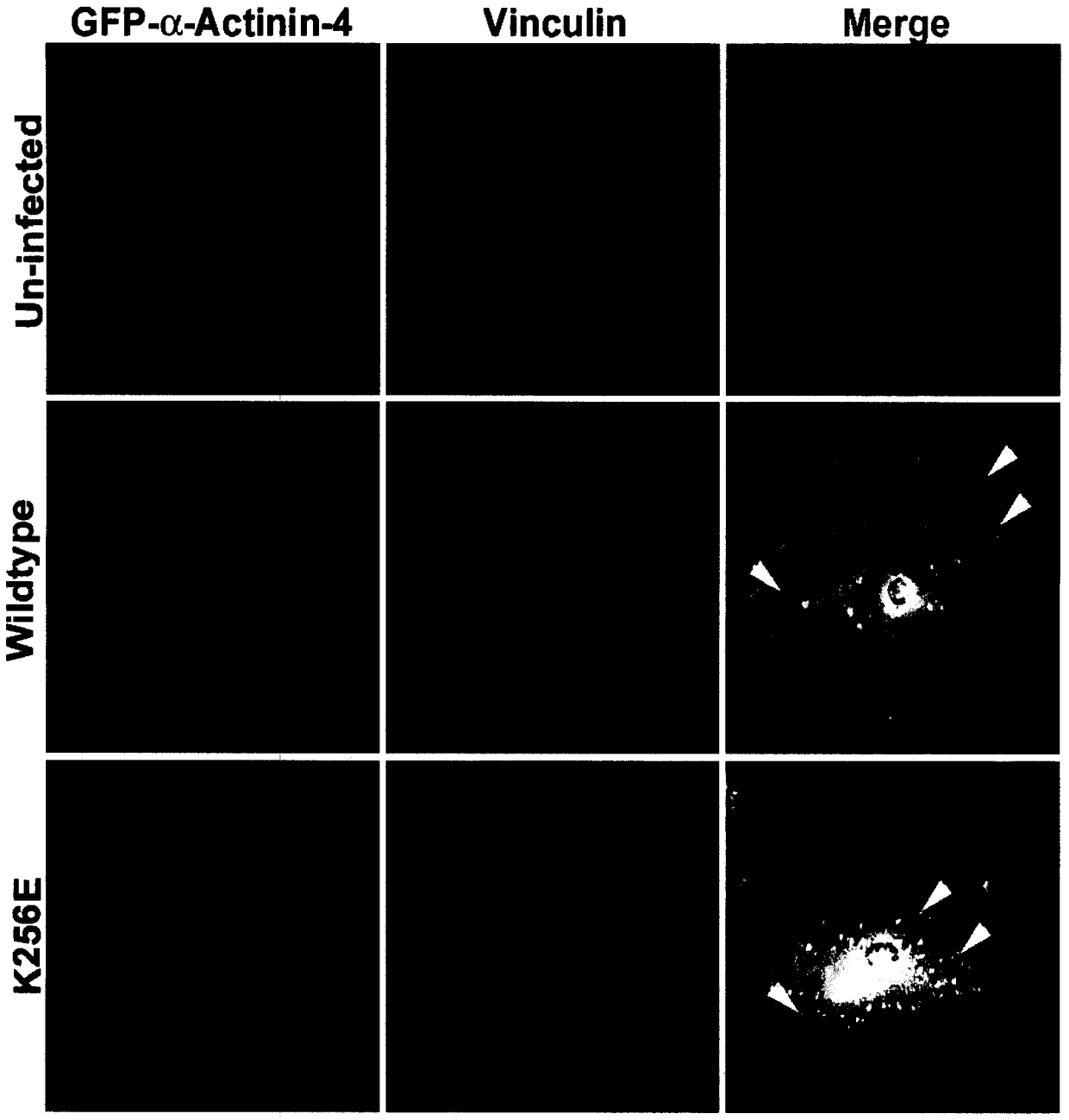
GFP-α-Actinin-4
Vinculin
Merge
Un-infected
Wildtype
K256E

6.2.5 Akt Phosphorylation Within Podocytes Overexpressing Wildtype and K256E α-Actinin-4

Akt plays a critical role in controlling the balance between survival and apoptosis. This protein is activated by various growth and survival factors involving PI3-kinase [60]. Upon phosphorylation, Akt inhibits apoptosis by inactivating several proteins involved in cell death [81-83]. In podocytes Akt is stimulated by PI3-kinase via the association of two important proteins of the slit diaphragm, nephrin and CD2AP [9].

A recent study showed that α-actinin-4 can interact with Akt. Interestingly, siRNA-mediated ACTN4 silencing down-regulated Akt phosphorylation by blocking Akt translocation to the membrane in hOSE cells [69]. Such inhibition of Akt phosphorylation could result in inhibition of cell proliferation and survival. Since the K256E α-actinin-4 is reluctant to dissociate from actin filaments, we hypothesized that it may not be able to facilitate Akt translocation and phosphorylation and thereby dysregulate cell survival pathways in podocytes.

To investigate the levels Akt phosphorylation in podocytes, cells were infected with adenoviral constructs encoding either wildtype or K256E α-actinin-4 tagged with HA. The immunoblots were probed with an anti-phospho-Akt (Ser473) antibody (Figure 6.15A) or an anti-total Akt antibody (Figure 6.15B). Densitometric quantification of immunoblots revealed that baseline Akt phosphorylation and total Akt expression are unchanged within podocytes expressing either wildtype or K256E α-actinin-4. Furthermore, podocytes serum starved for 2 hours and treated with 10% FBS for 30 minutes prior to cell lysis exhibited significant Akt phosphorylation (Figure 6.16A). The immunoblots were probed with an anti-total Akt antibody (Figure 6.16B) or an anti-HA

antibody to verify transfection efficiency (Figure 6.16C). However, no differences in serum-induced Akt phosphorylation were detected in podocytes expressing either K256E or wildtype α-actinin-4 (Figure 6.16A).

Figure 6.15 Akt Phosphorylation in Podocytes Overexpressing Wildtype or K256E α-Actinin-4

Podocyte cells were infected with adenoviral constructs encoding either wildtype or K256E α-actinin-4 tagged with HA (blots are representative of three repeated experiments.). **A –** Immunoblots were probed with an anti-phospho-Akt antibody and an anti-total Akt antibody (the ultra-sensitive Pierce SuperSignal Femto kit was required to detect baseline phospho-Akt levels) **(B). C -** Densitometric quantification representing the three repeated experiments adjusted for total Akt expression (normalized to mutant) shows no significant difference in the levels of Akt phosphorylation within podocytes expressing either wildtype or K256E α-actinin-4 (n=3).

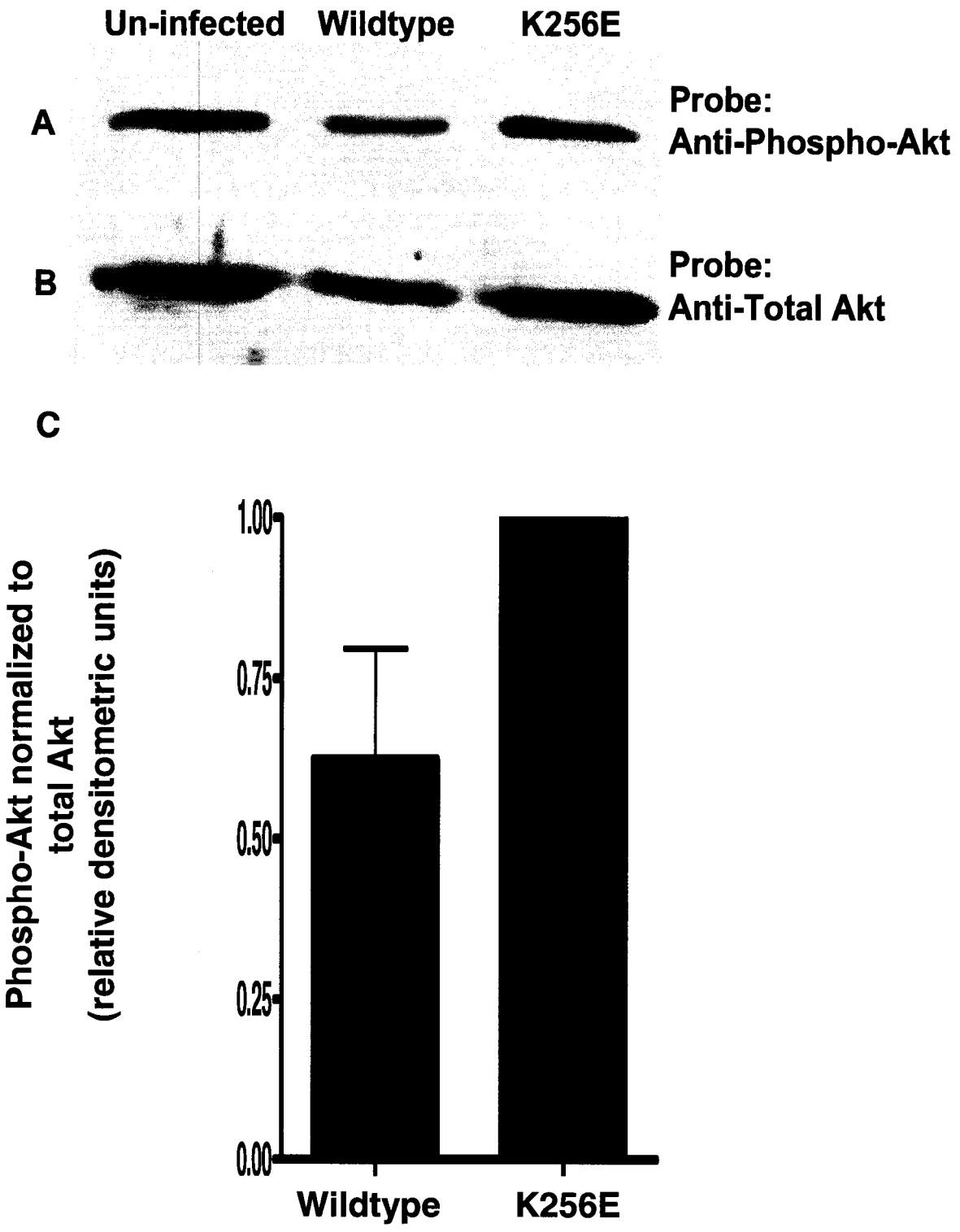
Un-infected
Wildtype
K256E
A
Probe:
Anti-Phospho-Akt
B
Probe:
Anti-Total Akt
C
Phospho-Akt normalized to total Akt (relative densitometric units)
1.00
0.75
0.50
0.25
0.00
Wildtype
K256E

Figure 6.16 Akt Phosphorylation in Serum-Stimulated Podocytes

Podocyte cells were either un-infected or infected with adenoviral constructs encoding wildtype or K256E α-actinin-4 tagged with HA. Cells were then serum starved for 2 hrs and treated with 10% FBS for 30 minutes prior to lysis. **A –** Immunoblots were then probed with an anti-phospho-Akt antibody or an anti-total Akt antibody **(B). C -** Equal expression of α-actinin-4 was detected within each cell lysate. Blots are representative of two repeated experiments.

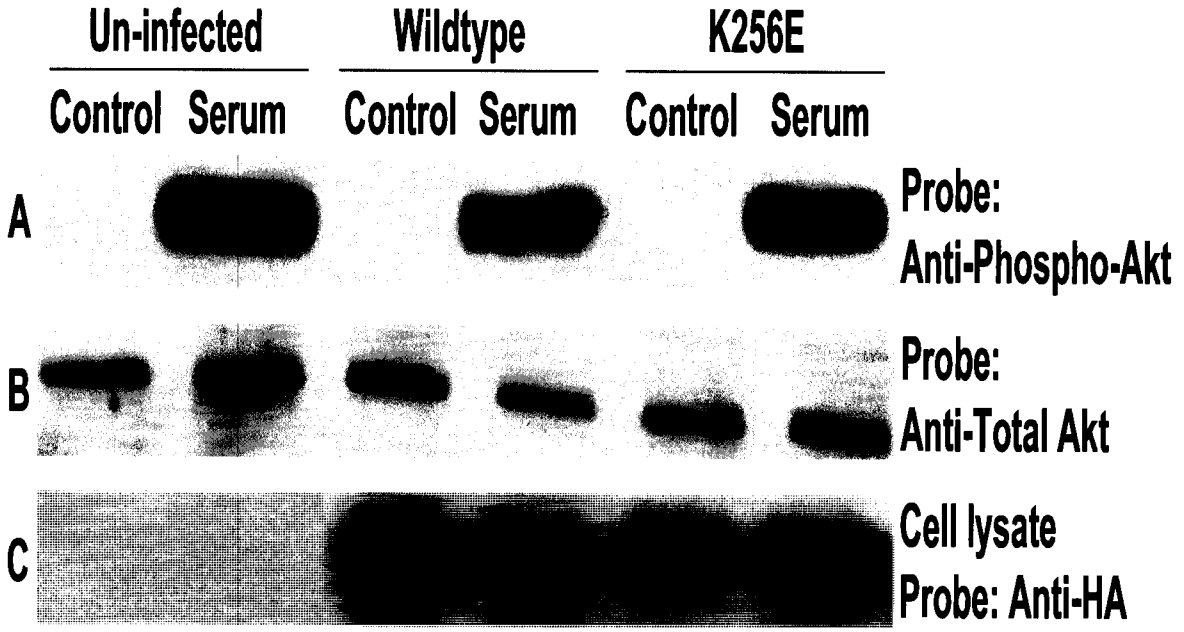
Un-infected
Wildtype
K256E
Control Serum
Control Serum
Control Serum
A
Probe:
Anti-Phospho-Akt
B
Probe:
Anti-Total Akt
C
Cell lysate
Probe: Anti-HA

6.3 MORPHOLOGICAL CHANGES OF PODOCYTES EXPRESSING WILDTYPE AND K256E α-ACTININ-4 IN RESPONSE TO MECHANICAL STRETCH

6.3.1 Co-localization of α-Actinin-4 and The Actin Cytoskeleton During Mechanical Stretch

Increased glomerular capillary pressure, which includes hydrostatic and oncotic pressures, contributes towards glomerulosclerosis in FSGS [84]. When the intraglomerular pressure is increased it causes stress-tension and stretch of glomerular cells, including podocytes [85]. These cells respond and adapt to applied mechanical forces by remodeling their actin cytoskeleton. Since the FSGS-associated mutation in α-actinin-4 increases its affinity for actin filaments, we hypothesized that the remodeling of the actin cytoskeleton would be impaired in podocytes expressing K256E α-actinin-4 and this would compromise their architectural integrity.

To test our hypothesis, podocytes were cultured on collagen-I coated silicone membranes and an equibiaxial mechanical stretch was applied to mimic the glomerular capillary pressure in vivo. Cells were infected with adenoviral constructs encoding either GFP-tagged wildtype or K256E α-actinin-4 (Figure 6.17). A Flexercell Tension Plus – FX-4000T system was employed to deliver equibiaxial cyclic stress (0.5 Hz and 10% linear strain) over the time course of 1 to 24 hours. Using phalloidin-FITC, co-localization of wildtype or K256E α-actinin-4 with the actin cytoskeleton was determined. Un-infected podocytes and those overexpressing wildtype α-actinin-4 exhibit adaptation to the mechanical stretch at each time point. The actin stress fibers respond to the application of stretch by initially disassembling (after 1 hour stretch) and subsequently reassembling (after 4 hours to 24 hours). The cell surface area was

maintained throughout the 24 hours of stretch. Conversely, podocytes expressing K256E α-actinin-4 became progressively elongated beginning at 4 hours, and by 24 hours the actin cytoskeleton became extensively condensed.

Figure 6.17 Mechanical Stretch of Podocytes Overexpressing Wildtype or K256E α-Actinin-4

Podocytes were cultured on collagen-I coated silicone membranes. Equibiaxial cyclic stress (0.5 Hz and 10% linear strain) was applied to the membranes for various durations (1 and 24 hour time points shown). Using phalloidin-FITC, co-localization of GFP-tagged wildtype and K256E α-actinin-4 with the actin cytoskeleton was determined (Images are representative of three repeated experiments.). Un-infected podocytes and those overexpressing wildtype α-actinin-4 exhibit adaptation to the mechanical stretch at each time point by reorganizing the actin cytoskeleton. Conversely podocytes expressing K256E α-actinin-4 become thin and elongated after 24 hours of stretch.
Data represent three repeated experiments (n=3).

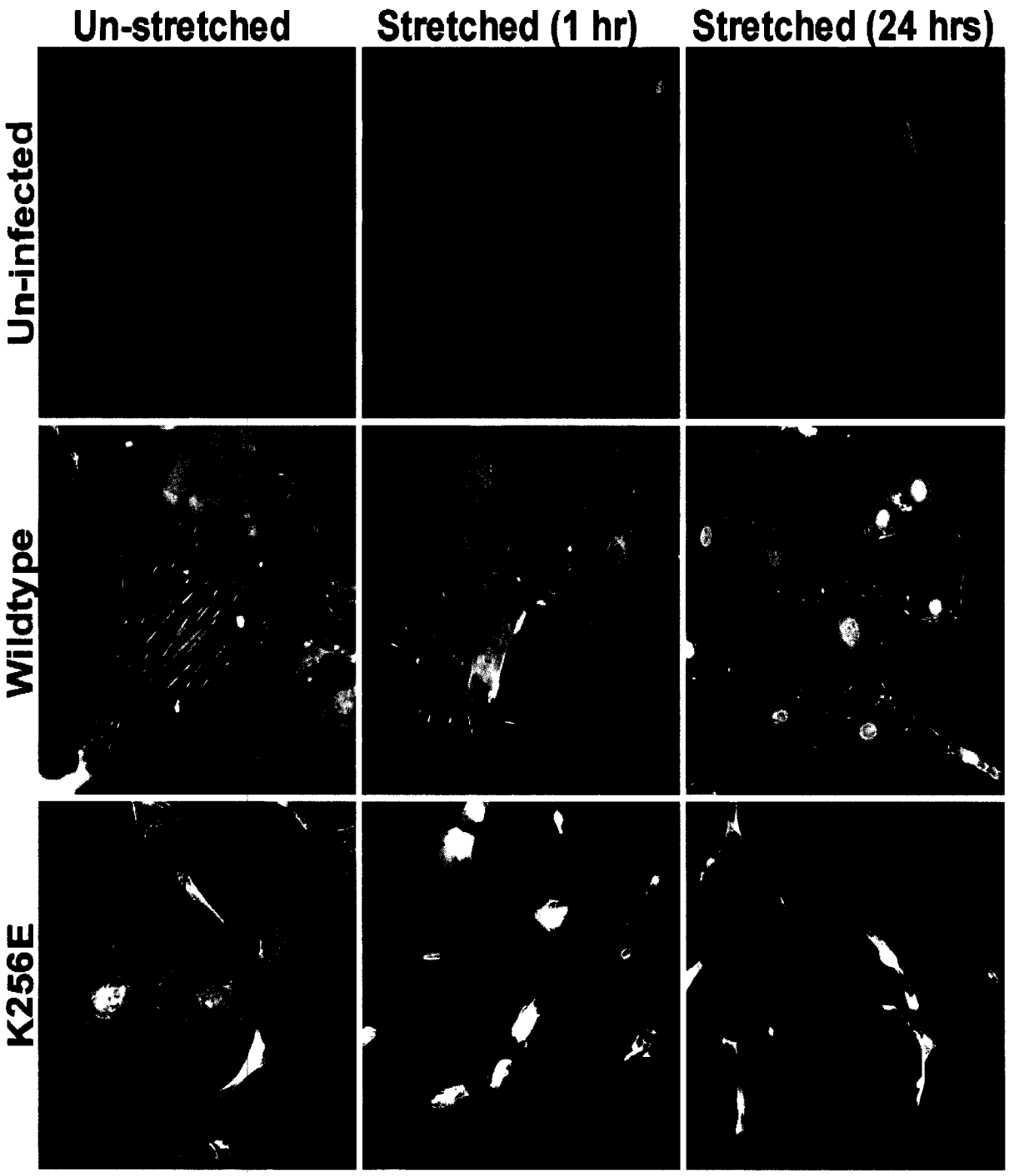
Un-stretched
Stretched (1 hr)
Stretched (24 hrs)
Un-infected
Wildtype
K256E

6.3.2 Podocyte Surface Area and Cell Number Following Mechanical Stretch

The surface area of cells was determined in mechanical stretch experiments using Kodak ID project software (Figure 6.18). The average surface area of un-infected podocytes not exposed to mechanical stretch ($1550 \pm 50\ \mu m^2$) was not statistically different from those that were stretched ($1550 \pm 200\ \mu m^2$). The surface area of those podocytes overexpressing wildtype α-actinin-4, either having remained un-stretched ($2050 \pm 150\ \mu m^2$) or stretched ($1600 \pm 100\ \mu m^2$) for 24 hours, remained similar. In contrast, podocytes over-expressing K256E α-actinin-4 showed a significant reduction in surface area after 24 hours of stretch ($300 \pm 20\ \mu m^2$) compared to non-stretched podocytes over-expressing K256E α-actinin-4 ($1800 \pm 200\ \mu m^2$).

Since podocytes expressing K256E α-actinin-4 exhibited abnormal structure and reduced cell surface area following 24 hours of stretch we investigated whether the mechanical stretch induced cell detachment in a manner resembling the detachment of podocytes from the GBM in vivo during the onset of FSGS. Cell number was determined by counting DAPI-stained nuclei (Figure 6.19). Podocytes overexpressing either wildtype or K256E α-actinin-4 showed no significant difference in cell number; thus, mechanical stretch forces cells expressing the K256E mutation to become thin and elongated but they remain attached to the collagen-I coated silicone membrane.

Figure 6.18 Surface Area Analysis from Mechanical Stretch Experiments

Podocytes were cultured on collagen-I coated silicone membranes. Equibiaxial cyclic stress (0.5 Hz and 10% linear strain) was applied to the membranes for up to 24 hours. Un-infected podocytes and those overexpressing wildtype α-actinin-4 exhibit normal surface area after 24 hours of stretch. Conversely podocytes expressing K256E α-actinin-4 show a significant reduction in their surface area after 24 hours of stretch (**P<0.01). Data are from three repeated experiments (n=3).

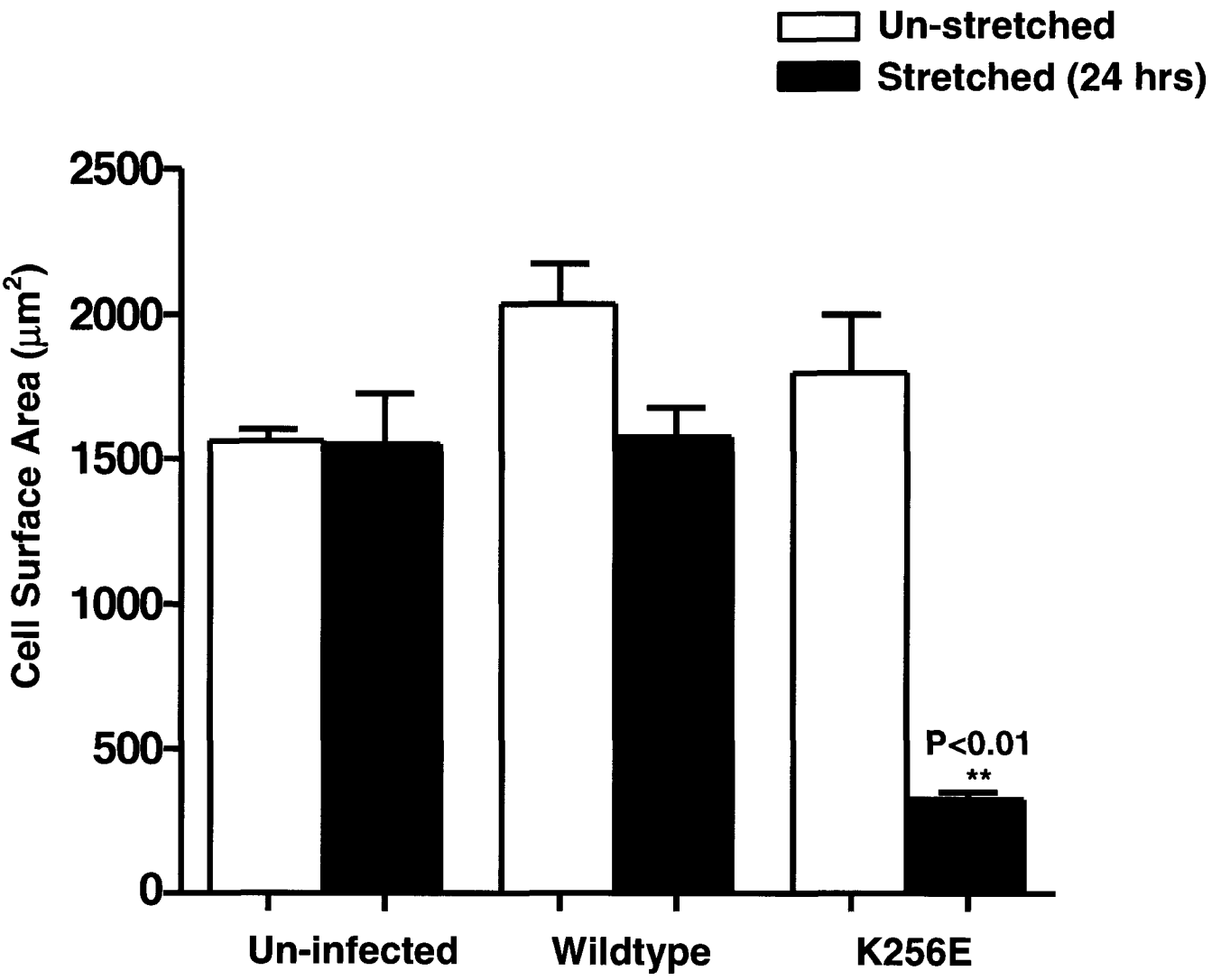
Un-stretched
Stretched (24 hrs)
Cell Surface Area (μm²)
2500
2000
1500
1000
500
0
P<0.01
**
Un-infected
Wildtype
K256E

Figure 6.19 Quantitative Analysis from Mechanical Stretch Experiments

Podocytes were cultured on collagen-I coated silicone membranes. Equibiaxial cyclic stress (0.5 Hz and 10% linear strain) was applied to the membranes for 24 hours. Cell number was determined by manually counting cells stained with DAPI. Podocytes overexpressing wildtype or K256E α-actinin-4 show no significant difference in the number of cells; thus, cells expressing K256E α-actinin-4 become thin and elongated but show no reduction in quantity. Data are from three repeated experiments (n=3).

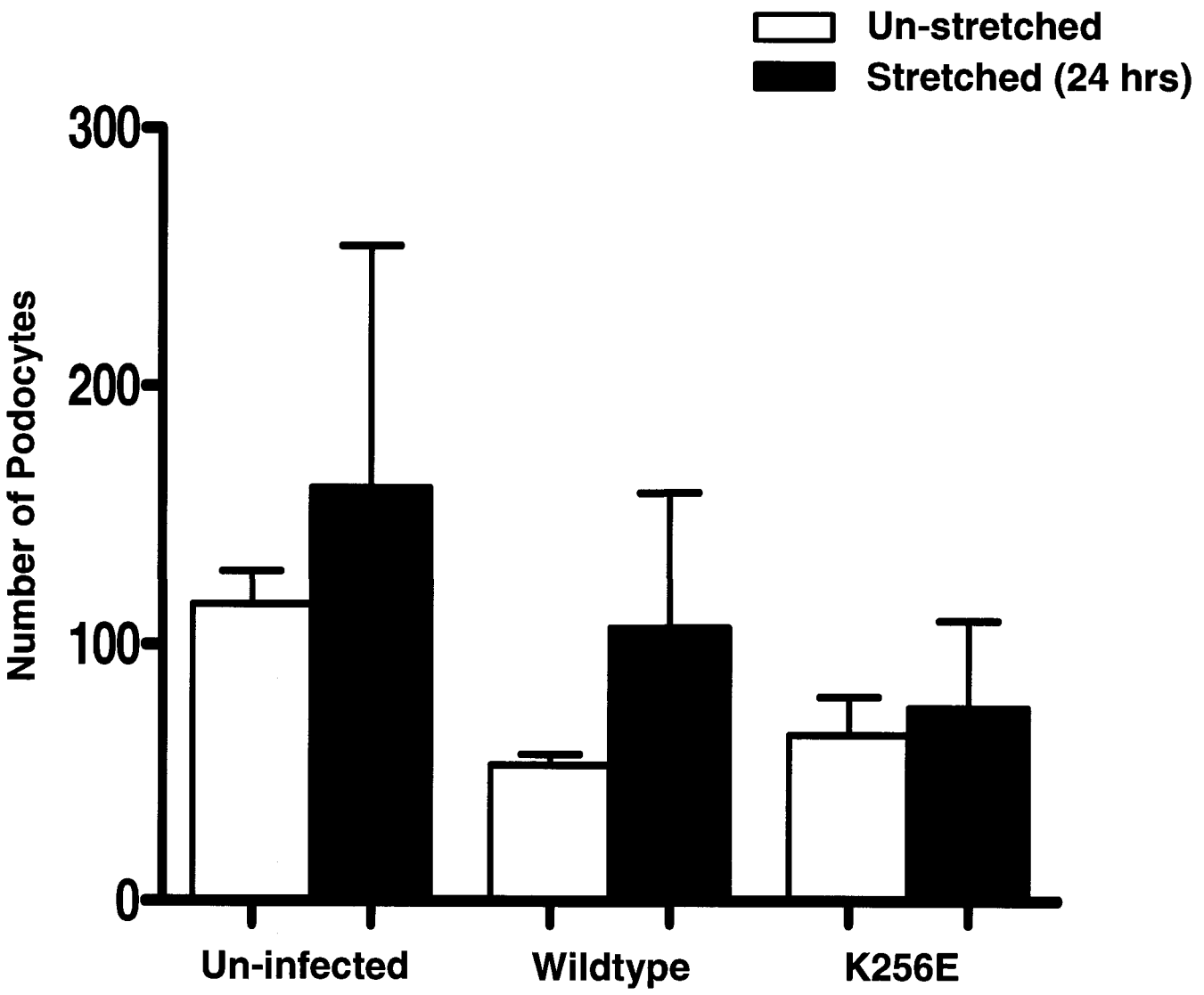
Un-stretched
Stretched (24 hrs)
300
200
100
0
Number of Podocytes
Un-infected
Wildtype
K256E

7 DISCUSSION

α-Actinin-4 is an actin filament crosslinking protein that is highly expressed in podocytes, where it supports the structure and function of the foot processes of the glomerular filtration barrier. Mutations in the α-actinin-4 gene lead to a familial form of glomerular disease called FSGS [1]. Each of the disease-causing mutations (e.g., K256E) dramatically increase the affinity of α-actinin-4 for F-actin [2], perturbs cellular migration and spreading, while altering its intracellular localization in podocytes [3]. Due to these defects in K256E α-actinin-4 biology, we hypothesized that K256E mutation would affect the interaction between α-actinin-4 and its known association partners involved in a variety of cellular processes, including FAK, β-catenin, synaptopodin, MAGI-1, vinculin, and Akt.

7.1 PHOSPHORYLATION AND α-ACTININ-4 ACTIN AFFINITY

A variety of protein kinases phosphorylate target proteins in order to regulate their actions, associations, and localization within the cell. FAK is a major tyrosine kinase involved in signaling events originating at focal adhesions and its actions influence cell proliferation, cell migration and survival by regulating the turnover of the adhesion complexes on the underside of the cell.

α-actinin-1, an isoform of α-actinin-4, can be phosphorylated by FAK in adherent platelets, but not in other cell types such as Cos-7, NIH 3T3, or HeLa cells unless intracellular phosphatases are inhibited with sodium orthovanadate. This indicates that

phosphorylation of α-actinin-1 is tightly regulated by phosphatases in these cells. Importantly, phosphorylation of α-actinin-1 reduced its affinity for actin filaments as evidenced by the introduction of glutamic acid in place of tyrosine 12 on α-actinin-1 to mimic phosphorylation. Additionally, phosphorylation of α-actinin-1 was dependent upon co-expression of FAK since cells lacking FAK were unable to exhibit phosphorylation of α-actinin-1 [41]. Since α-actinin-1 has an affinity for actin filaments and localizes to focal adhesions it was concluded that phosphorylation of α-actinin-1 by FAK could facilitate the turnover of adhesion complexes as well as the actin cytoskeleton thereby facilitating the process of migration and spreading. Interestingly, cells from FAK-deficient mice also exhibit reduced mobility in vitro [86], and cells treated with a FAK inhibitor exhibit impaired cell migration [87], similar to podocytes expressing K256E α-actinin-4. We believe that the association of α-actinin-4 with actin filaments is likewise tightly regulated in podocytes. As K256E α-actinin-4 associates with actin filaments with greater affinity than does wildtype α-actinin-4 it is possible that when mutated in this manner, α-actinin-4 loses the sensitivity of its regulatory sites (e.g. phosphorylation) and fails to dissociate from the actin filaments, thereby inhibiting the turnover of these filaments. Based upon these results and on regulation of α-actinin-1 by phosphorylation, we investigated whether α-actinin-4 could be phosphorylated by FAK. The amino acid sequences of α-actinin-1 and α-actinin-4 are highly homologous. The tyrosine amino acid residue of α-actinin-1 reported to be phosphorylated by FAK in Cos-7 cells, corresponds to tyrosine 32 on α-actinin-4. However, our results indicate that neither wildtype nor K256E α-actinin-4 are tyrosine phosphorylated by FAK in NIH 3T3 (Figure 6.1) and in Cos-7 (Figure 6.2) cells under our experimental conditions (Figure 6.3

and 6.4), despite the fact that FAK appeared to be autophosphorylated. Furthermore, we were unable to reproduce the findings of Izaguirre et al., with respect to FAK-induced phosphorylation of actinin-1. The reason for this discrepancy is presently unclear.

Subsequent to direct tyrosine phosphorylation studies we investigated the regulation of α-actinin-4/actin binding by indirect tyrosine phosphorylation of α-actinin-4. In this approach, cells were treated with the tyrosine phosphatase inhibitor, sodium orthovanadate (Figure 6.5) to prolong tyrosine phosphorylation within the cells. The soluble α-actinin-4 (Triton x-100 soluble) and actin bound α-actinin-4 (Triton x-100 insoluble) subcellular fractions were then obtained. If the interaction of α-actinin-4 with actin is regulated by tyrosine phosphorylation, either directly or indirectly, then it would follow that the distribution of α-actinin-4 in the Triton soluble fraction should have increased following treatment of the cells with sodium orthovanadate treated cells. However, our results illustrate that both wildtype and K256E α-actinin-4 showed no changes in their actin affinity under conditions of maximized cellular tyrosine phosphorylation levels.

Taken together, our findings suggest that tyrosine phosphorylation and signaling does not play a major role in regulating the interaction of α-actinin-4 with actin filaments. Therefore, it is likely that other signaling mechanisms play an important role in the regulation of α-actinin-4 in podocytes, and remain to be discovered.

7.2 INTERACTION AND CO-LOCALIZATION OF α-ACTININ-4 WITH BINDING PARTNERS

7.2.1 Interaction and Co-localization of α-Actinin-4 with β-Catenin in Podocytes

Cell to cell adhesion plays a critical role in establishing and maintaining the architecture and functional integrity of epithelial cells such as podocytes. Cell to cell contacts are regulated by a variety of adhesion structures (adherens junctions, focal contacts, and tight junctions) [88]. Each structure consists of distinct adhesion proteins that interact with the cytoskeleton. Any disruption in these interactions can lead to dysregulation of cell to cell adhesion and eventually lead to cell functional failure.

In podocytes, the cell to cell adhesion is particularly important to the integrity of the filtration barrier in the kidney and is maintained by the slit diaphragm which is a modified adherens junction. The structure/function of the slit diaphragm, aside from simply attaching two neighboring podocytes together, is that it forms the filtration barrier without which proteinuria will initiate a progression towards end stage renal disease.

It is becoming apparent that the structure of the slit diaphragm is maintained through its linkage to the cytoskeleton and disruption of these associations leads to disappearance of the slit diaphragm. For example, proteins such as CD2AP, podocin, ZO-1 or MAGI-1 are the adaptors that link nephrin to actin filaments by binding to actin filaments [8] directly or by binding to α-actinin-4. Loss of expression for nephrin, CD2AP or podocin in gene-targeted mice, or under experimental or clinical disease contexts, results in slit diaphragm destruction, foot process effacement and filtration barrier dysfunction [16, 18, 19, 89].

Another example includes β-catenin, which binds to α-actinin-4 and links actin filaments to P-cadherin, which is another transmembrane protein aside from nephrin that contributes to the zipper-like structure of the slit diaphragm. As β-catenin is an adherens junction protein and a binding partner of α-actinin-4 [42], the importance of this association was of great interest. We hypothesized that the FSGS-causing mutant might show altered interaction with β-catenin. Indeed our immunoprecipitation results show minimal interaction of K256E α-actinin-4 with β-catenin compared to wildtype α-actinin-4 (Figure 6.6). However, it seems that the intracellular location of β-catenin does not change (situated around cell periphery) within podocytes expressing K256E α-actinin-4. Furthermore, as K256E α-actinin-4 exhibits an aberrantly high affinity for actin filaments, it tends to be sequestered away from the cell periphery where β-catenin is found. This altered localization of K256E α-actinin-4 might affect its ability to co-localize and interact with β-catenin around cell periphery including filopodia and lamelopodia (Figure 6.7). The functional consequences of this reduced association are unclear, however, the podocytes of transgenic mice expressing FSGS-associated mutant α-actinin-4 exhibit loss of foot process structure and cell to cell adhesion resulting in effacement. It is unclear whether cell-cell contacts were perturbed between podocytes expressing K256E α-actinin-4. Nevertheless, our findings might explain one of the initial steps leading to podocyte effacement – that is disruption of adherens junction complexes due to loss of interaction between β-catenin and α-actinin-4. Further studies will be required to uncover the downstream molecular events that may be perturbed by the reduced association of β-catenin and K256E α-actinin-4. The regulation of this

interaction might be of great importance in maintaining the proper structure and function of podocytes.

7.2.2 Interaction and Co-localization of α-Actinin-4 with Synaptopodin in Podocytes

It is becoming increasingly apparent that the podocyte cytoskeleton is the common target for podocyte damage in glomerular diseases, as most mutations in proteins that lead to foot process effacement are cytoskeletal proteins, including actin binding proteins (such as α-actinin-4) or the proteins that are connected to the cytoskeleton (nephrin, podocin, and CD2AP) [16, 18, 19].

Synaptopodin is an actin binding protein that associates with α-actinin-4 and regulates actin bundling activity of α-actinin-4 in podocytes by inhibiting the branching of actin filaments induced by α-actinin-4 [47]. The interaction of α-actinin-4 with its binding partner, synaptopodin, was of great interest and we hypothesized that compared with wildtype α-actinin-4, the FSGS causing mutant might show a different pattern of association with synaptopodin – either increasing its interaction due to the enhanced actin association, or displacing synaptopodin from actin filaments. Indeed our data show that synaptopodin expression along stress fibers is reduced in podocytes expressing K256E α-actinin-4 (Figure 6.9). However, co-immunoprecipitation experiments showed no differences in association of synaptopodin with wildtype and K256E α-actinin-4 (Figure 6.8).

The apparently opposing results of the immunoprecipitation and immunofluorescence studies may be explained by at least two possibilities. First, in our

immunoprecipitation results, the α-actinin-4 located in the cytoplasm and α-actinin-4 around the cell periphery may be preferentially immunoprecipitated over that which is tightly associated with actin filaments. In that case the same amount of synaptopodin may be interacting with "unbound" wildtype and K256E α-actinin-4. Second, synaptopodin is not expressed in undifferentiated podocytes, thus, in our immunofluorescence results, podocytes expressing K256E α-actinin-4 may have reverted back towards an undifferentiated state, as compared with podocytes expressing wildtype α-actinin-4.

Overall our findings may indicate that the enhanced affinity of K256E α-actinin-4 for actin filaments may displace and prevent synaptopodin from regulating the actin cytoskeleton. This dysregulation may be one of the steps in inhibition of actin cytoskeleton turnover in podocytes resulting in cell migration and cell spreading impairments. Finally, we did not observe any apparent differences in actin branching levels in K256E α-actinin-4 expressing podocytes, that may have arisen due to the low levels of synaptopodin. It is possible that the gain of affinity activity of α-actinin-4 could have overridden these effects.

7.2.3 Interaction and Co-localization of α-Actinin-4 with MAGI-1 in Podocytes

The glomerular slit diaphragm is a modified adherens junction consisting of trafficking of proteins acting as a regulatory barrier and forming a signaling platform that regulates cell growth, proliferation and differentiation. As discussed earlier, mutations in the genes encoding for slit diaphragm proteins or altered interaction of these proteins can

lead to irregular downstream molecular events. This may cause podocyte damage and eventually lead to kidney disease.

MAGI-1, an important molecular scaffold protein that is expressed in many epithelial cells, and acts as a binding partner for α-actinin-4 and nephrin in podocytes [51, 52]. This association was of great interest since it indicates that MAGI-1 plays an important role in the structure of the slit diaphragm and may act as an adaptor to link the slit diaphragm to the cytoskeleton.

We speculated that the FSGS causing mutant might show different interaction with MAGI-1 and the outcome will be the disruption of the linkage between slit diaphragm and cytoskeleton that leads to foot process effacement. However our immunoprecipitation data shows that MAGI-1 associates with both wildtype and K256E α-actinin-4 equally (Figure 6.10). Furthermore immunofluorescence data shows that podocytes expressing wildtype and K256E α-actinin-4 exhibit similar intracellular localization of MAGI-1, around the cell periphery, along stress fibers and in the nucleus. However, wildtype α-actinin-4 tends to co-localize with MAGI-1 around cell periphery and along stress fibers and K256E α-actinin-4 co-localization is restricted only to stress fibers (Figure 6.11).

Even though interaction between MAGI-1 with wildtype and K256E α-actinin-4 seems similar, further studies are required to investigate the importance of the association of MAGI-1 with α-actinin-4 and the downstream molecular events that take place after this interaction. It is possible that in podocytes, when α-actinin-4 associates with MAGI-1 around the cell periphery the complex participates in a different signaling pathway compared to when α-actinin-4 associates with MAGI-1 around stress fibers. The former

interaction may be involved in regulation of the slit diaphragm and the latter may further inhibit the turnover of actin cytoskeleton by restricting filament flexibility.

7.2.4 Interaction and Co-localization of α-Actinin-4 with Vinculin in Cos-7 and Podocyte Cells

Aside from the structure of slit diaphragm, the attachment of foot processes to the GBM is also essential for the structural integrity of the podocyte foot process. Cell to matrix contacts are mediated by complex structures known as focal adhesions. Focal adhesions not only attach cells to their matrix they are also important within the cells for cell survival functions such as migration, spreading and lamellipodia extension [90] as they are required to assemble and disassemble, a phenomenon known as focal adhesion turnover [91]. Detachment of podocytes from the extracellular matrix represents a key event that follows foot process effacement during glomerular diseases such as FSGS. A cytoskeletal-initiated impairment of cell migration and spreading might involve the disruption of focal adhesion complexes and inhibition of its turnover. For example, cells that lack vinculin – a focal adhesion protein - exhibit impairment in cell adhesion, spreading, and fewer focal adhesions [55-57]. Furthermore, cells from FAK-deficient mice exhibit an increase in the number of focal adhesions and reduced cell migration [86], suggesting that deficiency in any of the focal adhesion proteins may either increase or decrease the number of focal adhesions within the cell and eventually affect the turnover of these complexes.

It is possible that in FSGS, podocytes either lose their focal adhesion complexes leading to their detachment from the GBM or they fail to regulate their focal adhesion

turnover leading to a more subtle impairment of their function. Two previous studies investigated the adhesion properties of podocytes in disease states in vitro and in vivo. The first study was carried out in our lab where we showed that podocytes expressing K256E α-actinin-4 do not exhibit reduced adhesion compared to podocytes expressing wildtype α-actinin-4. However, Martin Pollak's group detected podocytes in the urine of the mice deficient in α-actinin-4 suggesting a decrease in podocyte number through detachment from the GBM [92]. They also showed that α-actinin-4 deficient podocytes had decreased adhesion to glomerular basement membrane components suggesting that α-actinin-4 is important for podocyte attachment to GBM.

To follow up with these studies, we wanted to investigate whether α-actinin-4 binds to vinculin and if this interaction becomes aberrant once α-actinin-4 is mutated thereby explaining the impairment of adhesion properties, cell spreading and lamellipodia extension in podocytes. Interestingly, α-actinin-1 was demonstrated to associate with vinculin [58]. However, our results show that neither wildtype nor K256E α-actinin-4 associate with vinculin in either Cos-7 cells (Figure 6.12) or podocytes (Figure 6.13), despite an apparent co-localization with vinculin as determined by co-immunofluorescence experiments in podocytes (Figure 6.14). Our findings may be explained by at least two possibilities. The first is that there might be other focal adhesion proteins that require association with α-actinin-4 that regulate adhesion of podocytes to the GBM or disruption in the turnover of the focal adhesions when α-actinin-4 fails to interact with them. The second possible conclusion is that α-actinin-4 does not play a major role in maintaining the focal adhesion properties of podocytes to GBM. However, the role of α-actinin-4 in the turnover of focal adhesions is yet to be investigated. Overall,

based on our results the impairment in cell spreading and lamellopodia extension observed in podocytes [3] is not the result of disruption in the association of α-actinin-4 with vinculin.

7.2.5 Akt Phosphorylation within Podocytes Overexpressing Wildtype and K256E α-Actinin-4

The slit diaphragm maintains the functional integrity of podocytes by participating in signaling pathways that are triggered through nephrin. One of these pathways involves Akt, a serine/threonine kinase, which is phosphorylated downstream of PI3-kinase. Akt mediates cellular survival pathways by inhibiting apoptosis through inactivation of several proteins involved in cell death. A recent study showed that α-actinin-4 regulates Akt by mediating its translocation to the cell membrane in hOSE cells [69]. Thus, we wanted to test whether K256E α-actinin-4, being restricted to stress fibers, is incapable of regulating Akt phosphorylation in podocytes which might increase the susceptibility of these cells to apoptosis.

Our results indicated no significant differences in Akt phosphorylation in podocytes expressing either wildtype or K256E α-actinin-4 under basal conditions (Figure 6.15) or following serum stimulation of the cells (Figure 6.16). This may indicate that Akt activity is independent of α-actinin-4 in podocytes, such that other proteins might regulate its phosphorylation.

7.3 MORPHOLOGICAL CHANGES OF PODOCYTES EXPRESSING WILDTYPE AND K256E α-ACTININ-4 WHILE SUBJECTED TO MECHANICAL STRETCH

Kidney filtration is achieved by the cyclical application of both hydrostatic and oncotic pressure within the glomerular capillaries [85]. These pressures are continuously exerted on podocytes and therefore these cells, which cover the glomerular capillaries, need to be equipped with a flexible cytoskeletal network in order to contend with these pressures. FSGS is associated with an increased glomerular capillary pressure [84]. When these pressures are increased, one can imagine that podocytes with an aberrant cytoskeletal phenotype might not be able to adapt to the stress-tension and stretch. We therefore hypothesized that podocytes expressing K256E α-actinin-4 while subjected to mechanical stretch, would exhibit impaired morphological changes compared to podocytes expressing wildtype α-actinin-4.

Our results show that podocytes expressing wildtype α-actinin-4 are indeed able to adapt to the mechanical stretch over a 24 hours time period (Figure 6.17). The actin stress fibers, initially arranged in parallel bundles, initially disassemble upon the application of mechanical stretch in vitro. These stress fibers subsequently reassemble in a more random orientation over a 24 hour timeframe without affecting the cell surface area (Figure 6.18). As expected, podocytes expressing K256E α-actinin-4 have difficulty adapting to these distensive forces and become thin and elongated after 24 hours of stretch while the actin cytoskeleton condenses exhibiting numerous aggregates of actin/actinin-4 (Figure 6.17 and Figure 6.18).

Since detachment of podocytes from the GBM is observed in many glomerular lesions, we wanted to investigate whether podocytes expressing K256E α-actinin-4 lose

their focal adhesions and detach from the collagen-coated silicone membranes when they are subjected to mechanical stretch. Quantitative analysis from mechanical stretch experiments shows no significant difference in the number of cells between podocytes expressing wildtype and K256E α-actinin-4 (Figure 6.19). Perhaps 24 hours is insufficient to cause detachment of stretch. However, these findings are consistent with those of the adhesion assays as previously reported by our lab [3].

In this study we used in vitro mechanical stretch of cultured podocyte cells, which mimics the pressure within the glomerular capillaries. This approach provides an understanding of the architecture/function of podocytes as they depend on a dynamic actin cytoskeleton for survival when constantly subjected to stretch. It is likely that podocytes constantly need to remodel their actin cytoskeleton to contend with the forces exerted on them. However, the K256E mutant may inhibit the turnover of the actin filaments by binding forcefully thereby preventing any remodeling of actin. The result is that these cells become rigid and eventually fail to function as filtration barriers. Upon stretch podocytes expressing K256E α-actinin-4 resemble the podocytes in vivo when they are damaged as they appear elongated and condensed and unable to enwrap the glomerular capillaries (Figure 7.1).

Taken together, the data presented in this series of studies shows that a mutation in the gene encoding for α-actinin-4 that leads to a familial form of FSGS exhibits altered association with an important adherens junction protein, β-catenin, and it alters the expression and localization of synaptopodin along stress fibers. It also impairs the ability of the actin cytoskeleton to adjust to distensive forces while still maintaining its presence at focal adhesions. We can therefore conclude that the function of α-actinin-4 is crucial

for maintaining the structure of podocytes. This study also shows that α-actinin-4 is not regulated by tyrosine phosphorylation and does not regulate phosphorylation of Akt. Future studies will undoubtedly be aimed at investigating which regulatory domains of α-actinin-4 are muted by the FSGS-associated mutation(s), thereby leading to podocyte dysfunction.

Figure 7.1 Podocyte Damage in Vivo and in Vitro

When podocytes are damaged, the cells exhibit an effaced and elongated phenotype in vivo resembling what we observed in vitro. **A –** Illustrates a scanning EM of the normal podocytes enwrapping the glomerular capillaries resembling the podocytes overexpressing wildtype α-actinin-4 after 24 hours of stretch resembling **(B)**. **C –** Illustrates a scanning EM of the damaged podocytes resembling the podocytes overexpressing K256E α-actinin-4 after 24 hours of stretch **(D)**.

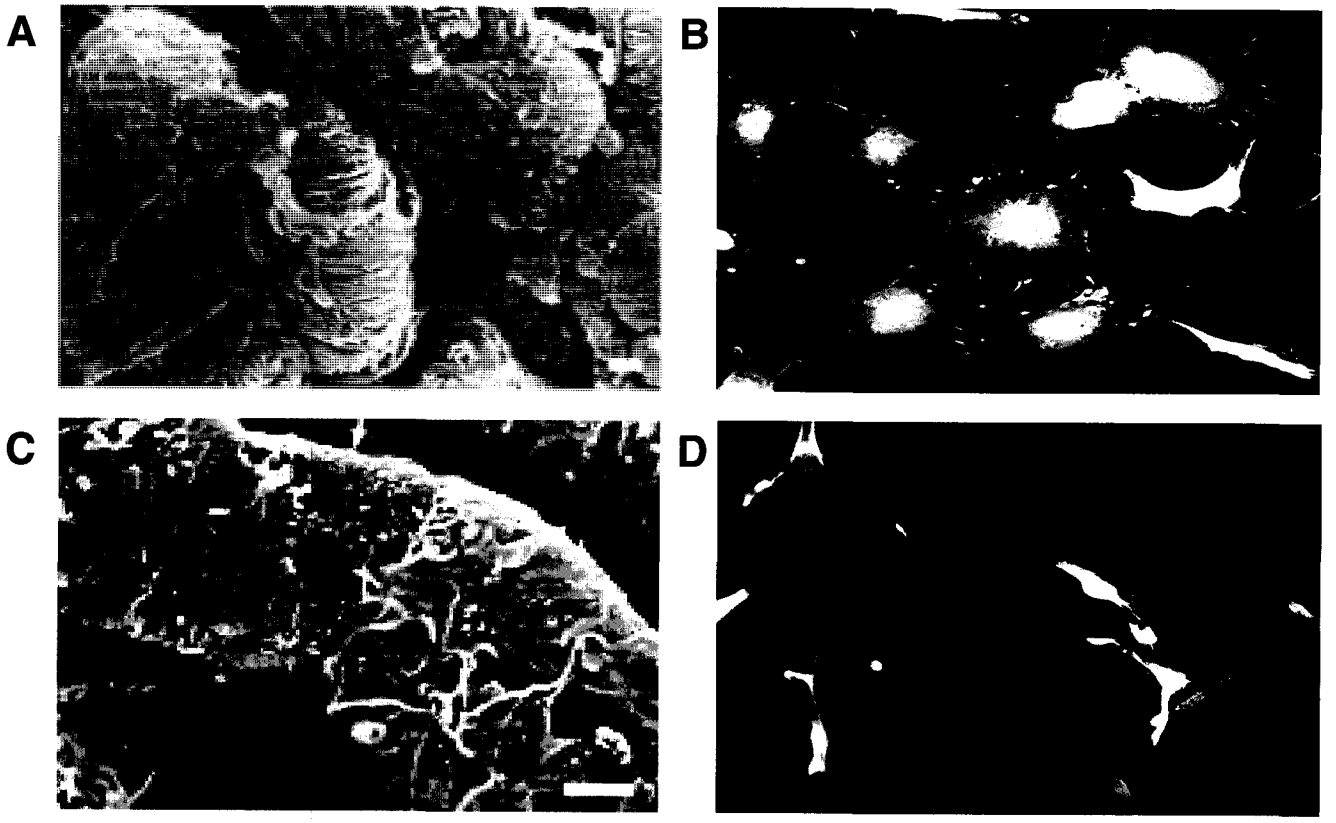
A
B
C
D

8 REFERENCES

1. Kaplan JM, Kim SH, North KN, et al: Mutations in ACTN4, encoding alpha-actinin-4, cause familial focal segmental glomerulosclerosis. *Nat Genet* 24(3):251-256, 2000

2. Michaud JL, Lemieux LI, Dube M, et al: Focal and segmental glomerulosclerosis in mice with podocyte-specific expression of mutant alpha-actinin-4. *J Am Soc Nephrol* 14(5):1200-1211, 2003

3. Michaud JL, Chaisson KM, Parks RJ, Kennedy CR: FSGS-associated alpha-actinin-4 (K256E) impairs cytoskeletal dynamics in podocytes. *Kidney Int* 70(6):1054-1061, 2006

4. Schauf C, Moffett D, Moffett S: *Human Physiology,* Pg. 953-959, 1990

5. Tortora GJ, Grabowski SR: *Principles of anatomy and physiology,* Pg. 953-959, 2003

6. Stockand JD, Sansom SC: Glomerular mesangial cells: electrophysiology and regulation of contraction. *Physiol Rev* 78(3):723-744, 1998

7. Loutzenhiser R: Inward rectifier currents in pericytes. *Am J Physiol Regul Integr Comp Physiol* 290(6):R1598-600, 2006

8. Pavenstadt H, Kriz W, Kretzler M: Cell biology of the glomerular podocyte. *Physiol Rev* 83(1):253-307, 2003

9. Huber TB, Hartleben B, Kim J, et al: Nephrin and CD2AP associate with phosphoinositide 3-OH kinase and stimulate AKT-dependent signaling. *Mol Cell Biol* 23(14):4917-4928, 2003

10. Lee DB, Huang E, Ward HJ: Tight junction biology and kidney dysfunction. *Am J Physiol Renal Physiol* 290(1):F20-34, 2006

11. Schnabel E, Anderson JM, Farquhar MG: The tight junction protein ZO-1 is concentrated along slit diaphragms of the glomerular epithelium. *J Cell Biol* 111(3):1255-1263, 1990

12. Garrod DR, Fleming S: Early expression of desmosomal components during kidney tubule morphogenesis in human and murine embryos. *Development* 108(2):313-321, 1990

13. Bazzoni G, Dejana E: Endothelial cell-to-cell junctions: molecular organization and role in vascular homeostasis. *Physiol Rev* 84(3):869-901, 2004

14. Benzing T: Signaling at the slit diaphragm. *J Am Soc Nephrol* 15(6):1382-1391, 2004

15. Hallman N, Norio R, Rapola J: Congenital nephrotic syndrome. *Nephron* 11(2):101-110, 1973

16. Putaala H, Soininen R, Kilpelainen P, et al: The murine nephrin gene is specifically expressed in kidney, brain and pancreas: inactivation of the gene leads to massive proteinuria and neonatal death. *Hum Mol Genet* 10(1):1-8, 2001

17. Verma R, Wharram B, Kovari I, et al: Fyn binds to and phosphorylates the kidney slit diaphragm component Nephrin. *J Biol Chem* 278(23):20716-20723, 2003

18. Ardiles LG, Carrasco AE, Carpio JD, Mezzano SA: Late onset of familial nephrotic syndrome associated with a compound heterozygous mutation of the podocin-encoding gene. *Nephrology (Carlton)* 10(6):553-556, 2005

19. Shih NY, Li J, Karpitskii V, et al: Congenital nephrotic syndrome in mice lacking CD2-associated protein. *Science* 286(5438):312-315, 1999

20. Winn MP, Conlon PJ, Lynn KL, et al: A mutation in the TRPC6 cation channel causes familial focal segmental glomerulosclerosis. *Science* 308(5729):1801-1804, 2005

21. Kaplan J, Pollak MR: Familial focal segmental glomerulosclerosis. *Curr Opin Nephrol Hypertens* 10(2):183-187, 2001

22. Blanchard A, Ohanian V, Critchley D: The structure and function of alpha-actinin. *J Muscle Res Cell Motil* 10(4):280-289, 1989

23. Virel A, Backman L: Molecular evolution and structure of alpha-actinin. *Mol Biol Evol* 21(6):1024-1031, 2004

24. Dixson JD, Forstner MJ, Garcia DM: The alpha-actinin gene family: a revised classification. *J Mol Evol* 56(1):1-10, 2003

25. Otey CA, Carpen O: Alpha-actinin revisited: a fresh look at an old player. *Cell Motil Cytoskeleton* 58(2):104-111, 2004

26. Beggs AH, Byers TJ, Knoll JH, et al: Cloning and characterization of two human skeletal muscle alpha-actinin genes located on chromosomes 1 and 11. *J Biol Chem* 267(13):9281-9288, 1992

27. Mills M, Yang N, Weinberger R, et al: Differential expression of the actin-binding proteins, alpha-actinin-2 and -3, in different species: implications for the evolution of functional redundancy. *Hum Mol Genet* 10(13):1335-1346, 2001

28. Tang J, Taylor DW, Taylor KA: The three-dimensional structure of alpha-actinin obtained by cryoelectron microscopy suggests a model for Ca(2+)-dependent actin binding. *J Mol Biol* 310(4):845-858, 2001

29. Honda K, Yamada T, Endo R, et al: Actinin-4, a novel actin-bundling protein associated with cell motility and cancer invasion. *J Cell Biol* 140(6):1383-1393, 1998

30. Pollak MR: Inherited podocytopathies: FSGS and nephrotic syndrome from a genetic viewpoint. *J Am Soc Nephrol* 13(12):3016-3023, 2002

31. Kos CH, Le TC, Sinha S, et al: Mice deficient in alpha-actinin-4 have severe glomerular disease. *J Clin Invest* 111(11):1683-1690, 2003

32. Yao J, Le TC, Kos CH, et al: Alpha-actinin-4-mediated FSGS: an inherited kidney disease caused by an aggregated and rapidly degraded cytoskeletal protein. *PLoS Biol* 2(6):e167, 2004

33. Hampton CM, Taylor DW, Taylor KA: Novel Structures for alpha-Actinin:F-Actin Interactions and their Implications for Actin-Membrane Attachment and Tension Sensing in the Cytoskeleton. *J Mol Biol* 368(1):92-104, 2007

34. Fraley TS, Tran TC, Corgan AM, et al: Phosphoinositide binding inhibits alpha-actinin bundling activity. *J Biol Chem* 278(26):24039-24045, 2003

35. Fraley TS, Pereira CB, Tran TC, et al: Phosphoinositide binding regulates alpha-actinin dynamics: mechanism for modulating cytoskeletal remodeling. *J Biol Chem* 280(15):15479-15482, 2005

36. Clark EA, Brugge JS: Integrins and signal transduction pathways: the road taken. *Science* 268(5208):233-239, 1995

37. Abbi S, Ueda H, Zheng C, et al: Regulation of focal adhesion kinase by a novel protein inhibitor FIP200. *Mol Biol Cell* 13(9):3178-3191, 2002

38. Chan PY, Kanner SB, Whitney G, Aruffo A: A transmembrane-anchored chimeric focal adhesion kinase is constitutively activated and phosphorylated at tyrosine residues identical to pp125FAK. *J Biol Chem* 269(32):20567-20574, 1994

39. Shen Y, Schaller MD: Focal adhesion targeting: the critical determinant of FAK regulation and substrate phosphorylation. *Mol Biol Cell* 10(8):2507-2518, 1999

40. Izaguirre G, Aguirre L, Ji P, et al: Tyrosine phosphorylation of alpha-actinin in activated platelets. *J Biol Chem* 274(52):37012-37020, 1999

41. Izaguirre G, Aguirre L, Hu YP, et al: The cytoskeletal/non-muscle isoform of alpha-actinin is phosphorylated on its actin-binding domain by the focal adhesion kinase. *J Biol Chem* 276(31):28676-28685, 2001

42. Hayashida Y, Honda K, Idogawa M, et al: E-cadherin regulates the association between beta-catenin and actinin-4. *Cancer Res* 65(19):8836-8845, 2005

43. Conacci-Sorrell M, Zhurinsky J, Ben-Ze'ev A: The cadherin-catenin adhesion system in signaling and cancer. *J Clin Invest* 109(8):987-991, 2002

44. Mundel P, Heid HW, Mundel TM, et al: Synaptopodin: an actin-associated protein in telencephalic dendrites and renal podocytes. *J Cell Biol* 139(1):193-204, 1997

45. Mundel P, Gilbert P, Kriz W: Podocytes in glomerulus of rat kidney express a characteristic 44 KD protein. *J Histochem Cytochem* 39(8):1047-1056, 1991

46. Deller T, Korte M, Chabanis S, et al: Synaptopodin-deficient mice lack a spine apparatus and show deficits in synaptic plasticity. *Proc Natl Acad Sci U S A* 100(18):10494-10499, 2003

47. Asanuma K, Kim K, Oh J, et al: Synaptopodin regulates the actin-bundling activity of alpha-actinin in an isoform-specific manner. *J Clin Invest* 115(5):1188-1198, 2005

48. Asanuma K, Yanagida-Asanuma E, Faul C, et al: Synaptopodin orchestrates actin organization and cell motility via regulation of RhoA signalling. *Nat Cell Biol* 8(5):485-491, 2006

49. Etienne-Manneville S, Hall A: Rho GTPases in cell biology. *Nature* 420(6916):629-635, 2002

50. Raftopoulou M, Hall A: Cell migration: Rho GTPases lead the way. *Dev Biol* 265(1):23-32, 2004

51. Patrie KM, Drescher AJ, Welihinda A, et al: Interaction of two actin-binding proteins, synaptopodin and alpha-actinin-4, with the tight junction protein MAGI-1. *J Biol Chem* 277(33):30183-30190, 2002

52. Hirabayashi S, Mori H, Kansaku A, et al: MAGI-1 is a component of the glomerular slit diaphragm that is tightly associated with nephrin. *Lab Invest* 85(12):1528-1543, 2005

53. Wu MH: Endothelial focal adhesions and barrier function. *J Physiol* 569(Pt 2):359-366, 2005

54. Coll JL, Ben-Ze'ev A, Ezzell RM, et al: Targeted disruption of vinculin genes in F9 and embryonic stem cells changes cell morphology, adhesion, and locomotion. *Proc Natl Acad Sci U S A* 92(20):9161-9165, 1995

55. Goldmann WH, Ingber DE: Intact vinculin protein is required for control of cell shape, cell mechanics, and rac-dependent lamellipodia formation. *Biochem Biophys Res Commun* 290(2):749-755, 2002

56. Goldmann WH, Schindl M, Cardozo TJ, Ezzell RM: Motility of vinculin-deficient F9 embryonic carcinoma cells analyzed by video, laser confocal, and reflection interference contrast microscopy. *Exp Cell Res* 221(2):311-319, 1995

57. Ezzell RM, Goldmann WH, Wang N, et al: Vinculin promotes cell spreading by mechanically coupling integrins to the cytoskeleton. *Exp Cell Res* 231(1):14-26, 1997

58. Belkin AM, Koteliansky VE: Interaction of iodinated vinculin, metavinculin and alpha-actinin with cytoskeletal proteins. *FEBS Lett* 220(2):291-294, 1987

59. Somanath PR, Razorenova OV, Chen J, Byzova TV: Akt1 in endothelial cell and angiogenesis. *Cell Cycle* 5(5):512-518, 2006

60. Vanhaesebroeck B, Alessi DR: The PI3K-PDK1 connection: more than just a road to PKB. *Biochem J* 346 Pt 3:561-576, 2000

61. Hemmings BA: Akt signaling: linking membrane events to life and death decisions. *Science* 275(5300):628-630, 1997

62. Andjelkovic M, Alessi DR, Meier R, et al: Role of translocation in the activation and function of protein kinase B. *J Biol Chem* 272(50):31515-31524, 1997

63. Cohen P, Alessi DR, Cross DA: PDK1, one of the missing links in insulin signal transduction? *FEBS Lett* 410(1):3-10, 1997

64. Alessi DR, Cohen P: Mechanism of activation and function of protein kinase B. *Curr Opin Genet Dev* 8(1):55-62, 1998

65. Kandel ES, Hay N: The regulation and activities of the multifunctional serine/threonine kinase Akt/PKB. *Exp Cell Res* 253(1):210-229, 1999

66. Chen WS, Xu PZ, Gottlob K, et al: Growth retardation and increased apoptosis in mice with homozygous disruption of the Akt1 gene. *Genes Dev* 15(17):2203-2208, 2001

67. Garofalo RS, Orena SJ, Rafidi K, et al: Severe diabetes, age-dependent loss of adipose tissue, and mild growth deficiency in mice lacking Akt2/PKB beta. *J Clin Invest* 112(2):197-208, 2003

68. Qian Y, Corum L, Meng Q, et al: PI3K induced actin filament remodeling through Akt and p70S6K1: implication of essential role in cell migration. *Am J Physiol Cell Physiol* 286(1):C153-63, 2004

69. Ding Z, Liang J, Lu Y, et al: A retrovirus-based protein complementation assay screen reveals functional AKT1-binding partners. *Proc Natl Acad Sci U S A* 103(41):15014-15019, 2006

70. Chartier C, Degryse E, Gantzer M, et al: Efficient generation of recombinant adenovirus vectors by homologous recombination in Escherichia coli. *J Virol* 70(7):4805-4810, 1996

71. He TC, Zhou S, da Costa LT, et al: A simplified system for generating recombinant adenoviruses. *Proc Natl Acad Sci U S A* 95(5):2509-2514, 1998

72. Ng P, Graham FL: Construction of first-generation adenoviral vectors. *Methods Mol Med* 69:389-414, 2002

73. Schiwek D, Endlich N, Holzman L, et al: Stable expression of nephrin and localization to cell-cell contacts in novel murine podocyte cell lines. *Kidney Int* 66(1):91-101, 2004

74. Hanks SK, Polte TR: Signaling through focal adhesion kinase. *Bioessays* 19(2):137-145, 1997

75. Ilic D, Damsky CH, Yamamoto T: Focal adhesion kinase: at the crossroads of signal transduction. *J Cell Sci* 110 (Pt 4)(Pt 4):401-407, 1997

76. Tamura M, Gu J, Takino T, Yamada KM: Tumor suppressor PTEN inhibition of cell invasion, migration, and growth: differential involvement of focal adhesion kinase and p130Cas. *Cancer Res* 59(2):442-449, 1999

77. Orsulic S, Huber O, Aberle H, et al: E-cadherin binding prevents beta-catenin nuclear localization and beta-catenin/LEF-1-mediated transactivation. *J Cell Sci* 112 (Pt 8)(Pt 8):1237-1245, 1999

78. Dobrosotskaya IY, James GL: MAGI-1 interacts with beta-catenin and is associated with cell-cell adhesion structures. *Biochem Biophys Res Commun* 270(3):903-909, 2000

79. Dobrosotskaya I, Guy RK, James GL: MAGI-1, a membrane-associated guanylate kinase with a unique arrangement of protein-protein interaction domains. *J Biol Chem* 272(50):31589-31597, 1997

80. Hirabayashi S, Tajima M, Yao I, et al: JAM4, a junctional cell adhesion molecule interacting with a tight junction protein, MAGI-1. *Mol Cell Biol* 23(12):4267-4282, 2003

81. Cardone MH, Roy N, Stennicke HR, et al: Regulation of cell death protease caspase-9 by phosphorylation. *Science* 282(5392):1318-1321, 1998

82. Datta SR, Dudek H, Tao X, et al: Akt phosphorylation of BAD couples survival signals to the cell-intrinsic death machinery. *Cell* 91(2):231-241, 1997

83. Meng F, Liu L, Chin PC, D'Mello SR: Akt is a downstream target of NF-kappa B. *J Biol Chem* 277(33):29674-29680, 2002

84. Petermann AT, Pippin J, Durvasula R, et al: Mechanical stretch induces podocyte hypertrophy in vitro. *Kidney Int* 67(1):157-166, 2005

85. Endlich N, Kress KR, Reiser J, et al: Podocytes respond to mechanical stress in vitro. *J Am Soc Nephrol* 12(3):413-422, 2001

86. Ilic D, Furuta Y, Kanazawa S, et al: Reduced cell motility and enhanced focal adhesion contact formation in cells from FAK-deficient mice. *Nature* 377(6549):539-544, 1995

87. Slack-Davis JK, Martin KH, Tilghman RW, et al: Cellular characterization of a novel focal adhesion kinase inhibitor. *J Biol Chem* 2007

88. Weis WI, Nelson WJ: Re-solving the cadherin-catenin-actin conundrum. *J Biol Chem* 281(47):35593-35597, 2006

89. Wolf G, Chen S, Ziyadeh FN: From the periphery of the glomerular capillary wall toward the center of disease: podocyte injury comes of age in diabetic nephropathy. *Diabetes* 54(6):1626-1634, 2005

90. Wu C, Keightley SY, Leung-Hagesteijn C, et al: Integrin-linked protein kinase regulates fibronectin matrix assembly, E-cadherin expression, and tumorigenicity. *J Biol Chem* 273(1):528-536, 1998

91. Webb DJ, Donais K, Whitmore LA, et al: FAK-Src signalling through paxillin, ERK and MLCK regulates adhesion disassembly. *Nat Cell Biol* 6(2):154-161, 2004

92. Dandapani SV, Sugimoto H, Matthews BD, et al: Alpha-actinin-4 is required for normal podocyte adhesion. *J Biol Chem* 282(1):467-477, 2007